Hill Slope Unsaturated Flowpaths and Soil Moisture Variability in a Forested Catchment in Southwest China

Lars-Erik Sørbotten

Norwegian University of Life Sciences
Department of Plant and environmental sciences
Master Thesis 60 credits 2011

Preface

The road from my first work on this thesis, via two field seasons in TieShanPing to the moment of final submission, has at times been long and frustrating, but nonetheless extremely rewarding, both on a professional and personal level. It would be too much to try to mention all the excellent people who should be thanked, but certain individuals have been central: Jan Mulder for calm, encouraging and insightful support through the entire process and not least for introducing me to China and the Chinese. Zhu Jing for much pleasant time spent together, with profound thanks for being both colleague, supervisor, interpreter, and indeed my only link to the outside world during my first stay in TieShanPing. Jannes Stolte for excellent supervision and design suggestions. Also thanks to Silja Solheimslid for great discussions and many late beers at TieShanPing, Li Zhenhua for valuable discussions, boxing and basketball workouts in TieShanPing, Professor Zhang Xiaoshan for putting me at my ease my first evening alone in China, Zou Shifu for great help in the field, everyone at Bioforsk Soil and Environment Division for helping me out when I needed it, Huang Hen Nen for digging all those profiles for me, and all the good people at our hotel in TieShanPing welcoming me and making my stay very enjoyable. And to the rest of the members of the team, Wang Yanhui, Yu Pengtao, Duan Lei, Peter Dörsch, Thorjørn Larssen, Rolf Vogt, Anja Nieuwenhuis: I hope I will have the opportunity to work with you in the future.

Finally, I wish to dedicate this thesis to my girlfriend Pernille Sandemose and son Sigbjørn, who have encouraged me when everything seemed hopeless, been proud of me when things were going well and together have provided all the motivation necessary to finish this thesis. I love you.

Lars-Erik Sørbotten, 03.08.2011

Institute of Plant and Environmental Sciences

Abstract

Forested catchments in subtropical southwest China are important sites for nitrogen, primarily due to denitrification. Denitrification depends strongly on soil moisture content and the residence time of soil water. Both depend on the hydrological properties of the soils. In this study we investigated the soil hydrological properties and water flow paths on a hill slope in the TieShanPing catchment around 25 kilometres north-east of Chongqing. Soils were sampled for analyses of water retention characteristics, grain size distribution, hydraulic conductivity, porosity and bulk density. In addition, TDR-generated soil moisture data were analysed with respect to volumetric water flow in response to precipitation events. A dye tracer experiment was also conducted for visual support of analyses. Hydraulic conductivity and chemical data support the hypothesis that episodic rain water does not generate overland flow, and TDR measurements support the hypothesis that episodic rain water mainly infiltrates through the upper 15-20 cm of the soil, due to a combination of functional saturation of the B1 horizon and subsequent infiltration excess. With an annual runoff coefficient of only 22 %, and accounting for an evapotranspiration of up to 60 %, there is still a deficiency in the water budget of at least 18 % which may indicate that a not insignificant amount of water percolates to deep groundwater and is lost from the sub-catchment. In future efforts, it will be important to ensure that the placement of soil moisture sensors is representative of the entire system to be described. Other sampling, including water samples for chemical analyses, discharge readings and ground water level readings, should be automatic and be set to high sampling frequencies during episodes.

Sammendrag

Skogkledte nedbørfelt i det subtropiske Sørvest-Kina er viktige områder for nitrogen, hovedsakelig på grunn av denitrifisering. Denitrifisering er sterkt avhengig av jordvanninnhold og jordvannets oppholdstid. Begge disse avhenger av jordens hydrologiske egenskaper. I denne studien undersøkte vi jordens hydrologiske egenskaper og vannets strømningsbaner i en bratt dalside i et nedbørfelt i TieShanPing, ca. 25 kilometer nordøst for Chongqing. Jordprøver ble tatt ut og analysert for vannretensjonsegenskaper, kornstørrelsesfordeling, hydraulisk konduktivitet, porøsitet og jordtetthet. I tillegg ble TDR-genererte jordvannsdata analysert med hensyn på volumetrisk vannstrømning som respons på nedbørsepisoder. Et fargetracereksperiment ble også gjennomført for visuell støtte for analysene. Hydraulisk konduktivitet og kjemiske data støtter hypotesen at episodenedbør ikke fører til overflateavrenning, og TDR-målingene støtter hypotesen om at episodenedbør hovedsakelig infiltrerer i de øvre 15-20 cm av jorden, grunnet en kombinasjon av funksjonell metning av B1-sjiktet og etterfølgende infiltrasjonsbegrensning. Med en årlig avrenningskoeffisient på 22 % av nedbøren og en evapotranspirasjon som kan være på opptil 60 %, har vi fortsatt et underskudd i vannbalansen på minst 18 %. Dette kan tyde på at en ikke ubetydelig andel av nedbøren infiltrerer til dypere grunnvann og strømmer ut av sidenedbørfeltet. I fremtidige undersøkelser vil det være viktig å sikre at plasseringen av jordvannssensorer er representativ for hele systemet som skal beskrives. Annen prøvetaking, herunder vannprøver for kjemisk analyse samt avlesning av vannføring og grunnvannsnivå, bør så langt det er mulig automatiseres, og det bør tas hyppige prøver under episoder.

Table of Contents

1 Introduction

During the past decades, the subtropical region of southwest China has experienced increased levels of nitrogen (N) deposition and is expected to receive more in the future, largely due to increased energy production and agricultural activities (Busch et al. 2001; Chen 2006). In principle, N is an important, often growth-limiting plant nutrient. However, in ecosystems with abundant external supply N may occur in excess. In temperate and boreal forests excess N has caused "nitrogen saturation", characterized by elevated leaching of nitrate (NO_3^-) to groundwater and surface water, with associated toxification, acidification and possible eutrophication of coastal waters. Recent studies (Larssen et al. 2011) suggest that despite N saturation and associated NO_3^- leaching from root zones in sub-tropical forest soils of south China, NO_3^- runoff with stream water is small. It has been hypothesized that this quantitatively important N sink in N saturated sub tropical forest is due to denitrification. Denitrification of NO_3^- is the primary pathway for production of N_2O, which is one of the important greenhouse gases (GHGs). Production of N_2O requires near saturated conditions, and the hydrological conditions are therefore of controlling importance for N_2O emission. This thesis is concerned primarily with investigating the varying hydrological conditions which control N_2O emission through creating conditions for nitrification or denitrification.

1.1 Increased nitrogen deposition and related problems

1.1.1 The N cycle

N_2O is a regular intermediary product denitrification of inorganic N such as NO_3- in the soil under reducing conditions (Koba et al. 2009; Wrage et al. 2001). It is also produced to a certain extent through nitrification, nitrifier denitrification and coupled nitrification-denitrification. The denitrification from inorganic N through N_2O to N_2 happens largely at low O_2 levels, i.e. when soils are near water saturated. Thus, hydrological conditions will as such have a major controlling influence on the N cycling in general. The released ratio of N_2O/N_2 also increases at low pH as this inhibits N_2O reductase (Wrage et al. 2001).

A great number of studies have been conducted on N cycling and ecological response to N deposition in forested catchments in temperate and boreal zones (Aber 1992; Dise & Wright 1995; Tietema 1998), but there is a lack of research done in subtropical areas (Chen 2006). The research which exists for tropical areas suggests that the processes differ from those in temperate and boreal zones; there are indications that tropical forest ecosystems are naturally N saturated due to high biological activity and phosphorous limitation and may not be able to

absorb anthropogenic N to the same degree as temperate forest ecosystems (Aber et al. 1989; Hall & Matson 1999). Given these differences, we should not assume that subtropical ecosystems exhibit identical responses to temperate or tropical ecosystems, and further study on subtropical systems is required.

1.1.2 The role of hydrology in understanding and predicting denitrification

In order to understand when and where we can expect emission of N_2O, which requires high values of water-filled pore space, we need to understand the principal hydrological processes that affect the nitrogen turnover. This research should ideally be conducted at a catchment level in order to produce an integrated understanding of these perspectives.

Hydrological parameters

In addition to availability of labile organic matter to drive the reduction process as well as available nitrate as substrate, N_2O production is also dependent on near saturated conditions to drive the denitrification. Hence an understanding of soil water flowpaths and the hydrological parameters that determine soil water variability are crucial to predicting N_2O emission. Vadose zone water transport is usually predicted using an approximation of unsaturated hydraulic conductivity (K_{unsat}) obtained from soil water retention characteristics and saturated hydraulic conductivity (K_{sat}). However, these measurements regard the soil as a uniform matrix through which water flows evenly, while in reality flowpaths to varying degrees will follow macropore structures which are unevenly spread throughout the soil matrix. This makes vadose zone flowpaths in hillslopes notoriously difficult to predict, and the greater the distribution of the macropores and the difference between macropore influence and matrix hydraulic conductivity, the more difficult such prediction will be.

1.2 Theory

1.2.1 Hillslope hydrology

Hillslope hydrology is mainly concerned with the fate of precipitation on its way through the hillslope vegetation and soils. Just as is the case for the general water balance, some water is lost through evapotranspiration, both through interception and from the soil after infiltration, and some water percolates to the groundwater and contributes to storage. The remainder is partitioned between overland flow, either Hortonian (also called ‘infiltration excess’) or saturation, subsurface flow and return flow (Kirkby 1988). Hortonian overland flow is overland flow generated when the precipitation rate exceeds the soil’s infiltration rate (its

capacity to absorb and transport the received water), whereas saturation overland flow is generated when the soil's storage capacity is exceeded, and the soil is effectively saturated.

History

Since hillslope hydrology emerged as a distinct hydrologic discipline in the 1960s and -70s (Kirkby 1988), much has changed in the understanding of the dynamics and importance of the particular flow paths that are generated under hill slope conditions.

Before the 1960s, R.E. Horton's theories on infiltration capacities versus rainfall intensity and the generation of surface flows (Horton 1933) were the generally accepted view. Infiltration and transport were largely viewed as purely Darcian processes, and surface water rises were generated by Hortonian overland flow. Later, it was shown that surface water variability could be predicted without the need to refer to overland flow at all, but could be generated purely by subsurface flow (Kirkby 1988).

In the 1970s and -80s and onwards, the role of macropores was investigated (Aubertin 1971; Beven & Germann 1982; Kirkby 1988), and it became evident that macropores and their connectivity had a significant controlling effect on effective hydraulic conductivity and on localisation of flow paths, particularly under saturated conditions. This was an important turning point, particularly since this would cast doubt on the applicability of the Darcian approach for predicting water movement. Studies on macropore effect on water transport has led to the design of models which use a bimodal, dual-permeability approach, such as is used in the HYDRUS model (Simunek & van Genuchten 2008; Simunek et al. 2008), which operates with two different hydraulic conductivities that act under different soil water content conditions.

Lately, it has been suggested that the importance of macropores may prove to be even more important. Numerical models employing the Darcian-Buckingham law, both for macropore and matrix flow as well as dual-permeability modelling, fail to yield accurate fits, as reported by Lamy et al. (2009) in a recent study. They also found that macropores may have an even greater impact on the preferential flow paths than previously suspected, and that in order for given mass of solute to be transferred through a macropore and achieve fits between observed results and modelling results, the effective flow path zone of a macropore must be considered to extend beyond the actual pore diameter. Thus, even accounting for macropore volume, we may underestimate the effect of macropores.

Current status

Different factors are of varying relative importance during different moisture conditions. Under dry conditions, the variability in soil surface water content seems to be mostly influenced by relative elevation, slope angle and clay content, while under wet conditions, the dominating factors are porosity and hydraulic conductivity (Famiglietti et al. 1998).

As earlier mentioned, macroporosity is a major factor in determining the redistribution of soil water, particularly in the upper soil horizons (Beven & Germann 1982; Noguchi et al. 2001). Hydrological modelling in catchments with steep hill slopes suggests that lateral subsurface flow becomes important during wet periods, when soil lateral hydraulic conductivity plays a greater part due to interconnected macropores (Bronstert & Plate 1997; Ridolfi et al. 2003). The importance of preferential flows in macropore networks seems to increase with soil moisture, and can become a dominating factor over matrix hydraulic conductivity during stormflows (Cheng 1988; Sidle et al. 2001), partly because the capillary forces are negated under saturated conditions, but also due to changes in connectivity and a self-organizing capacity in macropore networks, which contributes to increasing flow capacity (Nieber & Sidle 2010; Sidle et al. 2001). Meerveld & Weiler (2008) also found that inclusion of preferential flow in hillslope models gave simulations that more closely matched the observed ranges of maximum depths of saturation.

It has also been demonstrated that the topography of the underlying bedrock, and thus spatial variability of soil depth, may have a significant impact on mobility and mixing of subsurface water (McGlynn et al. 2002). Virtual experiments have been conducted which confirms the importance of soil depth variability (Weiler & McDonnell 2004; Weiler & McDonnell 2006), and this is backed up by a later study in by Meerveld & Weiler (2008), who also found that bedrock leakage also plays a major part in long-term modelling.

In a study of a number of Swiss grassland hill slopes, Scherrer & Naef (2003) designed a decision scheme to indicate the dominant runoff process (DRP), divided between Hortonian overland flow (HOF), saturation overland flow (SOF), subsurface lateral flow (SSF) and deep penetration to groundwater (DP), with subtypes within the three first categories. This scheme combines various characteristics such as vegetation coverage, presence of humus, compaction of matrix, slope, presence of macropores, soil depth and permeability to make a rough estimation of the dominant hydrological flow paths. While the scheme is based on a study of grasslands, it is interesting to see if its validity extends beyond Swiss grasslands to Chinese

forested hillslopes. Based on the scheme, slope, macroporosity, soil depth and permeability seem to be controlling parameters (Figure 1).

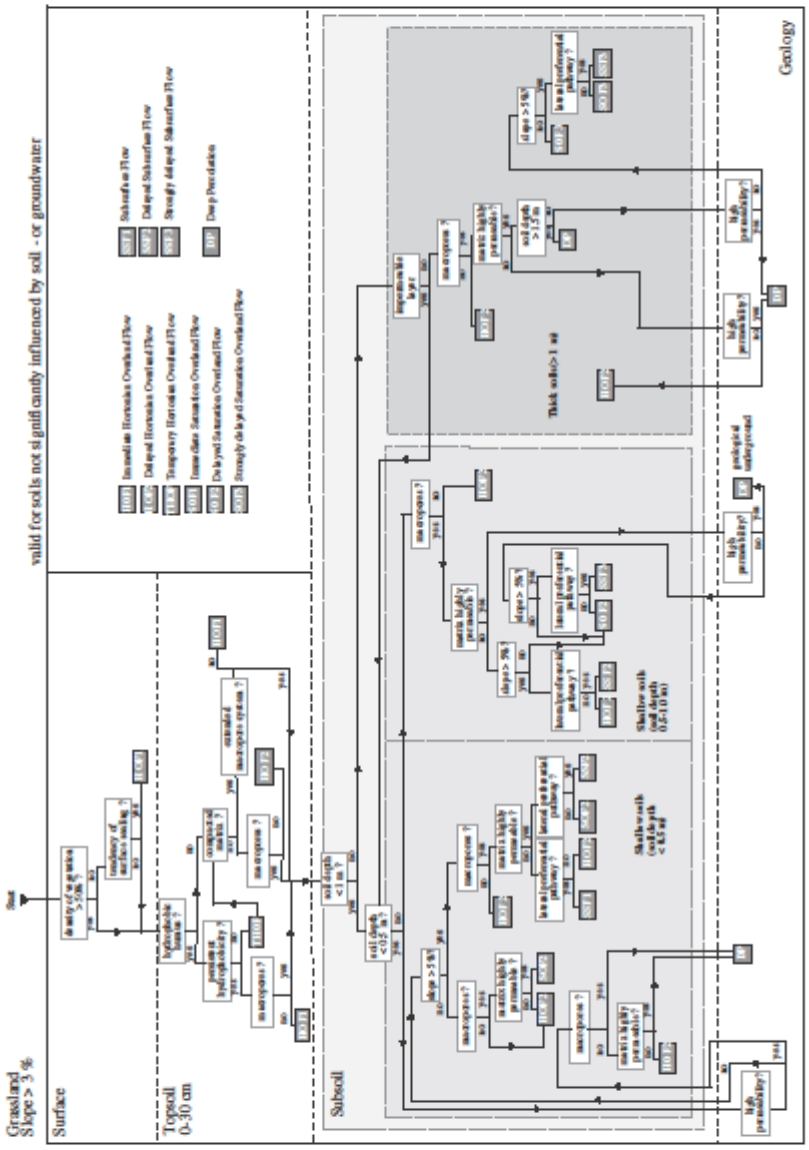

Figure 3. Decision scheme for grassland sites (slope > 3%) to evaluate dominant runoff process at the plot scale

Figure 1. Scherrer and Naef's decision scheme to identify the dominant runoff processes. From the paper "A decision scheme to indicate dominant hydrological flow processes on temperate grassland".

In summary, to understand hill slope hydrology, there are many controlling factors to be taken into account: Traditional Darcian matrix flow; macropore size, distribution and connectivity; soil depth and soil depth variability, slope angle, clay content and subsurface topography, either bedrock topography or topography of underlying soil horizons with significantly lower hydraulic conductivities.

1.2.2 Implications for this study

In order to determine potentials for N_2O production, the most important soil moisture conditions are those occurring at the surface and at the shallow soil horizons where the N_2O productions occurs, as these are the environments where there is both ample organic matter to drive reduction and sufficient nitrate to serve as substrate for denitrification. Therefore, this thesis will primarily be concerned with determining how episode rainwater input into the system is distributed between overland flow (either Hortonian or saturation), lateral subsurface flow over the B horizon and deep percolation to the groundwater zone. This will of course vary with space and time.

Because it has implications for the mixing of old and new water in the soil profile, it is also of interest to establish what the dominant runoff process in the sub-catchment is, specifically how any subsurface flow is generated. If subsurface runoff is primarily generated through saturation from below, there should be sufficient soil water contact between macropores and soil matrix, as well as between soil horizons, to allow for good exchange of water. Conversely, in the case of subsurface flow based on infiltration excess, new soil water does not effectively penetrate to deeper soil horizons, and soil water exchange should be limited (Scherrer & Naef 2003).

1.3 Aims and objectives

The aim of this thesis will be to find out how soil moisture and flow paths responds to spatial variations in soil physical parameters and temporal variations in rainfall, air temperature and other relevant climate drivers.

1.3.1 Objectives

1. To describe the movement of water through a steep hill slope in a dense loam soil dominated by macropores in the TieShanPing subtropical forest catchment for use in predicting hydrological response and soil moisture variability.

2. To obtain hydrologic information which can be used as an explanatory variable for rates of denitrification and N_2O emission on a landscape level.

Both these objectives will be achieved through the following:

1. Soil physical parameter analysis
    a. Soil water retention characteristic (pF curves)
    b. Porosity
    c. Bulk density
    d. Saturated hydraulic conductivity (K_{sat})
2. Data analyses of precipitation, temperature and discharge
3. Qualitative dye tracer experiment
4. Chemical fingerprint analysis

A modelling of the spatial and temporal soil moisture variation was also attempted using the SUTRA model from the USGS. Due to problems encountered both with software and parameterisation, this was aborted, but the experiences are discussed, and recommendations for future attempts are given.

1.3.2 Hypothesis

The initial hypothesis to be tested is that episode precipitation over the hill slope is primarily channelled through the upper 10-25 cm (the AB horizon) of the soil, and there is little Hortonian overland flow and deep percolation to groundwater. This will be tested by the means outlined in the objectives section.

2 Site description, materials and methods

2.1 Site description

2.1.1 Location

The studied sub-catchment is situated in Tie Shan Ping (29°37'N, 106°41'E), in a national protected forest region situated approximately 25 km north-east of downtown Chongqing, People's Republic of China (Figure 2). The sub-catchment area is approximately 4.64 ha in size.

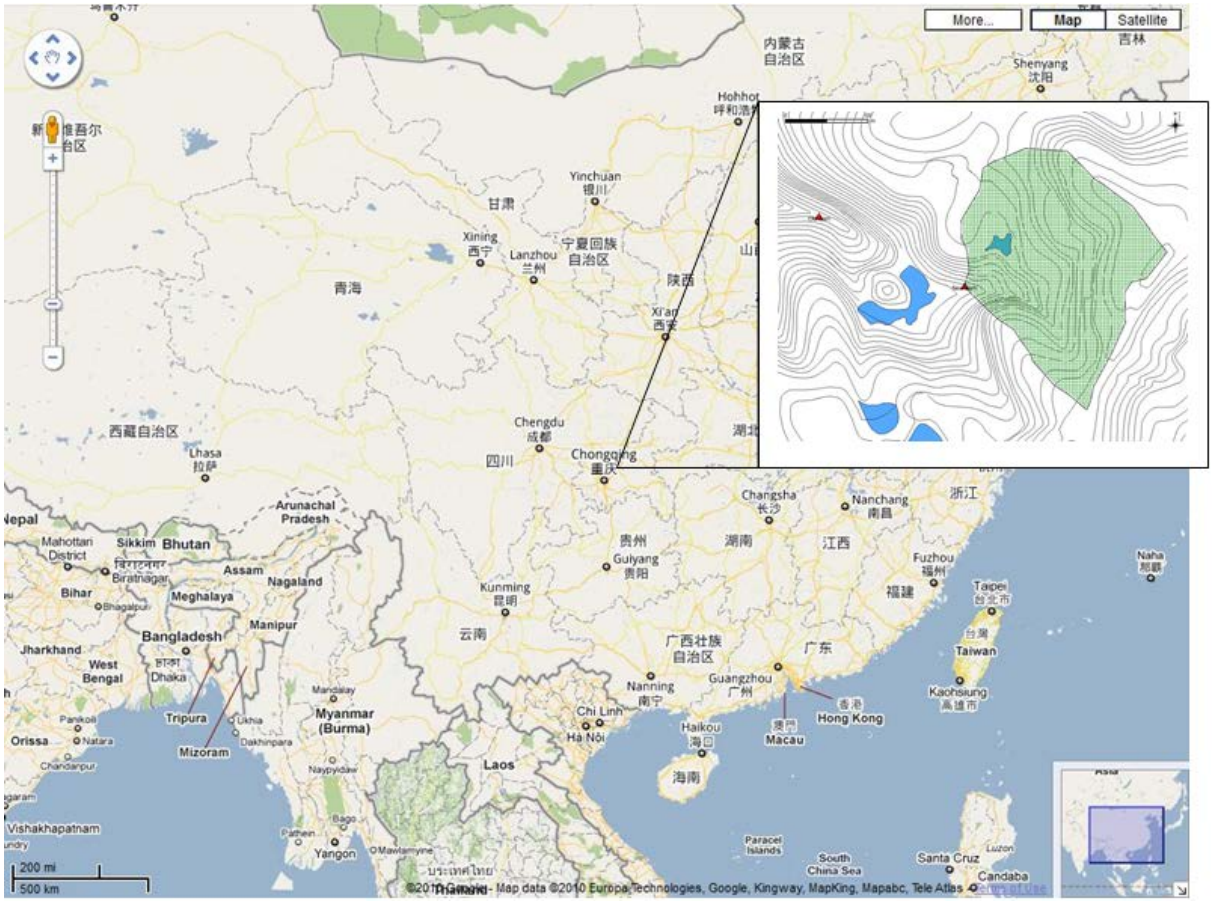

Figure 2. Location of study site in southwest China. Source: Google Maps.

2.1.2 Soil

The dominant soil type is a yellow mountain soil, clay-rich loam classified as a Haplic Acrisol, developed from the sandstone which is the predominant bedrock in the area. The soil in the studied area is characterized by a very thin O horizon (+2–0 cm), which is kept thin due to high biological activity caused by the hot and humid summers. The O/A horizon on average stretches from 0 to 5 cm, AB from 5 to 17 cm, B1 from 17 to 27 cm followed by the B2 horizon. The AB, B1 and B2 horizons are homogenous, but contain at times large and

frequently occurring fragments of regolithic sandstone as well as fragments of brick from human activities. Below this, there is a gradual transition to the C horizon (or R horizon), consisting of regolithic sandstone. Complete soil profile descriptions can be found in the appendix.

2.1.3 Forest ecology

The forest is predominantly a mixture of coniferous and deciduous trees, mostly coniferous, as represented by the Masson pine (*Pinus massoniana*) and Chinese fir (*Cunninghamia spp.*). The deciduous fraction is dominated by species of Rhododendron. The undergrowth consists mainly of ferns. The area is also very rich in insect life, and the soil is home to many invertebrates.

2.1.4 Hydrology

The sub-catchment is a steeply sloped valley, with six or seven terraces in the valley bottom, or groundwater discharge zone (GDZ). These terraces may be remnants of old vegetable gardens, now long since abandoned. The GDZ also slopes quite steeply, in terraces, and drains into a pond just below the study area. The ground water is generally very near the surface in the GDZ, and it forms a wetland with sparse forest vegetation, mainly ferns and shrubs, whereas the hill slopes are quite densely wooded. While the soil itself consists of relatively dense and clayey loam, plant roots and invertebrates form large macropores, increasing soil permeability.

2.1.5 Sampling and measurement sites

Transect T1

Five profiles were excavated on the hill slope along a transect hereafter referred to T1 (Figure 3). The five profiles are referred to as T1-1 through T1-5. In the summer of 2009, the original profiles were excavated for extraction of samples for the water retention curves. These were filled in at the end of the summer to minimise the impact on the natural processes. In summer 2010, five new profiles were excavated to extract soil samples for hydraulic conductivity analysis and grain size distribution. These profiles were dug as close as possible to the original profiles in order to obtain comparable samples, and they are referred to with the same names as the original profiles, T1-1 through T1-5.

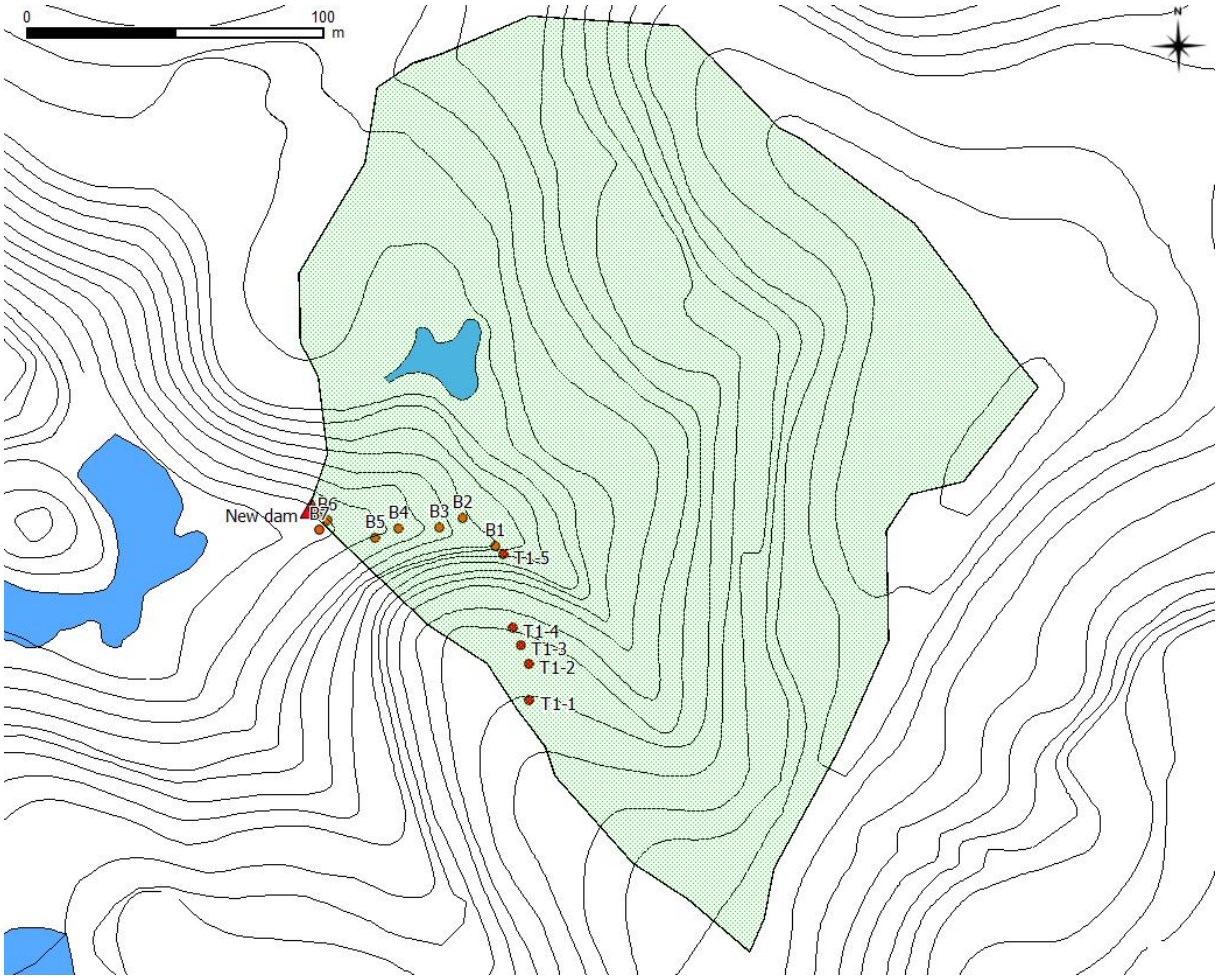

Figure 3. Position of profiles T1-1 through T1-5 and B1 through B7.

Transect B

Another transect, transect B, was established along the flow path of the groundwater discharge zone (GDZ). This transect includes plots B1 through B7, where lysimeters and groundwater piezometers are installed. This transect is used for the chemical analysis of lysimeter water from the GDZ and groundwater level measurements, but does not otherwise play any significant role in this thesis.

2.2 Soil physical and hydrological measurements

2.2.1 Sampling

For pF, porosity and bulk density

To determine the soil water retention characteristic, porosity and bulk density in the soils of the hill slope, soil samples were taken in 100 cc (h = 37.5 mm, r = 29.5 mm) steel cylinders from each of the five profiles, at four different depths; 3.5–7.2 cm, 10–13,7 cm, 25–28,7 cm

and 50–53,7 cm[1]. These depths (hereafter termed 3.5, 10. 25 and 50 cm, respectively) correspond to the O/A, AB, B1 and B2 horizons respectively in profiles. Triplicate samples were taken for each depth. The samples were taken back to UMB for analysis at the laboratory for soil physics.

For hydraulic conductivity and grain size distribution

Hillslope:

In each profile, three horizontal and three vertical samples were taken from the AB horizon and three from below the AB horizon. In profile T1-1 only two vertical samples could be taken from the lower horizons and in T1-4 only the horizontal samples were taken from the lower horizons; frequent rock fragments preventing the extraction of more undisturbed samples.

Groundwater discharge zone:

A few samples were taken from the B2 (0-3.75 cm) and B3 (0-3.75 cm, 6-9.75 cm and 12-15.75 cm) sites for comparison with the hill slope samples. A pumping test was attempted, but was aborted due to lack of time and equipment.

2.2.2 The soil water retention characteristic

Procedure

The samples were analysed for water retention potential at seven different negative pressures; -10 cm, -50 cm, -100 cm, -500 cm, -1000 cm, -3000 cm and -15000 cm. The -10 and -50 cm pressures were carried out in a sandbox setup from Eijkelkamp Agrisearch, and the remaining pressures were carried out in 5 bar (-100, -500, -1000 and -3000 cm) and 15 bar (-15000 cm) ceramic plate extractors from Soilmoisture Equipment, California.

Up to -1000 cm, the samples were still in their original cylinders during pF determination (undisturbed samples), and for -3000 cm and -15000 cm, the samples were dried, broken up, sieved and placed into small plastic rings for the pF determination (disturbed samples). Due to uncertainty as to whether the undisturbed soil in the cylinders had sufficient contact with the ceramic plates for accurate pF determination at stronger negative pressures, additional tests on the -500 cm and -1000 cm pressures were performed with disturbed samples in plastic rings for comparison.

[1] Due to thinner soil layer at profile T1-4, samples were not taken at 50 cm on this site. In T1-5, the lowest samples were collected at 40 cm.

Experimental setup

Sandbox

In the sandbox setup, the cylinders are placed on a layer of fine sand inside a box with an adjustable hanging water column. The bottoms of the cylinders are covered with a fine cloth to prevent soil escaping from the cylinders during the weighings. The hanging water column is adjusted to create an pressure of -10 cm and -50 cm, respectively. For detailed explanations on setup and procedure, see section on pF determination in Reeuwijk (2002).

5 bar ceramic plate extractor

The pressures of -500, -1000 and -3000 cm were performed in a 5 bar ceramic plate extractor from Soilmoisture Equipment, California. The -100 cm pressure was performed using 1 bar ceramic plates and connecting the extractor to a 100 cm water column, creating a -100 cm pressure in the extractor. The -500 cm to -1000 cm pressures were performed using 1 bar ceramic plates and connecting the extractor to a compressed-air system. The -3000 cm pressure was performed using 5 bar ceramic plates. The -100 cm to -1000 cm pressures were performed on undisturbed samples in original cylinders, and the -3000 cm test was performed using disturbed samples in plastic rings. In addition, a second test was performed on -500 cm and -1000 cm using disturbed samples in plastic rings.

15 bar ceramic plate extractor

The -15000 cm pressure was carried out in a 15 bar ceramic plate extractor from Soilmoisture Equipment, California, with disturbed samples in plastic rings.

Procedure using disturbed samples in plastic rings

For the alternative run of -500 and -1000 cm as well as the -3000 and -15000 cm pressures, the samples were taken out of their original sample cylinders, finely ground and placed in plastic rings in the ceramic bars in order to ensure that the soil had sufficient contact with the ceramic plate. As the structure of the soil is destroyed in this process, this could be expected to influence the water retention characteristic. However, at strong pressures of -3000 cm and more, soil structure is expected to have little influence on soil water retention, as the macropores should be emptied at pressures far below these (Børresen 2009).

Details on the analysis procedure are described in Reeuwijk (2002).

Calculations

For all samples, soil water content is calculated as described in Reeuwijk (2002):

First, the weight percentage of water is calculated using the following formula:

$$\theta_w = \frac{M_{net\ pressure} - M_{net\ dry}}{M_{net\ dry}} \times 100\%,$$

Where θ_w is weight percentage of water in the sample (%), $M_{net\ pressure}$ is the net mass of the sample after each individual pressure (g) and $M_{net\ dry}$ is the net dry mass of the sample (g).

Volumetric soil moisture (%) is then obtained by multiplying the weight percentage with bulk density:

$$\theta_v = \theta_w \times \rho_b,$$

Where θ_v is the volumetric water content of the sample (%),θ_w is weight percentage of water in the sample (%) and ρ_b is the bulk density of the sample (g/cm^3).

Van Genuchten parameter calculation

The soil water retention curve can be characterized by the van Genuchten model, as expressed in the following equation:

$$\theta(h) = \theta_r + \frac{\theta_s - \theta_r}{\left[1 + (\alpha|h|)^n\right]^{1-1/n}}$$

where

$\theta(h)$ is the volumetric water content as a function of soil suction [$L^3\ L^{-3}$];

$|h|$ is the negative pressure ([L^{-1}] or cm of water);

θ_s is the volumetric water content at saturation [$L^3\ L^{-3}$];

θ_r is the residual volumetric water content [$L^3\ L^{-3}$];

α is related to the inverse of the air entry suction, $\alpha > 0$ [L^{-1}] and

n is a measure of the pore size distribution [-].

The α and n parameters are obtained through parameter optimisation by curve fitting. The van Genuchten model was used to express the water retention curve in a form that can be used to parameterize the SUTRA model.

2.2.3 Bulk density and porosity

The values for porosity and bulk density were obtained from the soil water retention characteristic. Bulk density (ρ_b) is expressed in mass per volume, e.g. g/cm^3, kg/dm^3 or mg/m^3, and was calculated using the following formula:

$$\rho_b = \frac{M_{dry}}{V_{sample}},$$

where M_{dry} is the dry mass of the soil (g) and V_{sample} is the volume of the soil sample (cm^3).

Porosity (ϕ) is normally expressed as a fraction and is defined as the volume of pores divided by the total volume of the sample. The pore volume is found by weighing a water saturated sample, then drying the sample for 24 hours at 105 °C and weighing the dry sample. Porosity is then calculated using the following formula:

$$\phi = \frac{M_{saturated} - M_{dry}}{V_{sample}},$$

where $M_{saturated}$ is the mass of the saturated sample (g), and M_{dry} is the dry mass of the sample (g). For simplicity, porosity will be expressed as a percentage in the presentation of results.

Obtaining porosity using particle density

Due to a fault in the sandbox measuring equipment, the $M_{saturated}$ value was not recorded for some of the samples. For these, porosity was calculated using bulk density (ρ_b) and particle density (ρ_p) in the formula

$$\phi = (1 - \frac{\rho_b}{\rho_p})$$

where ρ_p was determined through water pycnometer analysis as described in Børresen & Haugen (2003). This procedure is based on the procedure outlined by Blake & Hartge (1986).

2.2.4 Soil texture (grain size distribution)

Sampling

The soil texture was determined from a selection of the samples used in the determination of the saturated hydraulic conductivity. See page 17 for details on sampling.

Pre-treatment

The soil was first passed through a 2 mm sieve to separate the gravel fraction and coarse roots from the fine earth. Afterwards, the <2 mm fractions were analysed using the pipette method as described in Krogstad *et al.*, (1991) and Rutsinda (2010). However, since we included an extra treatment to remove iron oxides, a brief description of the procedure follows below.

Each sample was pre-treated in series of 10 samples, which were further divided into seven fractions using the pipette method:

Particle size (mm)	Fraction
< 0.002	Clay
0.002 – 0.006	Fine silt
0.006 – 0.020	Medium silt
0.020 – 0.063	Coarse silt
0.063 – 0.200	Fine sand
0.2 – 0.600	Medium sand
0.6 – 2.000	Coarse sand

Approximately 10 g of soil was weighed into 800 ml labelled beakers, and the soil was then stirred and dispersed in 20 ml of deionised water. To each beaker 10 to 30 ml of 35 % hydrogen peroxide (H_2O_2) was added in order to oxidise any organic material. The beakers were covered with watch glasses to prevent desiccation and left overnight to react. The next morning the beakers were placed on an adjustable hot plate and heated to around 90 °C until no more reactions were visible. The beakers were then filled with water up to the 200 ml mark and evaporated to 90 ml at 90 °C without watch glasses. Soil stuck on the beaker walls was flushed with deionised water.

As these soils are relatively rich in iron oxides, the soils were deferrated using sodium dithionite (Reeuwijk 2002). 200 ml of buffer solution of 0.3 M sodium citrate (Na-citrate.$2H_2O$) and 0.1 M sodium bicarbonate ($NaHCO_3$) was added to the beakers and heated to 75 °C. For each beaker, approximately 1 g sodium dithionite was added, and the solution was then stirred continuously for 1 minute and then occasionally for 5 minutes. Sodium dithionite was added again until any reddish colour had disappeared, maximum three times in total. The samples were allowed to settle completely and the supernatant was then siphoned off. Next, the samples were stirred for 1 minute with 500 ml 1 M NaCl, allowed to settle overnight and the supernatant then siphoned off.

Next, 10 ml 2 M HCl was added to remove any carbonates. The samples are stirred for 1 minute and filled to the 800 ml mark with deionised water, allowed to settle overnight and the supernatant siphoned off. The samples are then again filled with deionised water, allowed to settle overnight and the supernatant siphoned off.

To ensure proper dispersion, 50 ml 0.05 sodium pyrophosphate ($Na_4P_2O_7$) were added to the samples, which were then stirred with an electrical stirrer for 1 minute. The suspension was left overnight to disperse and then transferred to cylinders where deionised water was added to make 400 ml of suspension. The suspension was then covered with watch glasses and left for a few hours until the water temperature stabilised at 21 °C.

Analysis

For each sample, seven small beakers were weighed and placed on an aluminium tray. The four smallest fractions were separated using the pipette method, where an equal volume of suspension is pipetted at specified distances from the surface at the times specified below:

Particle size (mm)	Fraction	Distance from surface (cm)	Time after stirring (21 °C)
< 0.002	Clay	15	45 sec
0.002 – 0.006	Fine silt	4	1 min 49 sec
0.006 – 0.020	Medium silt	4	20 min 10 sec
0.020 – 0.063	Coarse silt	4	3 hrs 1 min

Sedimentation speed (v) is determined using Stoke's law:

$$v = \frac{(\mu_s - \mu_w)}{18\omega} g d_e^2,$$

where d_e equals effective particle diameter (m), ω equals the viscosity of the water (N s/m^2), μ_s equals particle density (kg/m^3), μ_w equals the density of water (kg/m^3) and g equals gravitational acceleration (m/s^2).

The correlation between particle size, sedimentation length and sedimentation time is determined by the following equation:

$$d_e = 1.054 \times 10^{-2} \sqrt{\frac{h}{t}},$$

where h equals sedimentation distance in cm, t equals sedimentation time in seconds, and d_e equals particle diameter in cm (Krogstad et al. 1991).

After pipetting, the remainder of the suspension was washed through sieves with apertures of 600, 212 and 63 μm to separate the coarse sand, medium sand and fine sand fractions, respectively, and each fraction transferred flushed into the final three small beakers using deionised water from a small squirting bottle.

The small beakers were then dried at 105 °C overnight, left to cool sufficiently for handling and then weighed to a precision of 3 decimal places. The volume percentages were then calculated automatically through computer software connected to the electronic scales (Krogstad *et al.* 1991).

2.2.5 Saturated hydraulic conductivity (K_{sat})

Saturated hydraulic conductivity (K_{sat}) is an important and highly sensitive parameter in modelling water flow. Since we are interested to see if there is a significant difference between the upper soil horizons (primarily AB, as the O/A horizon in most places was too thin to sample) and the lower B horizons, six samples, three vertical and three horizontal, were taken at the AB horizon, collectively termed "upper", and six more at the B1 and B2 horizons collectively termed "lower" in later analyses.

Procedure

Experimental setup

The samples were analysed for hydraulic conductivity using a constant-head setup, as described by Stolte (1997). The setup was constructed in TieShanPing using mostly materials at hand, as well as some fittings brought from Norway.

The lack of running water and drain in the local laboratory precluded the use of a constant water supply with overflow and necessitated the construction of a closed system. A Mariotte system was constructed using a 5 l plastic water flask with an airtight stopper through which a water supply hose ran to a level observation beaker (Figure 4). From this beaker, four individual water hoses were connected to extension rings attached to the top of the sample cylinders using rubber sealings. An air pipe through the airtight stopper down into the water in the 5 l water flask made it possible to adjust the constant head level to the desired position (my thanks to Jannes Stolte for this design suggestion).

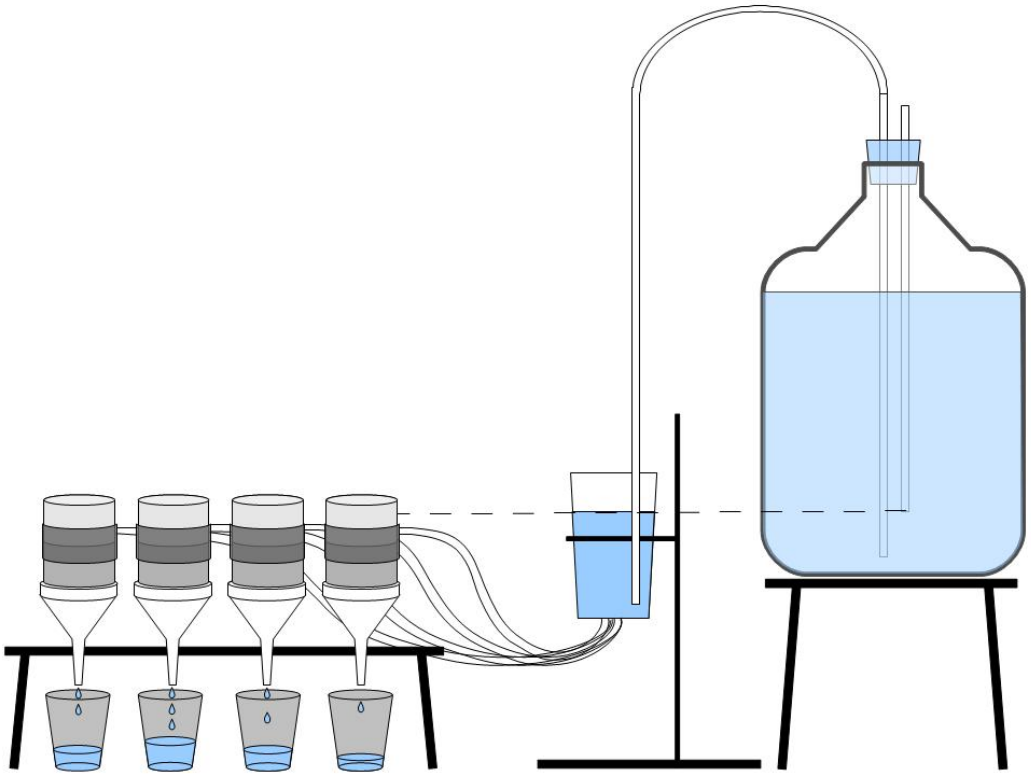

Figure 4. Home-made constant-head permeameter used in the field laboratory in TieShanPing. Dotted line shows the constant-head level.

The hydraulic conductivity was determined by collecting the water that ran through the samples, recording the time before a certain amount of water was collected and finally weighing the water and the collectors on an electronic scale with two decimals. The soil samples had a fixed length of 51 mm, and the water height was measured individually on each sample at the start of each run. The K_{sat} was then calculated using Darcy's equation:

$$K_{sat} = \frac{QL}{Ah},$$

Where Q (ml/sec) is the volume of water collected in the collection cups at the end of a run (ml), divided by the time (seconds) it took to collect it ($Q = \frac{V}{t}$), L is the length of the soil sample (cm), A is the sample area (cm^2) and h is the head (cm), i.e. the length of the soil sample plus the height of water on top of the sample.

2.3 Dye tracer experiment

In order to get visual, qualitative support for major flow paths of water, a dye tracer experiment was conducted at two sites at elevations corresponding to the T1-1 and T1-5

profiles, some 20 metres away from these. At these sites, a dye tracer was applied in two applications and the sites were later irrigated with fresh dye-free water to drive the tracer through the soil.

2.3.1 Procedure

At both sites, a 1 m x 1 m square relatively free of plant growth was outlined and cleared of debris and remaining vegetation. The squares were both slightly sloped, T1-1 at around 15 % and T1-5 at around 10 %. Dye tracer at a concentration of 4 g Brilliant Blue per litre was applied to the lower half of the square in two applications: First, two litres were applied, and ten minutes later, three more litres were applied to the same 0.5 m^2. This corresponds to 10 mm of precipitation.

Approximately ten minutes after dye application, the entire square metre was irrigated, first two times 8 litres at about 15-25 minutes' intervals, and later two applications of 32 litres each around three and five hours later, respectively. Thus, in addition to the tracer application, the plots were irrigated with 80 litres of water, the equivalent of 80 mm of precipitation over a period of approximately six hours. While this is a sizable episode, episodes of this intensity are relatively common in the area (see precipitation data in appendix; three equally large or larger episodes occurred in the monitoring period). The plots were excavated the following day and photographed at different stages of excavation for future visual analysis of dye penetration and distribution. Soil temperature, volumetric water content and electrical conductivity of the moist soil were measured before dye application, after irrigation and just before excavation using a portable TDR probe (Hydraprobe SDI-12, analogue) equipped with a Hydra Data Reader.

2.4 Data analysis of climate, discharge and soil moisture data

As a means of quantifying the water fluxes and the relative distribution of water on its way through the sub-catchment, various parameters were calculated based on climate, discharge and soil moisture data. TDR probes (Decagon 10HS) with loggers (Campbell CR200 Data logger) were installed at both T1-3 plot in the hill slope as well as in the B1 plot at the transition between the hill slope and the groundwater discharge zone. The weather station used to collect climate data is a WeatherHawk 232 (WeatherHawk 2011).

Collected data for precipitation, discharge and soil moisture were analysed with respect to runoff coefficient, infiltration and infiltration partitioning over different episodes. The data were also correlated with temperature, relative air humidity and antecedent soil moisture.

The analyses for soil moisture are based on the TDR measurements for the T1-3 plot, as this site is typical of the hill slope soil and does not receive as much water from higher up the slope as the B1 plot. Thus we expect it to take longer time before soil moisture returns to pre-episode conditions at the B1 plot.

In hydrological studies, episodes are specific hydrological events which supply information on the characteristics and behaviour of a catchment. An episode was defined as starting with the first rainfall and lasting until measured values for discharge and/or soil moisture were back to pre-episode levels, or until the start of the next episodic rainfall.

As the groundwater discharge zone stored a significant amount of precipitation water and therefore buffered discharge response at low to moderate precipitation rates, all episodes where daily rainfall exceeded 20 mm were identified, and at seven of these episodes there were reliable data for analysis. Equipment malfunction of TDR sensors and water height sensors at the stream precluded the use of any remaining episodes.

The following parameters were calculated:

$$C_r = \frac{Q}{P}$$

where C_r = runoff coefficient [fraction], Q = discharge [mm] and P = precipitation [mm],

ΔS, or change in soil water storage, was calculated using measured soil moisture values at T1-3 at 10 cm, 20 cm and 40 cm depths and applied to reasonable depth ranges, where the 10 cm values were applied to the 0-15 cm (thickness = 0.15 m) range, the 20 cm values to the 15-30 cm (thickness = 0.15 m) range and the 40 cm values to the 30-50 cm (thickness = 0.2 m) range. It was assumed that there was no significant change in soil water storage below the 50 cm depth. The ΔS was then calculated as follows:

$$\Delta S = (\theta_{\max} - \theta_{start}) * M * 1000\ mm$$

where θ = volumetric soil moisture [m^3/m^3] and M = thickness of the depth range to which the soil moisture measurement is applied [m].

In addition, the precipitation intensity was calculated, measured in mm/hour.

As a measure of the partitioning of the increase in soil water storage in the various soil layers in response to precipitation, the following equation was used:

$$I_d = \frac{\Delta S_d}{\Delta S} * 100$$

where I_d = percentage of changed water storage occurring in depth range d, ΔS_d = change in soil water storage at depth range d and ΔS = sum of change in soil water storage at all depths.

Traditionally, saturation is calculated as soil water content obtained from field measurements as a percentage of total pore space obtained from soil physical analysis, as expressed in the following equation:

$$Sat = \frac{\theta}{\phi} * 100\ \%,$$

where Sat = saturation [%], θ = soil water content [cm^3/cm^3], and ϕ = total pore space [%]. However, in dense, clayey soils a significant proportion part of the total pore space is capillary and is not easily drained, and only to a limited degree participates in the water transport. Comparing water content with total porosity in such soils may make it appear that there is very little variability in saturation, and it may make more sense to relate saturation to the *drainable* porosity (ϕ_D), which can be defined as the pore space which is emptied of water when the soil is drained to field capacity (pF 2), which is also obtained from soil physical analysis:

$$\phi_D = \phi - \theta_{fc},$$

where ϕ_D = drainable porosity [%], ϕ = total porosity [%] and θ_{fc} = soil water content at field capacity [cm^3/cm^3] .

Drainable saturation can then be defined as follows:

$$Sat_D = \frac{\theta - \theta_{fc}}{\phi_D} * 100\ \%,$$

where Sat_D = drainable saturation [%], θ = soil water content [cm^3/cm^3], θ_{fc} = soil water content at field capacity [cm^3/cm^3] and ϕ_D = drainable porosity [%].

As an additional parameter, it may be interesting to relate the laboratory obtained porosity and saturation to the range of actual soil moisture variability, and which may be termed *active* porosity. This active porosity is obtained purely from field TDR measurements and is the difference between observed minimum and maximum soil water content:

$$\phi_A = \theta_{max} - \theta_{min},$$

where ϕ_A = active porosity [%], θ_{max} = maximum observed soil moisture [cm^3/cm^3] and θ_{min} = minimum observed soil moisture [cm^3/cm^3].

The active saturation may then be defined as:

$$Sat_A = \frac{(\theta - \theta_{\min})}{\phi_A} * 100\,\%,$$

where Sat_A = active saturation [%], observed soil water content [cm^3/cm^3], θ_{min} = minimum observed soil moisture [cm^3/cm^3], and ϕ_A = active porosity [%].

In order to establish how subsurface runoff is generated, either as saturation subsurface runoff (corresponding to Scherrer & Naef's (2003) SSF2) or as infiltration excess subsurface runoff (corresponding to SSF1), elapsed time from initial precipitation until soil moisture response at the 10 cm, 20 cm and 40 cm depths were also calculated. In addition, to establish the degree of saturation at a given depth at the time of first soil water response in the horizon above, drainable (Sat_D) and active (Sat_A) saturation for these depths and times.

2.5 Chemical fingerprint analysis of water samples

The samples for chemical analyses were collected by Zhu Jing and the Chongqing Institute of Environmental Science in the 2009 and 2010 season and analysed primarily at the Institute in Chongqing. All data are courtesy of Zhu Jing. Soil water sample depths are labelled 1-4, where 1 = 5 cm, 2 = 10 cm, 3 = 20 cm and 4 = 40 cm. Average pH, NO_3^- and NH_4^+ concentrations in soil water are drawn from the IMPACTS project (IMPACTS 2004).

Ideally, chemical data should be available on the same temporal resolution as soil moisture and precipitation. Since data of this resolution is not available and indeed would be extremely costly, and very few episodes have been sampled, the data have instead been analysed on a longer time scale with an emphasis on seasonal variation.

All data analyses were carried out with respect to three seasons: the dry season, with little rainfall and discharge, lasting from November through March; early summer, with more regular precipitation, from April through June; and late summer, with more variable rainfall, heavier episodes, lasting from July through October.

In addition to being plotted over time, concentrations of NO_3^-, NH_4^+ as well as pH were viewed by season, NO_3^- and NH_4^+ were correlated with discharge, minimum and maximum concentrations were also viewed over the three seasons, and finally, average stream and soil water concentrations were compared with input chemistry from canopy throughfall and litter layer data.

2.6 Modelling

One of the goals of the investigation was to parameterise a 2D SUTRA model from U.S. Geological Survey (USGS 2010b; Voss & Provost 2002), with subsequent simulation of soil moisture variability according to real precipitation data. The parameterisation is based on porosity, permeability and unsaturated properties (van Genuchten parameters) and the driver data consists of precipitation data and evapotranspiration data. The van Genuchten parameters were obtained from soil water retention analysis using the Appia software, which is again based on the RETC for Windows software (van Genuchten 1992). The SUTRA version was a modified version of SUTRA 2.1, adapted by Toon Leijnse (version 4) to enable time-dependent input of driver data as well as spatially variable van Genuchten parameters (Leijnse 2009).

The model was run using the SutraGUI graphical user interface, version 2.1 (USGS 2010a) run in an ArgusONE environment (Argus Holdings 2010).

3 Results

3.1 Soil physical and hydrological parameters

Please note that for statistical analysis of the soil physical parameters, the results from the 40 cm sampling depth in T1-5 is grouped with the results from 50 cm in the other profiles. Due to thinner soil layer and frequent occurrences of fragmented rock in T1-4, it was impossible to sample below the 25 cm depth.

3.1.1 The soil water retention characteristic (pF curve)

The complete soil water retention characteristic data can be viewed in the appendix.

The pF curves show a general trend towards less steep curves at shallower depths, with higher volumetric soil water content (θ) at saturation (θs) and a lower residual water content at the highest suctions (θr), in the upper soil layers. Steeper curves, with a smaller difference between θs and θr are found in the lower horizons (Figure 5).

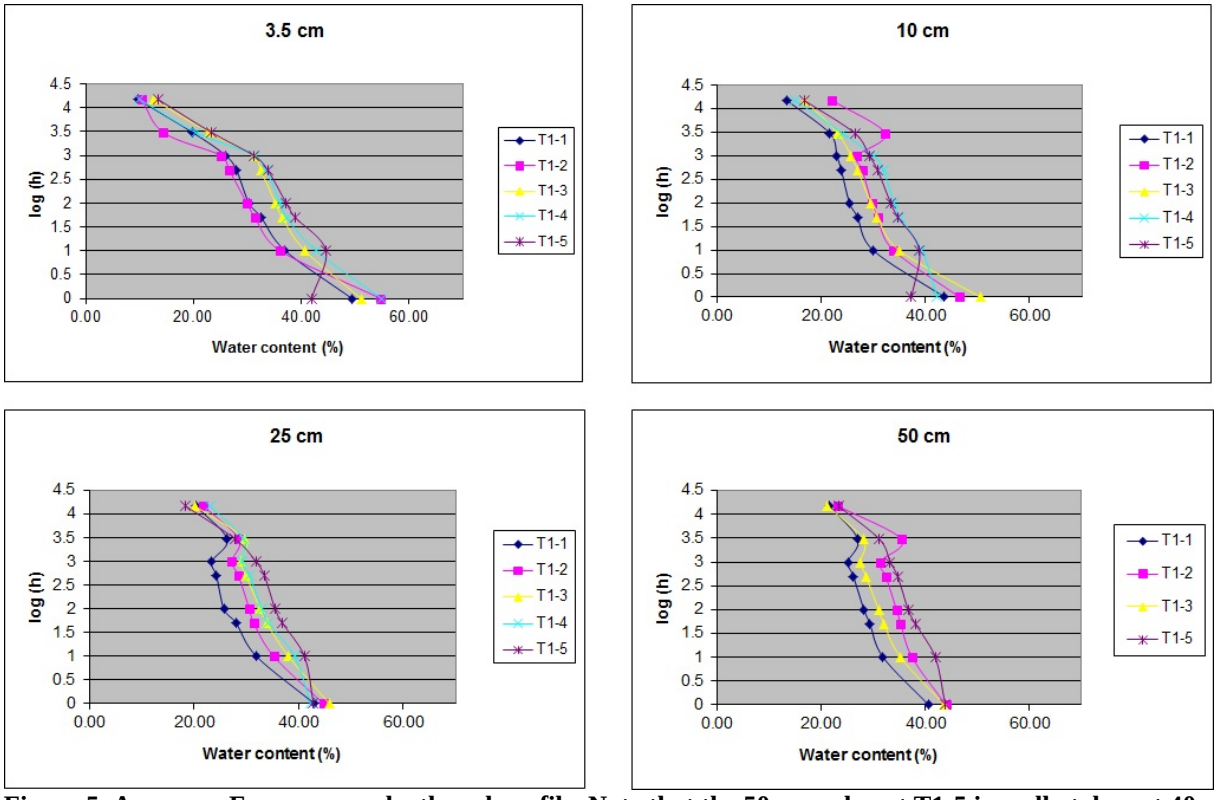

Figure 5. Average pF curves per depth and profile. Note that the 50 cm value at T1-5 is really taken at 40 cm depth due to thinner soil layer.

When we substitute disturbed samples at pressures -500 cm and -1000 cm for the undisturbed samples, we see that soil water content suddenly increases dramatically at pF 2.7 (-500 cm) (Figure 6) for the 10 cm to 50 cm depths.

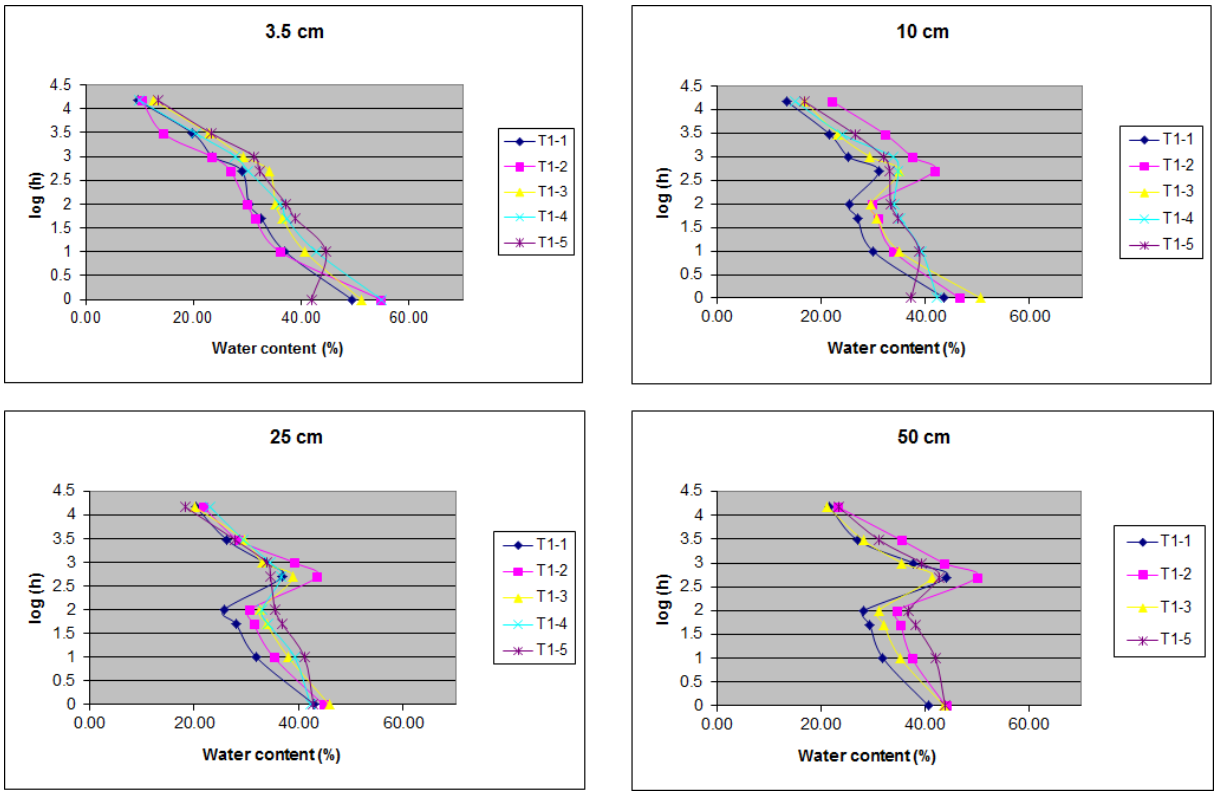

Figure 6. Average pF curves per depth and profile using disturbed samples at pressures -500 cm and -1000 cm.

The data from the pF curves was input into the Appia software to produce curves. An example of an output curve is shown below (Figure 7). All calculated curves can be viewed in the appendix.

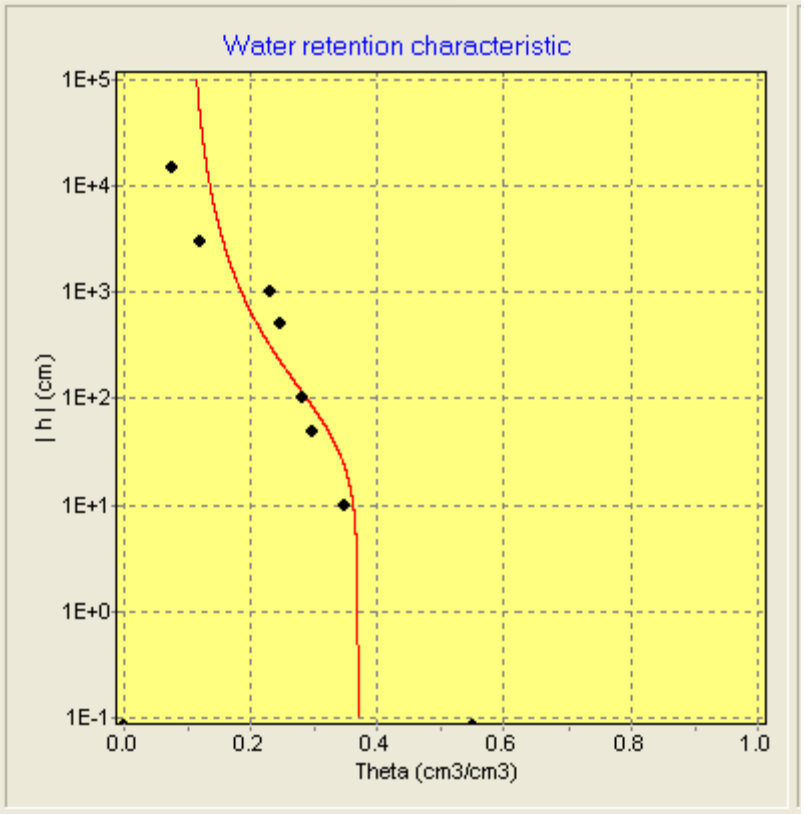

Figure 7. pF curve for T1-2, 3.5 cm. Theta-R = 0.1, Theta-S = 0.37, alpha = 0.02, n = 1.381, l = 0.5, m = 0.276. Note that Theta-S (saturation water content) needed to be adjusted from a real value of 0.553 to 0.37 to fit the curve.

Sources of error

Sampling

Due to very dry conditions during sampling, it was difficult to get smooth samples which gave good contact with the ceramic plates during analysis. As a result, the analysis results from the lower suctions with undisturbed samples may display too high theta (volumetric soil moisture content) values because of lack of contact (Bittelli & Flury 2009). Despite the fact that sample containers were capped to minimise evaporation, lack of cooling facilities in the field may have caused some drying and cracking during storage, generating preferential flow paths and leading to underestimation of the soil moisture content at strong negative pressures, particularly at field capacity (pF 2) by effectively increasing the macropore fraction. This may have an impact on both the pF curves and the van Genuchten parameters calculated from the pF curves.

Analysis

Due to technical problems, saturation was not measured on the T1-4 and T1-5 samples. These values were calculated using the water pycnometer method. Interestingly, the saturation

values for these samples yielded pF curves which were more in tune with ideal curves than the measured values, which gave significantly higher saturation values. However, it may appear that water pycnometer saturation values are incorrect, particularly for the 3.5 cm and 10 cm depths. It is unlikely that this is due to process or measurement errors, since the error is most pronounced for the 3.5 cm and 10 cm depths. It is more likely caused by the fact that some of the organic matter fraction may be displaced and removed from the pycnometer during vacuum extraction, and this will result in an underestimation of the particle density in soils with higher organic content. We do see a more reasonable fit with depth, where there is also less organic matter. If we compare both the calculated particle densities (from saturation) with the measured particle densities (from the water pycnometer method), we find that the average particle density derived from the saturation values (2.6 g/cm^3) correspond more closely to the standard particle density of 2.65 than the average measured particle density (2.47 g/cm^3). Compared to standard particle density, the pycnometer calculated values underestimate total porosity by an average of 2.6 % per cent porosity with a 95 % confidence interval range from 2.04 to 3.26.

3.1.2 Bulk density (ρ_b)

Figure 8 and Figure 9 show selected statistics for bulk density. Bulk density generally increases with depth, with a significant difference ($p = 0.000$) between the 3.5 cm depth and the greater depths.

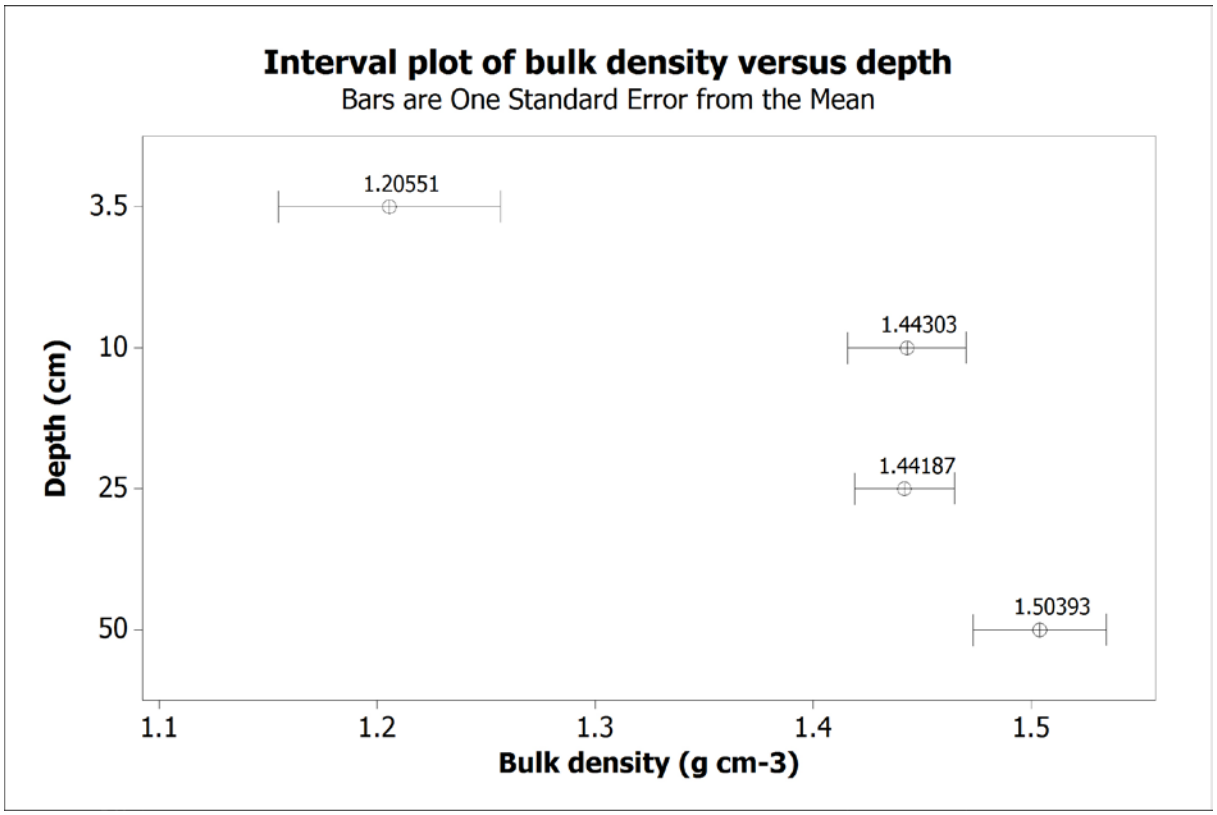

Figure 8. Interval plot of bulk density (g cm-3) versus depth (cm) across all profiles T1-1 through T1-5.

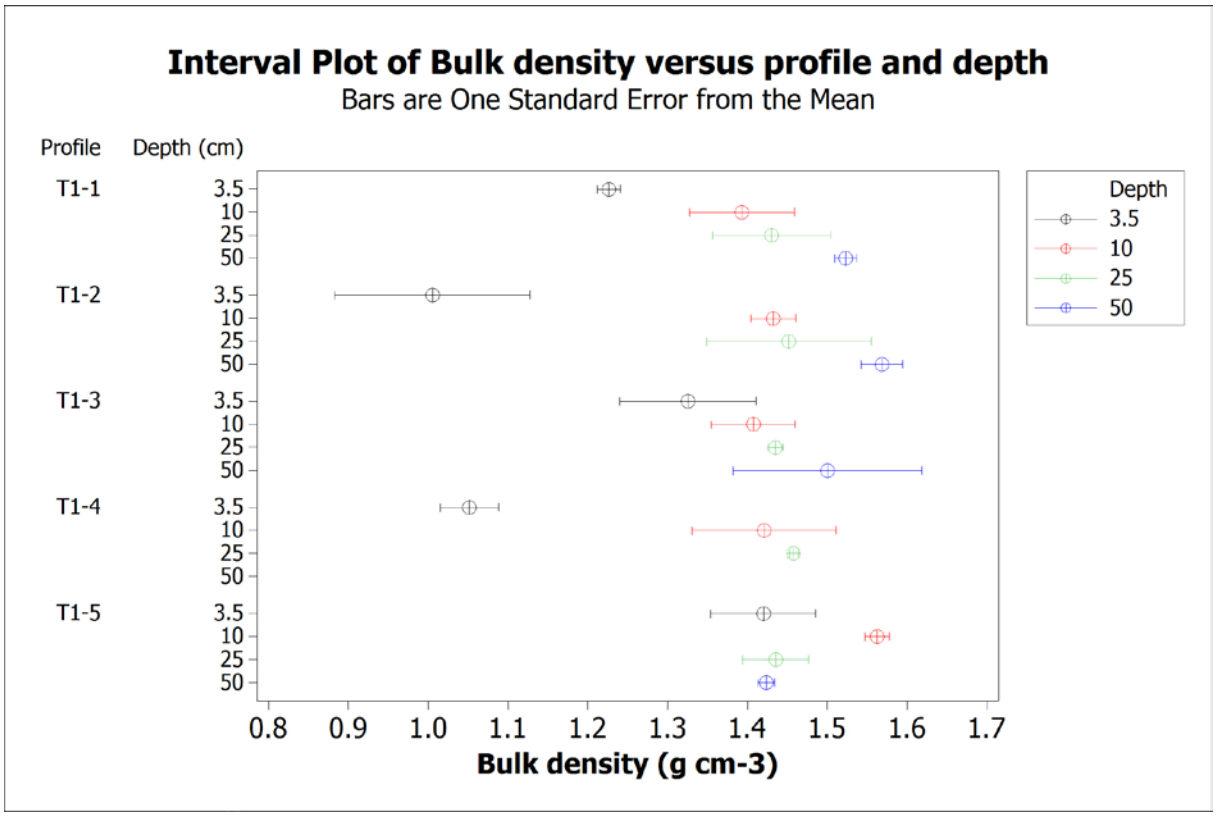

Figure 9. Interval plot of bulk density (g cm-3) versus profile and depth (cm).

3.1.3 Porosity (ϕ)

Figure 10, Figure 11 and Figure 12 show selected statistics for porosity. Porosity generally decreases with depth, with a significant (p = 0.000) difference between the 3.5 cm depth and the lower depths.

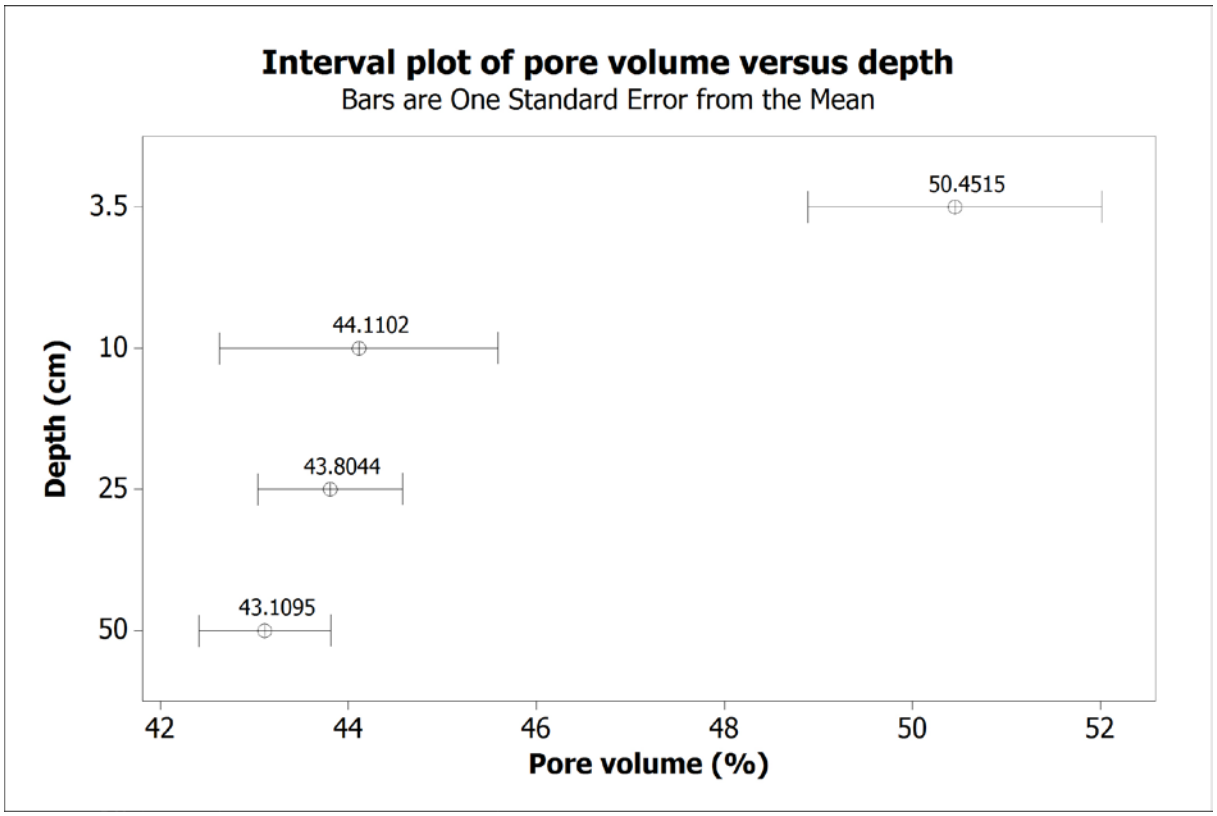

Figure 10. Interval plot of porosity (%) versus depth (cm) across all profiles T1-1 through T1-5.

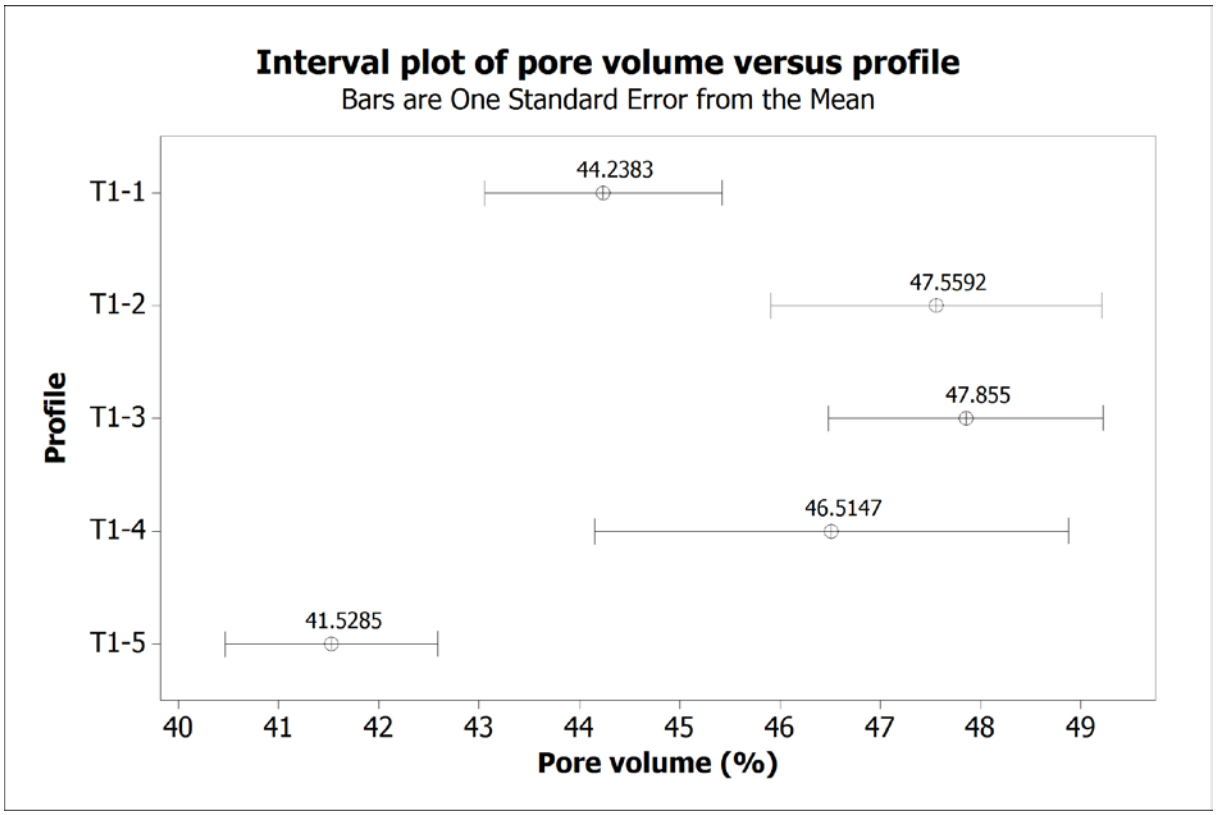

Figure 11. Interval plot of porosity (%) versus profile.

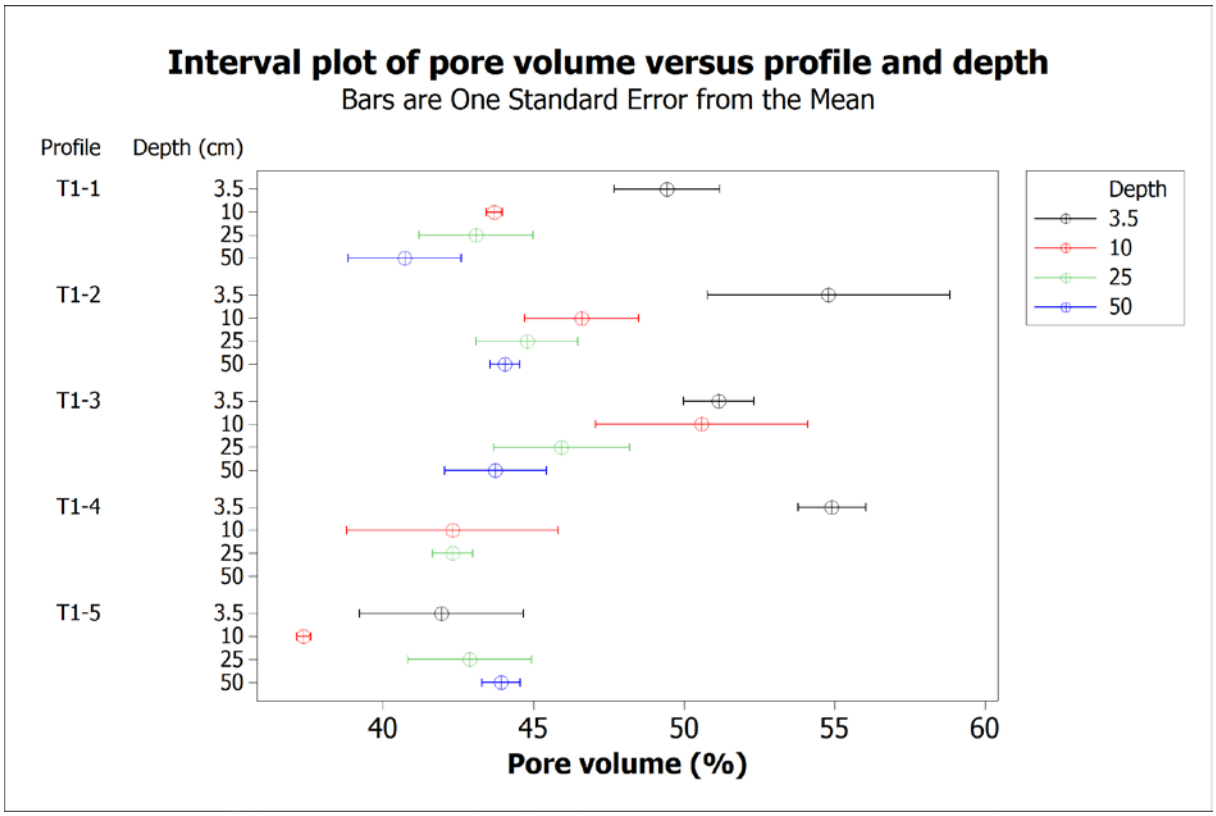

Figure 12. Interval plot of porosity (%) versus profile and depth (cm).

3.1.4 Grain size distribution (texture analysis)

Results of the texture analysis are shown below for only the fine earth fraction (Table 1) and including the > 2 mm fraction (Table 2). Profiles T1-2 to T1-4 have a somewhat higher clay content than T1-1 and T1-5, and T1-3 is the only profile where the clay content changes enough to change soil texture definition from the upper to the lower horizons.

Table 1. Soil texture for the fine earth fraction. Samples in grey are from the groundwater discharge zone below the T1 transect.

Percentage excluding > 2 mm fraction						
Sample profile	Depth (cm)	Horizon	Clay	Silt	Sand	Soil type
T1-1	4 - 7.75	AB	22.8	61.4	15.8	Silt loam
T1-1	24 - 27.75	B1/B2	19.6	50.3	30.1	Silt loam
T1-2	10 - 13.75	AB	36.2	52.5	11.4	Silty clay loam
T1-2	34 - 37.75	B2	28.5	61.7	9.8	Silty clay loam
T1-3	14 - 17.75	AB	26.4	56.0	17.6	Silt loam
T1-3	40 - 43.75	B2	39.4	52.0	8.6	Silty clay loam
T1-4	6 - 9.75	AB	27.0	60.6	12.3	Silty clay loam
T1-4	17 - 20.75	B1	31.6	57.4	11.0	Silty clay loam
T1-5	10 - 13.75	AB	18.6	50.7	30.6	Silt loam
T1-5	25 - 28.75	B2	18.9	50.4	30.8	Silt loam
B2	0 - 3.75		16.1	36.1	47.8	Loam
B3	0 - 3.75		13.8	42.8	43.5	Loam
B3	12 - 15.75		20.6	58.1	21.3	Silt loam

Table 2. Soil texture including the coarse fraction. Samples in grey are from the groundwater discharge zone below the T1 transect.

Percentage including > 2 mm fraction						
Sample profile	Depth (cm)	Horizon	> 2 mm	Clay	Silt	Sand
T1-1	4 - 7.75	AB	7.52	21.09	56.78	14.61
T1-1	24 - 27.75	B1/B2	7.85	18.06	46.35	27.74
T1-2	10 - 13.75	AB	27.66	26.19	37.98	8.25
T1-2	34 - 37.75	B2	15.72	24.02	52.00	8.26
T1-3	14 - 17.75	AB	19.19	21.33	45.25	14.22
T1-3	40 - 43.75	B2	21.62	30.88	40.76	6.74
T1-4	6 - 9.75	AB	1.33	26.64	59.79	12.14
T1-4	17 - 20.75	B1	2.62	30.77	55.89	10.71
T1-5	10 - 13.75	AB	1.02	18.41	50.18	30.29
T1-5	25 - 28.75	B2	1.53	18.61	49.63	30.33
B2	0 - 3.75		1.52	15.86	35.55	47.08
B3	0 - 3.75		0.00	13.80	42.80	43.50
B3	12 - 15.75		0.00	20.60	58.10	21.30

Profiles T1-2 and T1-3 have a significantly higher gravel content and a correspondingly smaller silt or sand fraction. The sand and coarse fraction shows the highest variability.

3.1.5 Hydraulic conductivity (K_{sat})

The values for hydraulic conductivity were log transformed to achieve normal distribution. Two-sample t-test of log transformed hydraulic conductivities (log K) in the AB horizon (above 25 cm) versus the B horizons (below 25 cm) suggests a significant difference ($p = 0.000$) between means (Figure 13). Differences in K_{sat} between profiles are more diffuse and can only be identified between profile T1-1 and T1-5 (Figure 9b). Otherwise, there does not seem to be any systematic difference in conductivities between the profiles.

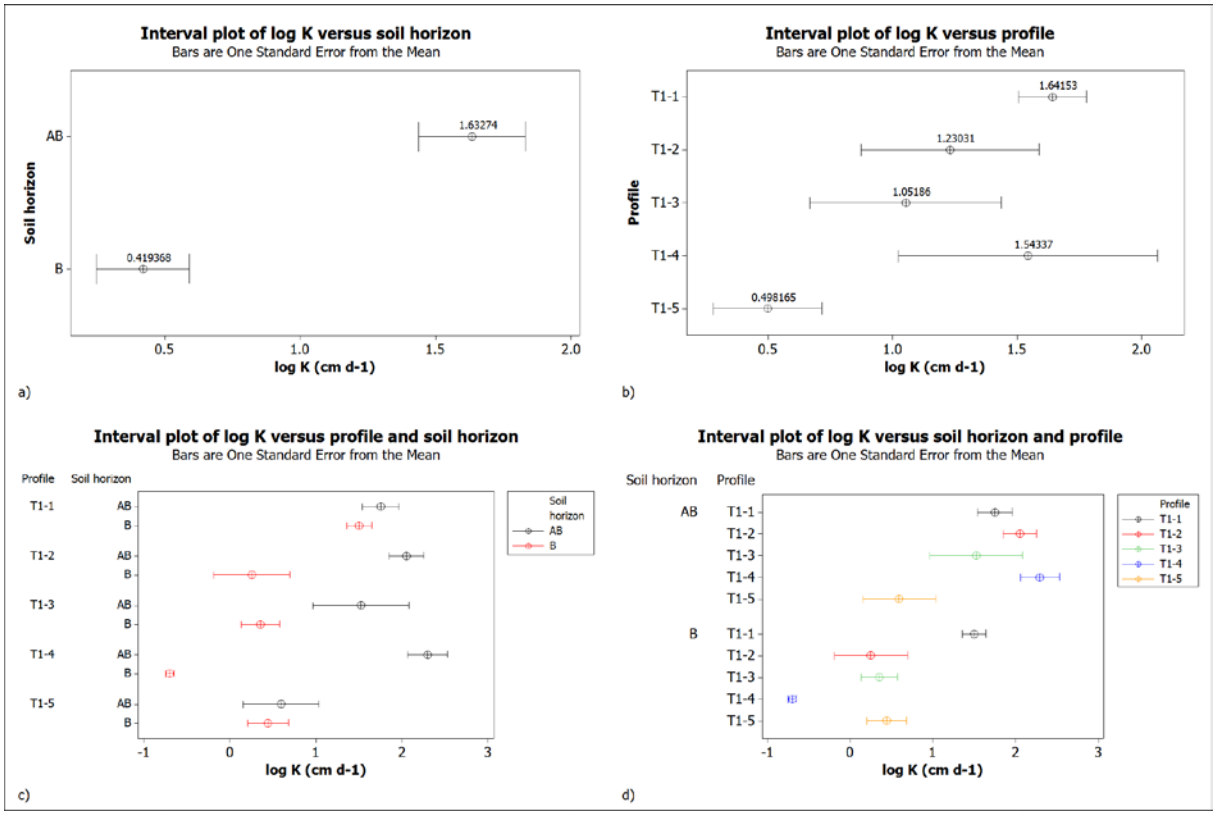

Figure 13. Interval plots for hydraulic conductivity (log K) in cm day-1: a) conductivity versus soil horizon; b) conductivity versus profile; c) conductivity versus profile and soil horizon; d) conductivity versus soil horizon and profile.

The difference between upper and lower soil layers appears greatest in the middle profiles, particularly T1-2 and T1-4, while upper and lower layers are more similar at T1-1 and T1-5.

3.2 Dye tracer experiment

3.2.1 Upper plot (T1-1)

Results from the excavation of the upper dye tracer plot are shown in Figure 14, Figure 15, Figure 16 and Figure 17. The colour is most intense in the upper 20 cm, while some dye penetrates through macropores to the lower horizons. There may be some return flow to the

surface, but this is difficult to read from the pictures. Generally it appears that the dye penetration is concentrated in the upper O/A and AB horizon.

Figure 14. Right-hand views (as seen from downslope) of the excavated upper profile. Photos: Lars-Erik Sørbotten.

Figure 15. Right-hand views (as seen from downslope) of the excavated upper profile, dyed areas highlighted. Photos: Lars-Erik Sørbotten.

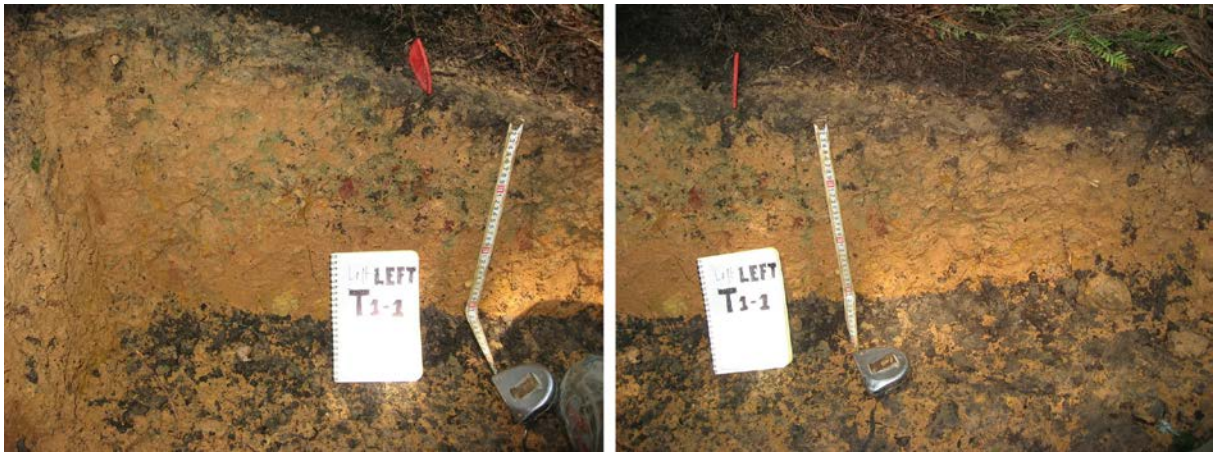

Figure 16. Left-hand views (as seen from downslope) of the excavated upper profile. Photos: Lars-Erik Sørbotten.

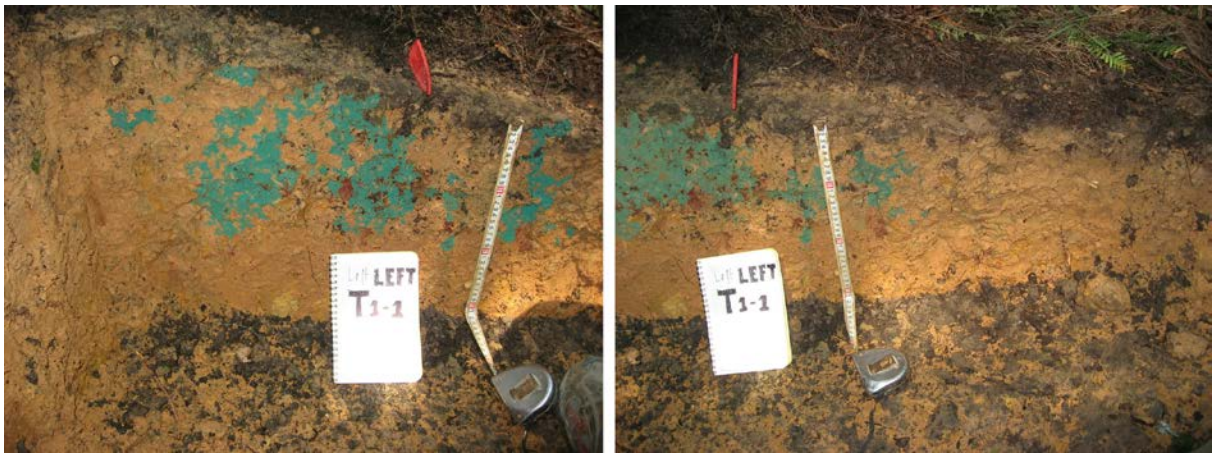

Figure 17. Left-hand views (as seen from downslope) of the excavated upper profile, dyed areas highlighted with colour. Photos: Lars-Erik Sørbotten.

3.2.2 Lower plot (T1-5)

Pictures from the excavation of the lower dye tracer plot. Due to the author suffering a mild heat stroke during excavation of the upper tracer plot, the excavation of the lower plot was kindly performed by prof. Jan Mulder (Figure 18 and Figure 19). The dye seems mostly to have penetrated through the upper 25 cm, with some deeper penetration at a few points. Dye also seems to have concentrated heavily around and below the small rocks in the profile.

Figure 18. Left- and right-hand views (as seen from downslope) of the excavated lower profile. Photos: Jan Mulder.

Figure 19. Left- and right-hand views (as seen from downslope) of the excavated lower profile, dyed areas highlighted. Photos: Jan Mulder.

3.3 Data analysis of climate, discharge and soil moisture data

3.3.1 Data availability

Due to problems with flooding of TDR logger boxes and power supply to the weather station and the water height logger in the dam, there are limited data series with precipitation, TDR and discharge data, and there exists only a five-month window with good data for all three. Figure 20 shows precipitation versus discharge and soil moisture at a daily resolution from March to August 2010.

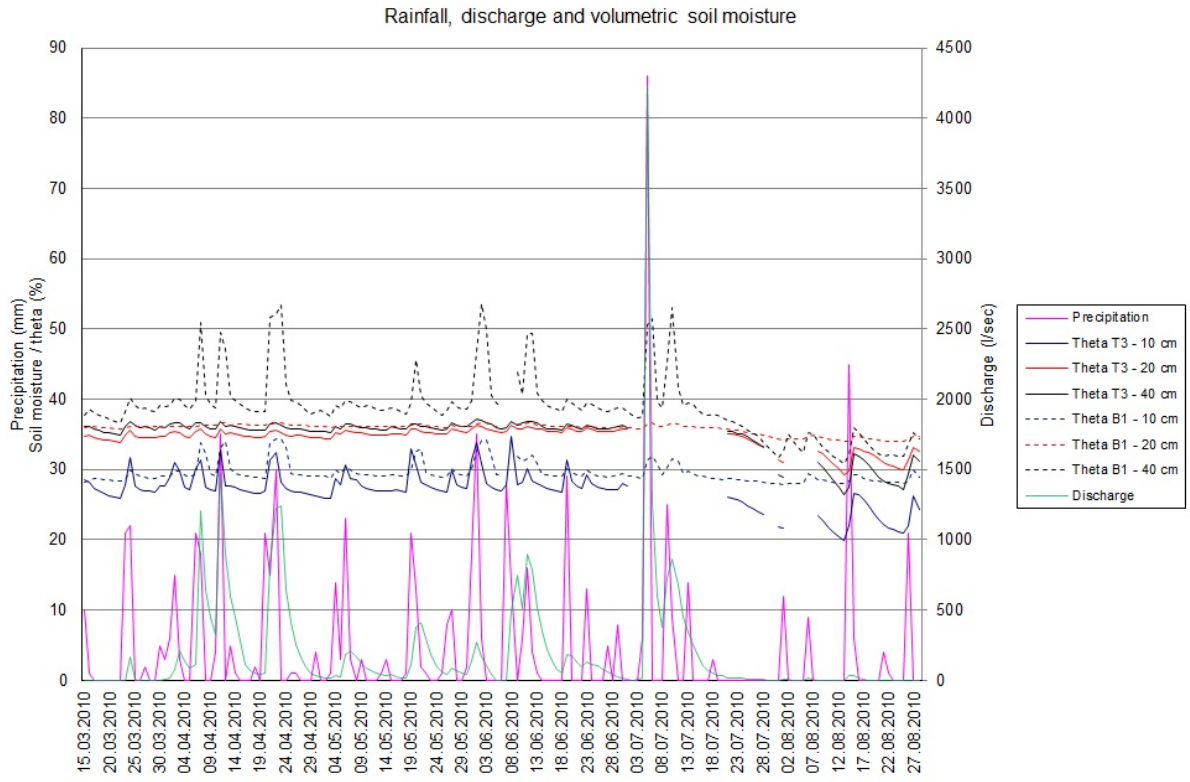

Figure 20. Precipitation, discharge and volumetric soil moisture in the period 15.03.2010-28.08.2010. Dotted lines are soil moisture values from the B1 profile.

3.3.2 Soil moisture response to precipitation

In this time window, seven episodes where daily rainfall exceeded 20 mm were identified (Table 3). Charts displaying precipitation, discharge and soil moisture data for these episodes can be viewed in the appendix.

Table 3. Seven episodes with > 20 mm daily rainfall identified in the period March to July.

Episode	Start	End	Duration (h)	P (mm)
1	23.03.2010 20:30	25.03.2010 06:50	34.33	36
2	06.04.2010 00:00	10.04.2010 22:30	118.50	39
3	10.04.2010 22:35	15.04.2010 15:25	112.83	45
4	20.04.2010 21:35	29.04.2010 15:10	209.58	66
5	06.05.2010 00:00	10.05.2010 00:00	96.00	29
6	18.05.2010 23:50	22.05.2010 01:10	73.33	38
7	31.05.2010 06:10	05.06.2010 06:30	120.33	59

Several climate factors and initial conditions were identified for each episode for correlation with the hydrological parameters (Table 4).

Table 4. Average rainfall intensity (mm/h), maximum rainfall intensity (mm/h), average air temperature (°C), average relative humidity (%), antecedent relative humidity (%), antecedent soil moisture at 10 cm, 20 cm and 40 cm (cm3/cm3) for the selected episodes.

Episode	P intensity (mm/h)	Max intensity (mm/h)	Average air temperature (°C)	Average relative humidity (%)	Antecedent humidity (%)	Antecedent θ 10 cm (cm^3/cm^3)	Antecedent θ 20 cm (cm^3/cm^3)	Antecedent θ 40 cm (cm^3/cm^3)
1	1.93	6	9.0	95	98	0.28	0.352	0.363
2	1.41	7	13.2	62	39	0.269	0.346	0.357
3	4.66	9	12.3	71	90	0.269	0.345	0.357
4	1.49	12	16.7	51	100	0.265	0.346	0.357
5	0.92	14	17.0	71	49	0.273	0.351	0.359
6	1.18	5	16.2	97	93	0.268	0.349	0.356
7	1.17	5	19.2	65	100	0.272	0.354	0.363

Visual inspection of the data shows a clear and quick soil moisture response to precipitation, most often 1 to 2 hours after the initial rainfall . The soil moisture increase was first visible at the 40 cm depth, followed by 20 cm and 10 cm, with the 10 cm response delaying up to 3:45 hours after the onset of the rainfall (Table 5).

Table 5. Time lag (hh:mm) for soil moisture response to onset of rainfall, drainable and active saturation (%) at the 20 cm depth at time of first response for the 10 cm depth, and drainable and active saturation (%) at the 40 cm depth at time of first response for the 20 cm depth.

Episode	Start rain	Time lag 10 cm	Time lag 20 cm	Time lag 40 cm	Sat_D 20 cm @ response time 10 cm	Sat_A 20 cm @ response time 10 cm	Sat_D 40 cm @ response time 20 cm	Sat_A 40 cm @ response time 20 cm
1	23.03.2010 20:30	01:40	01:30	01:30	39.02	71.79	39.42	38.18
2	06.04.2010 01:55	03:45	02:15	01:15	34.96	58.97	35.58	30.91
3	10.04.2010 22:35	03:15	02:05	01:15	40.65	76.92	40.38	40.00
4	20.04.2010 21:35	01:25	01:15	01:05	43.09	84.62	41.35	41.82
5	06.05.2010 03:00	00:10	00:10	00:00	43.09	84.62	45.19	49.09
6	18.05.2010 23:50	02:40	02:00	01:40	35.77	61.54	36.54	32.73
7	31.05.2010 06:10	02:10	02:00	01:50	43.90	87.18	40.38	40.00

At episodes 1, 4, 5 and 7, the responses follow very quickly across the soil horizons. It may be that 10 and 20 cm responds reasonably simultaneously, but the resolution (10-minute intervals) makes it difficult to tell. At 20 cm, there is also a marked difference between the drainable saturation and on the active saturation based on observed soil moisture variability, but this is not the case at 40 cm.

The active porosity (ϕ_A) at 20 cm and 40 cm is considerably smaller than the average drainable porosity (ϕ_D) calculated from the soil physical measurements (Table 6), while the values are reasonably similar at 10 cm. Both drainable and active porosity are dramatically smaller than total porosity (ϕ).

Table 6. Comparison of total, drainable and active porosity. φ = Average total porosity obtained from soil physical analysis, φD = average drainable porosity (φ - average θ at field capacity) and φA = active porosity (maximum observed soil moisture - minimum observed soil moisture). Note that the soil physical measurements are from 25 cm and 50 cm respectively where TDR measurements are taken at 20 cm and 40 cm.

Depth	Average ϕ	Average ϕ_D	ϕ_A
10 cm	0.441	0.137	0.113
20/25 cm	0.438	0.123	0.039
40/50 cm	0.431	0.104	0.055

3.3.3 Runoff coefficient

The runoff coefficient (Table 7) varies from 3 % of total rainfall to almost 53 %. The annual runoff coefficient for 2010 was 22.7 %.

Table 7. Precipitation (P), runoff, infiltration and runoff coefficient (Cr) for the selected episodes.

Episode	P (mm)	Runoff (mm)	Infiltration (mm)	C_r
1	36	1.11	17.00	0.03
2	39	17.56	22.65	0.45
3	45	23.67	27.30	0.53
4	66	31.93	22.35	0.48
5	29	4.46	17.95	0.15
6	38	6.02	20.80	0.16
7	59	4.61	19.9	0.08

Regression analysis shows a fit between the runoff coefficient and antecedent soil moisture across all horizons, most markedly at 20 cm, where r^2 = 95 % for a quadratic regression model (Figure 21) and r^2 = 87 % for a linear model (Figure 22). The runoff coefficient correlates negatively to antecedent soil moisture at 20 cm with a Pearson correlation of -0.944 (p = 0.001).

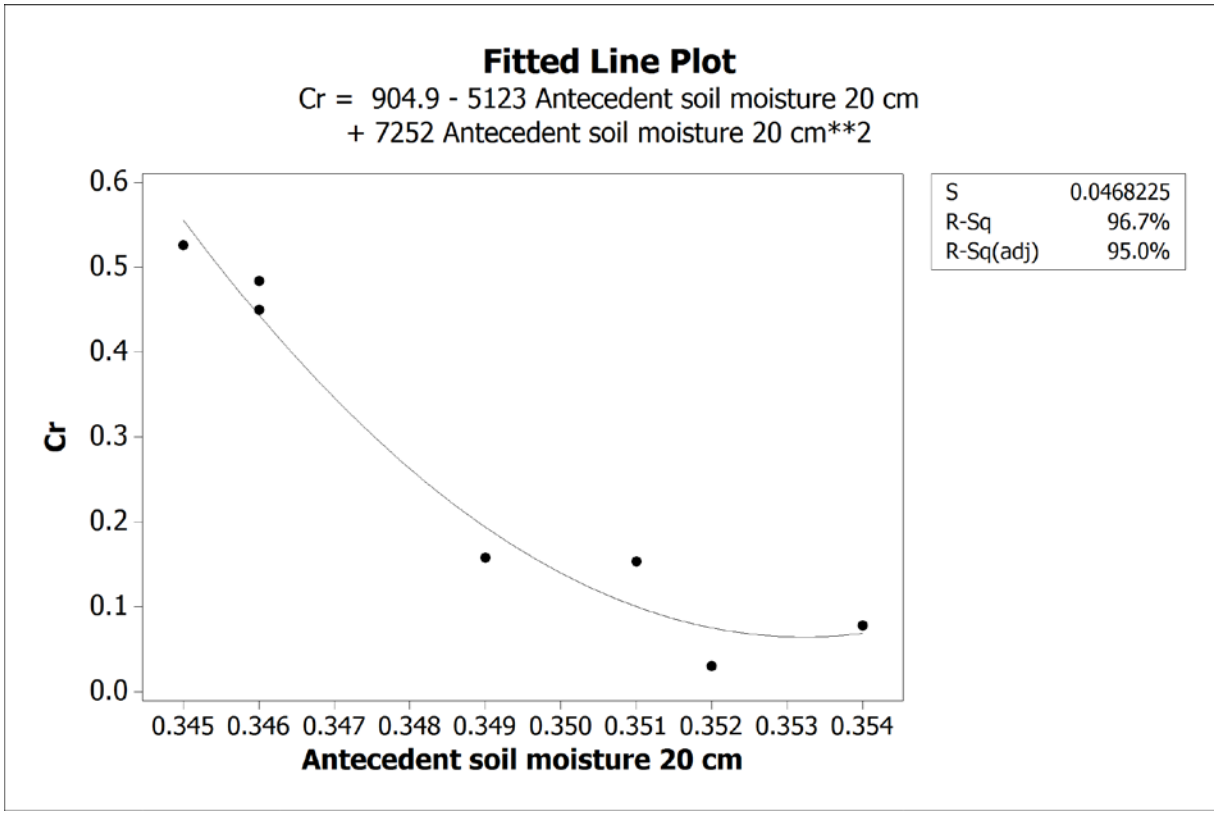

Figure 21. Quadratic regression fit of runoff coefficient (Cr) vs. antecedent soil moisture at 20 cm.

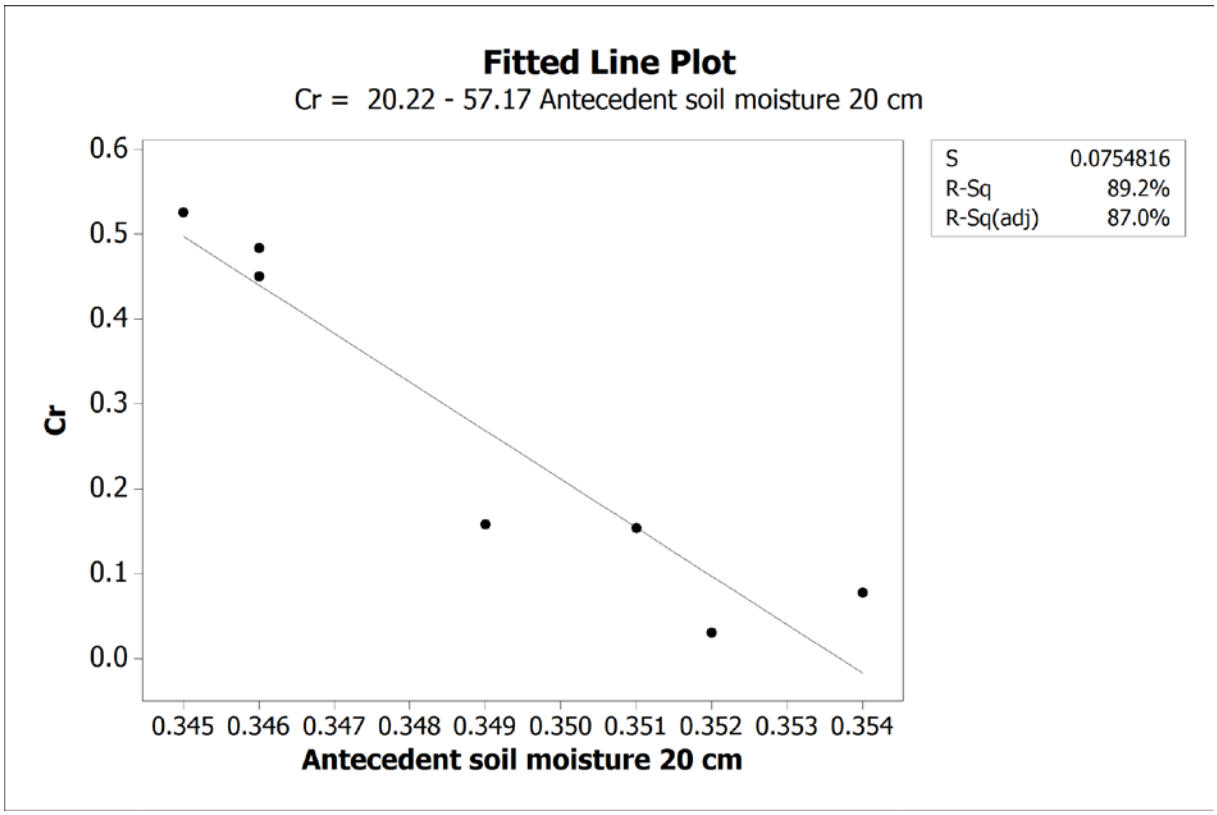

Figure 22. Linear regression fit of runoff coefficient (Cr) vs. antecedent soil moisture at 20 cm.

3.3.4 Distribution of soil moisture response

The change in soil water storage over an episode was calculated as θ_{max}-θ_{start} for each TDR sensor and calculated for the entire depth of the relevant soil horizon. The distribution between the soil horizons can be seen in (Figure 23).

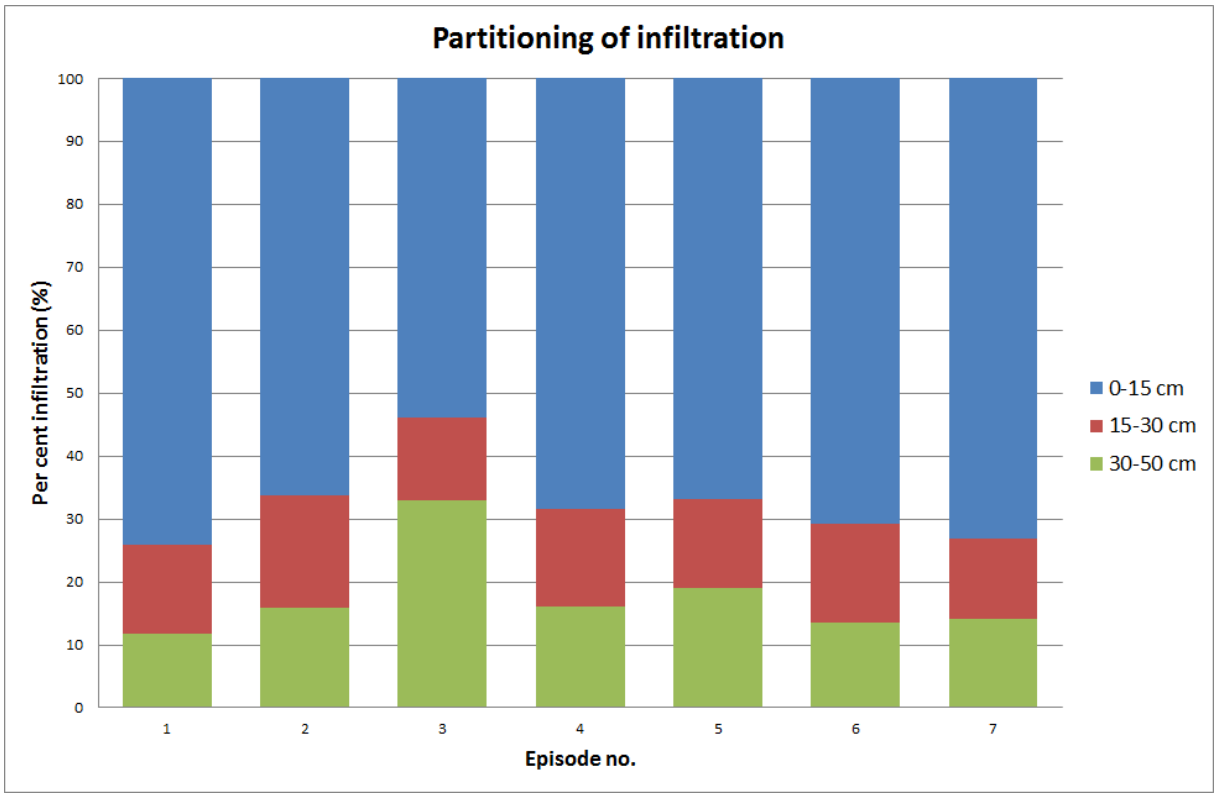

Figure 23. Partitioning of infiltration over soil horizons. 0-15 cm corresponds to the AB horizon, 15-30 cm to the B1 horizon and 30-50 cm to the B2 horizon.

3.4 Chemical fingerprint analysis of water samples

3.4.1 Stream water, soil water canopy throughfall and litter layer concentrations

Results from comparison of pH, NO_3-N and NH_4-N in stream water over three seasons, dry season (November-March), early summer (April-June) and late summer (July-October) can be found in Figure 24.

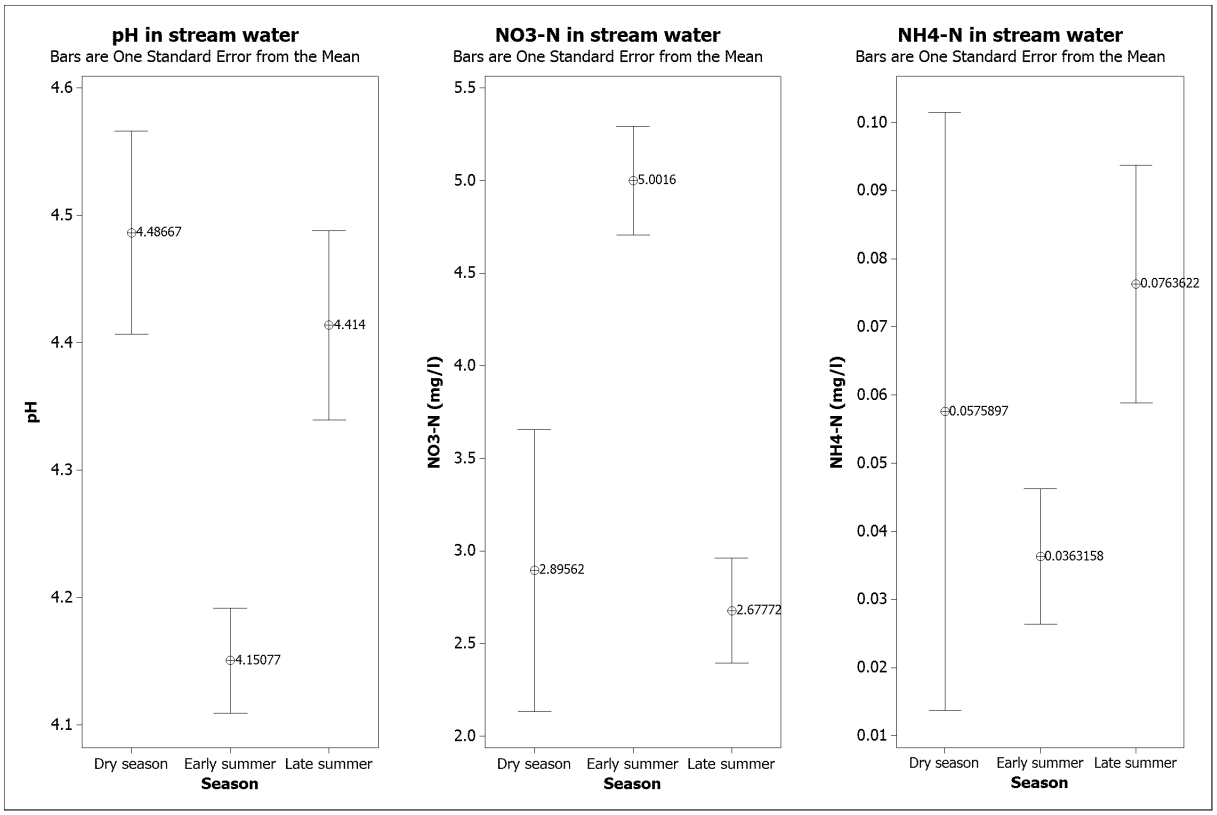

Figure 24. Interval plot of pH and concentrations of NO3-N (mg/l) and NH4-N (mg/l) in stream water over three periods: Dry season (November-March), early summer (April-June) and late summer (July-October).

Details from the one-way ANOVA analysis of pH, NO_3-N and NH_4-N in stream water can be seen in the appendix. Results indicate that pH is significantly lower ($p = 0.037$) and NO_3-N concentration is significantly higher ($p = 0.000$) in early summer than late summer and the dry season. Means could seem to indicate that NH_4-N concentration is lower in early summer, but the variation is too great to yield statistical significance ($p = 0.36$).

Results from comparison of pH, NO_3-N and NH_4-N (averages over soil depths) in soil water over the three seasons (Figure 25) indicate a similar pattern to stream water, although NO_3^- concentrations are lowest in early summer, not highest as in stream water.

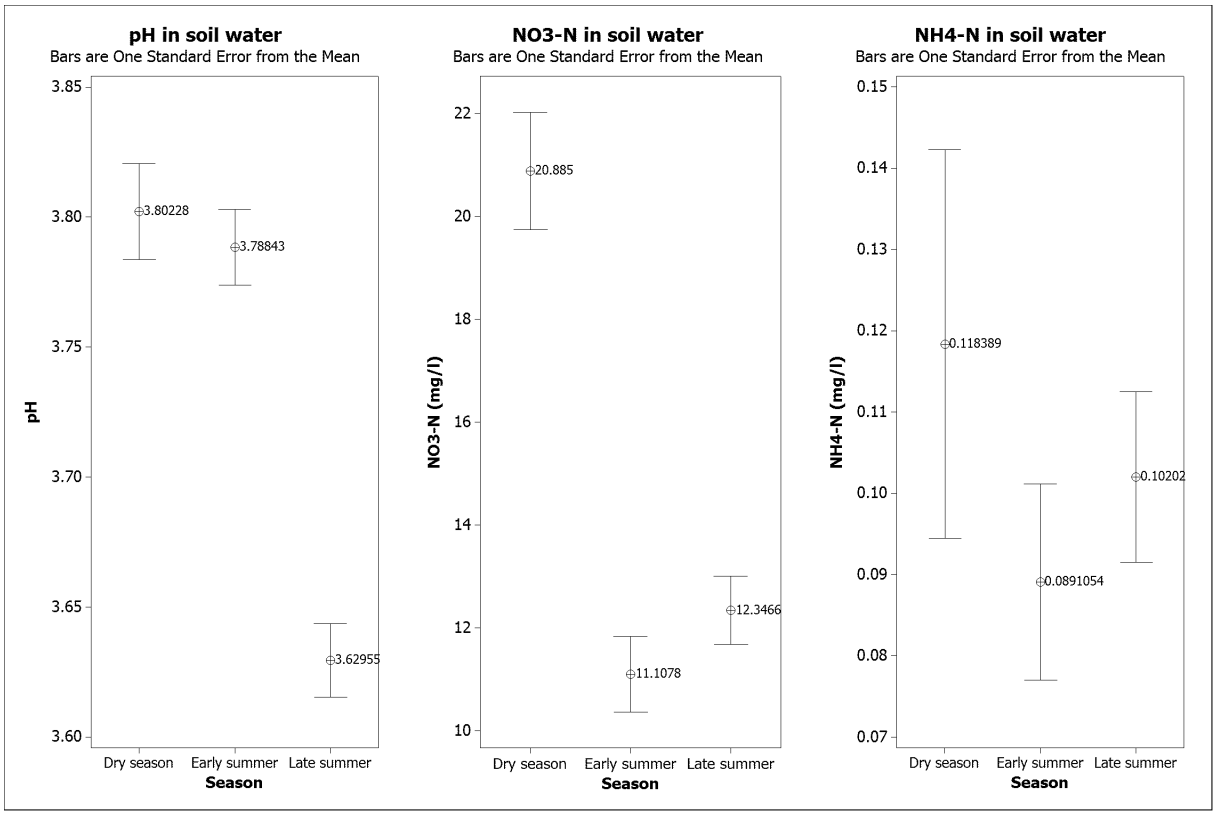

Figure 25. Interval plot of pH and concentrations of NO3-N (mg/l) and NH4-N (mg/l) in soil water over three periods: Dry season (November-March), early summer (April-June) and late summer (July-October).

Details from the one-way ANOVA analysis of pH, NO_3-N and NH_4-N in soil water can be seen in the appendix. pH is significantly lower in the late summer ($p = 0.003$) than the other seasons, while NO_3-N concentrations are significantly higher in the dry season ($p = 0.000$). NH_4-N concentrations show no statistically significant seasonal variation.

Comparison of canopy throughfall, litter layer water, soil water and stream water indicate a considerable difference (Figure 26). Ammonium-N increases slightly between CTF and the litter layer, and then decreases dramatically between the litter layer and the soil solution, and nitrate-N increases correspondingly. Canopy throughfall and litter layer data is from the IMPACTS project (IMPACTS 2004), and only the annual averages are known.

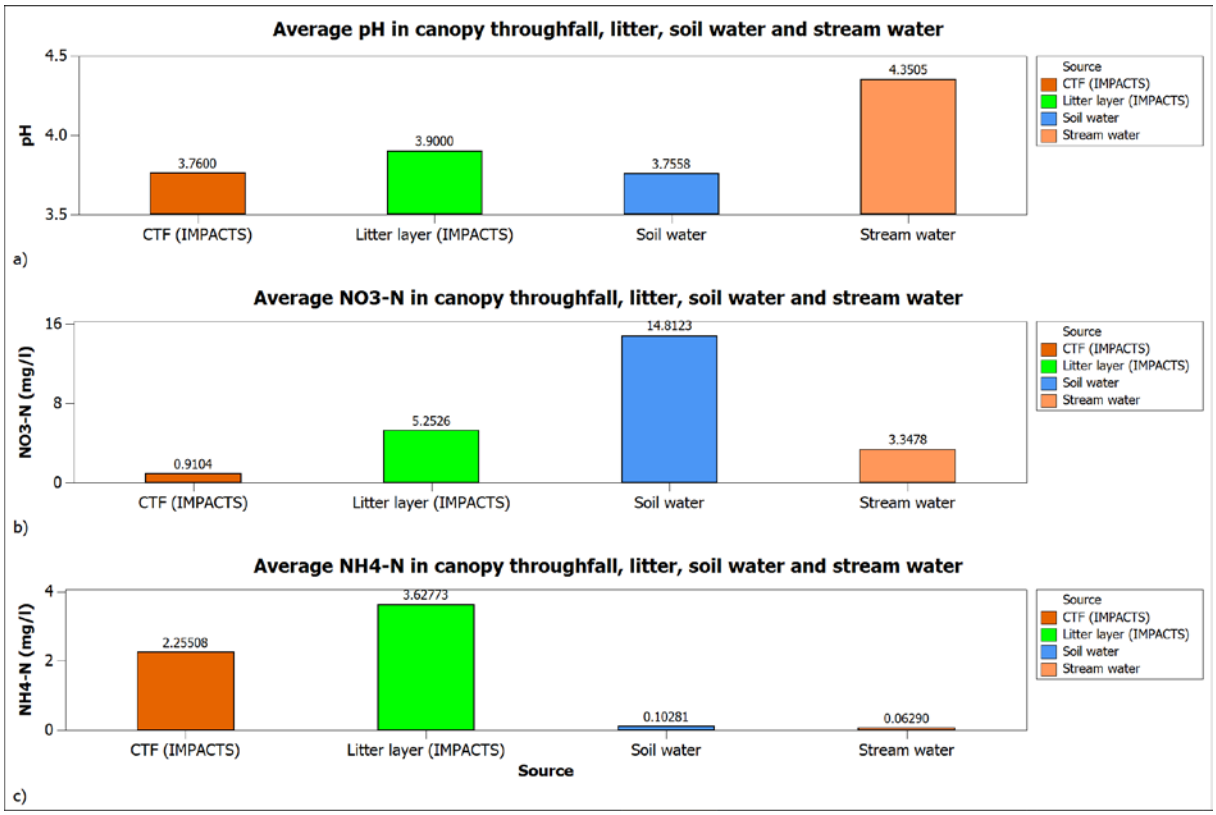

Figure 26. Average a) pH, b) NO3-N (mg/l) and c) NH4-N (mg/l) in canopy throughfall, litter layer, soil water and stream water, respectively.

Time plots of NO_3-N and NH_4-N versus precipitation and discharge for stream water (Figure 27) and soil water (Figure 28) indicate that NO_3-N and NH_4-N roughly co-vary in soil water, but responds inversely in stream water.

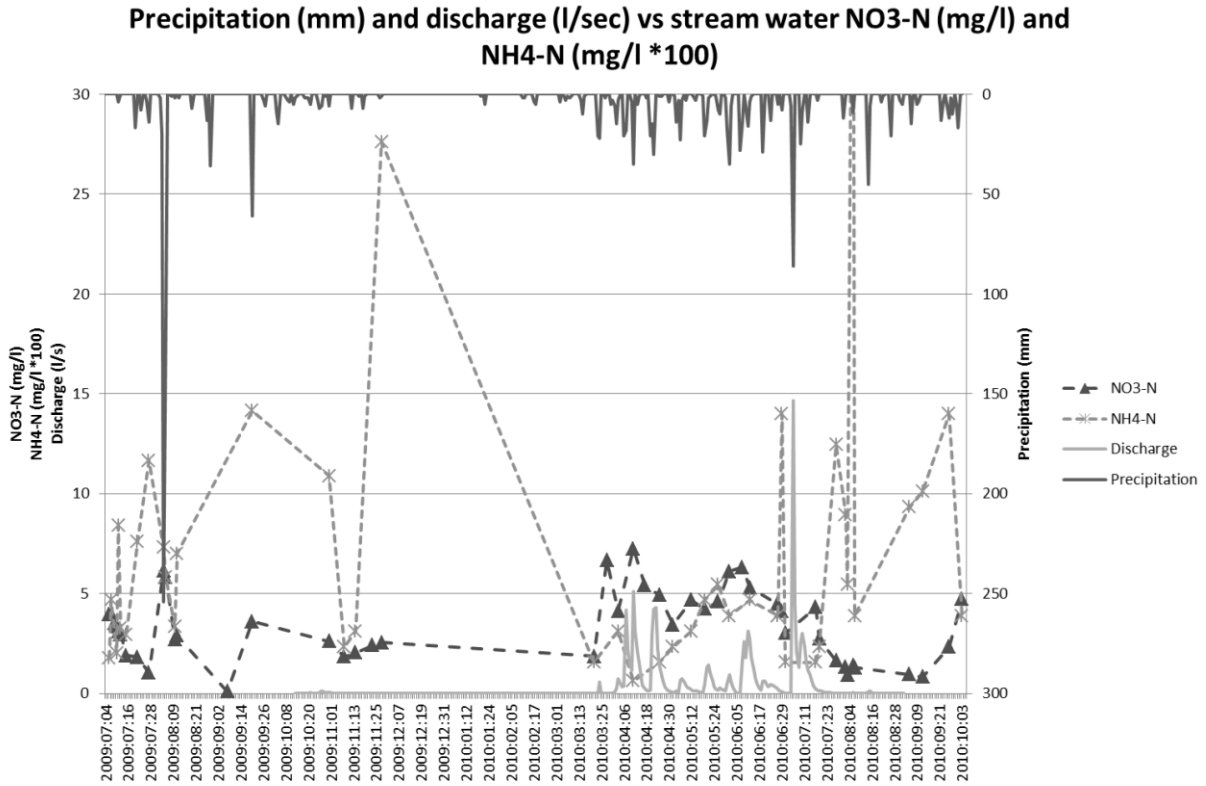

Figure 27. Time plot of precipitation, discharge and NO3-N (mg/l) and NH4-N (mg/l*100) concentrations in stream water.

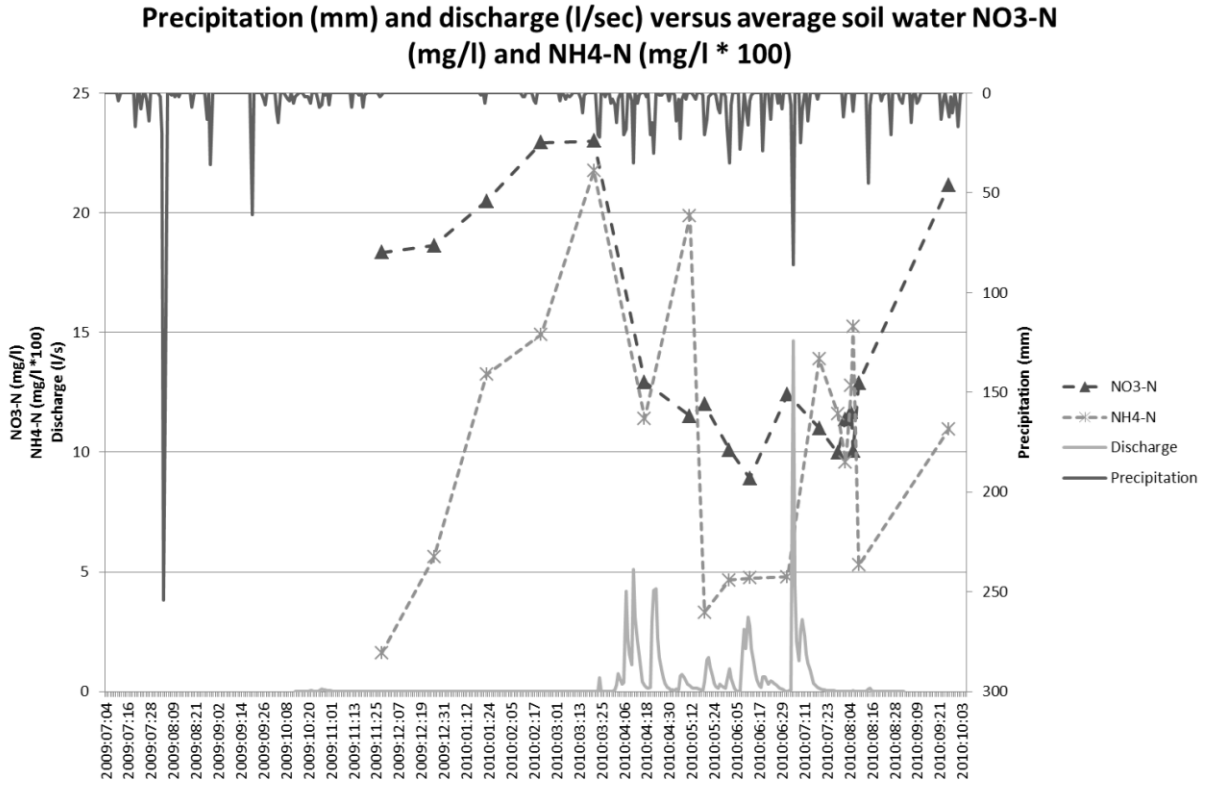

Figure 28. Time plot of precipitation, discharge and soil NO3-N (mg/l) and NH4-N (mg/l*100) concentrations in soil water.

Soil concentrations of NO_3-N and NH_4-N do not seem to correlate with precipitation ($p = 0.423$ and 0.131, respectively), but stream water concentrations of NO_3-N do show a positive correlation of 0.385 ($p = 0.008$) with precipitation (Figure 29). By contrast, stream water NO_3-N concentrations correlate negatively with stream water NH_4-N concentrations (Figure 30) (corr = -0.306; $p = 0.037$).

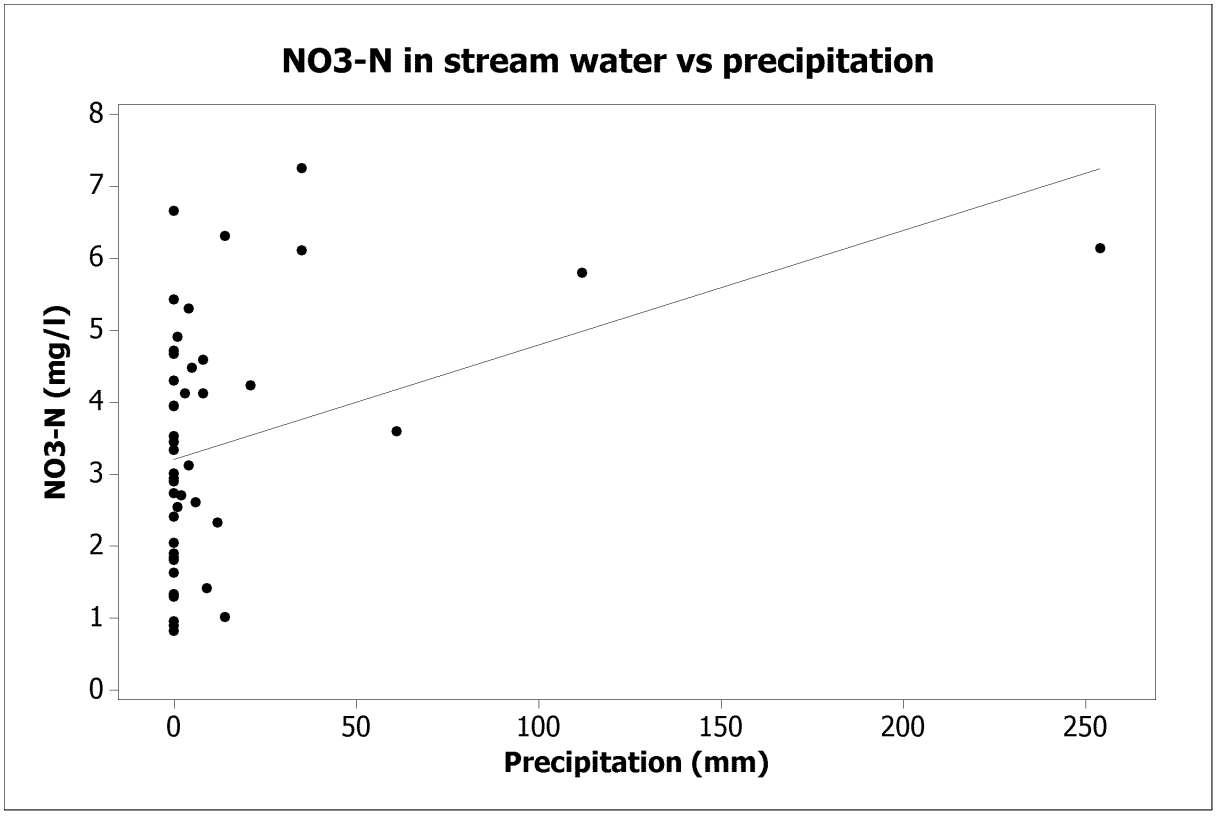

Figure 29. Regression line for stream water NO3-N concentrations (mg/l) vs precipitation (mm)

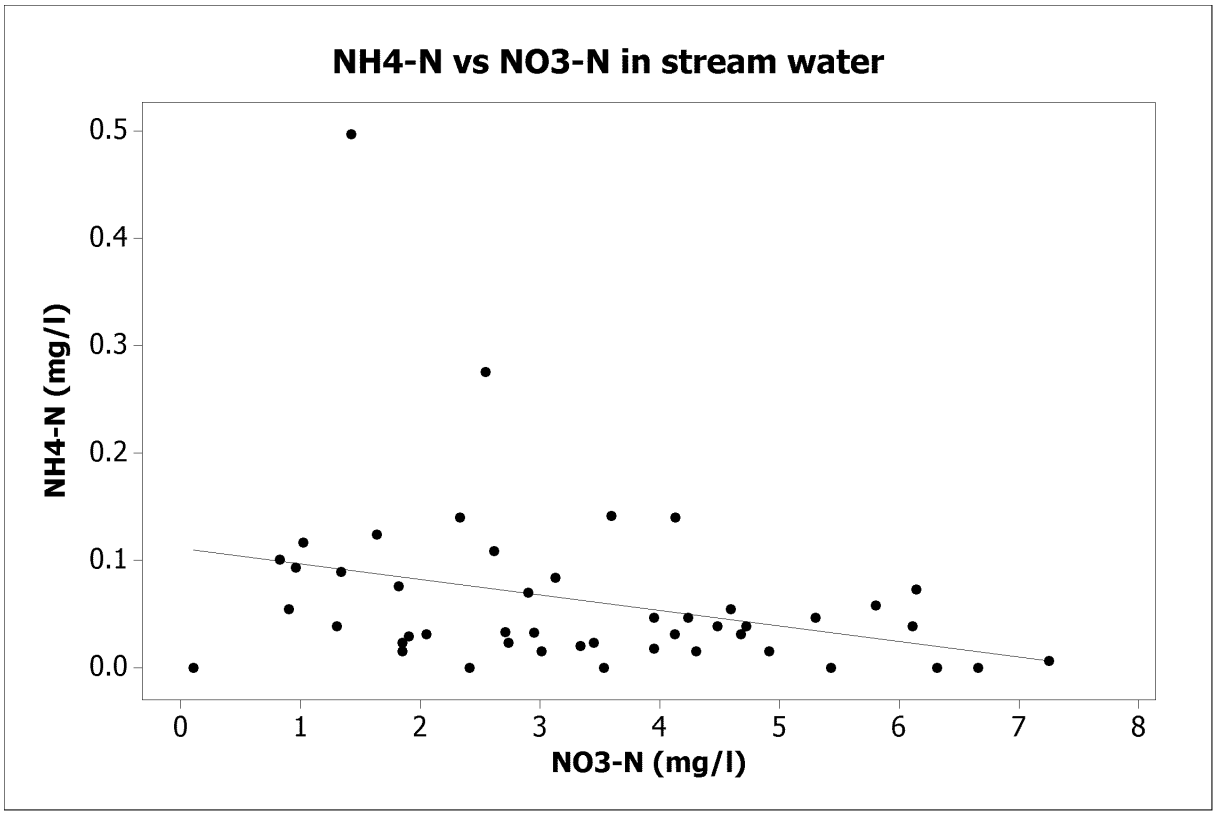

Figure 30. Regression line for soil water NH4-N concentrations (mg/l) vs NO3-N concentrations (mg/l).

3.4.2 Stream water vs discharge

Regression analyses were performed for stream water concentrations of NO_3-N and NH_4-N versus discharge by season. The regression fits can be seen in Figure 31 and Figure 32. Complete details of regression analyses can be found in the appendix.

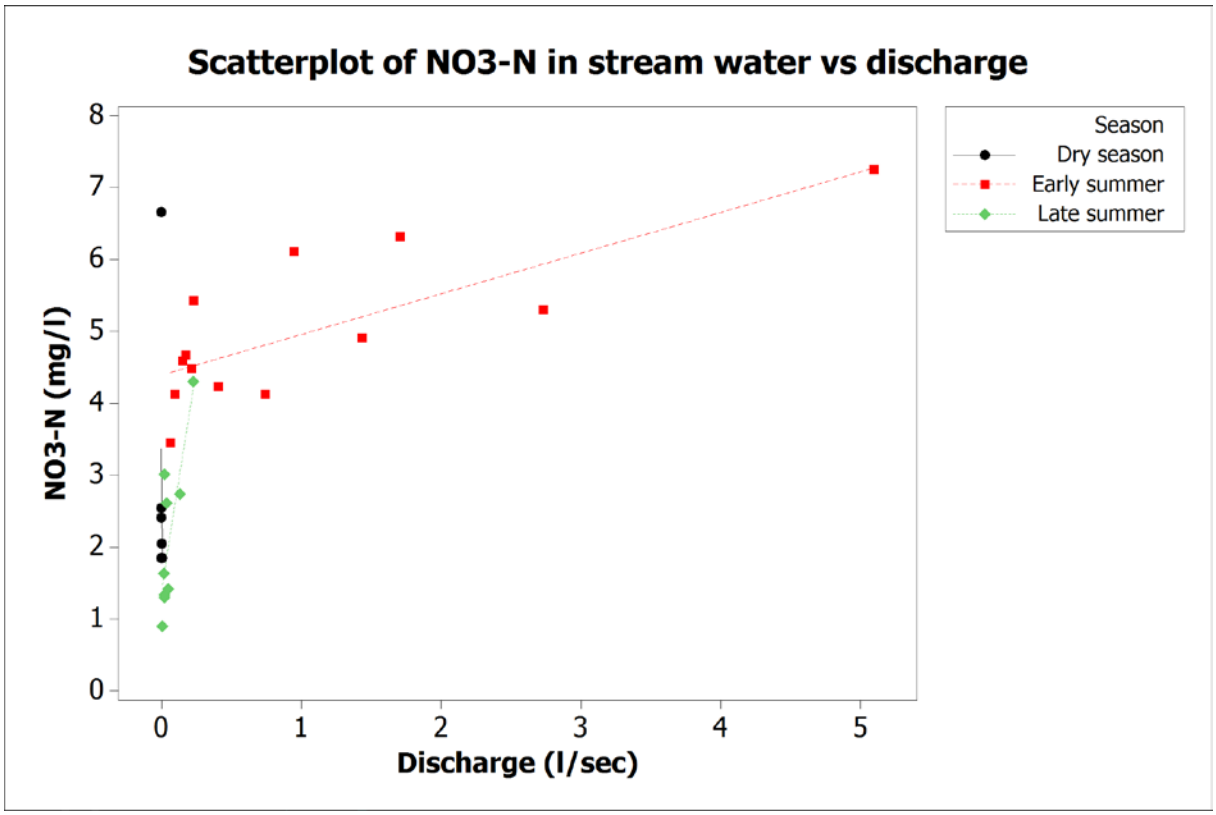

Figure 31. Regression lines for NO3-N concentrations (mg/l) vs daily discharge (l/sec).

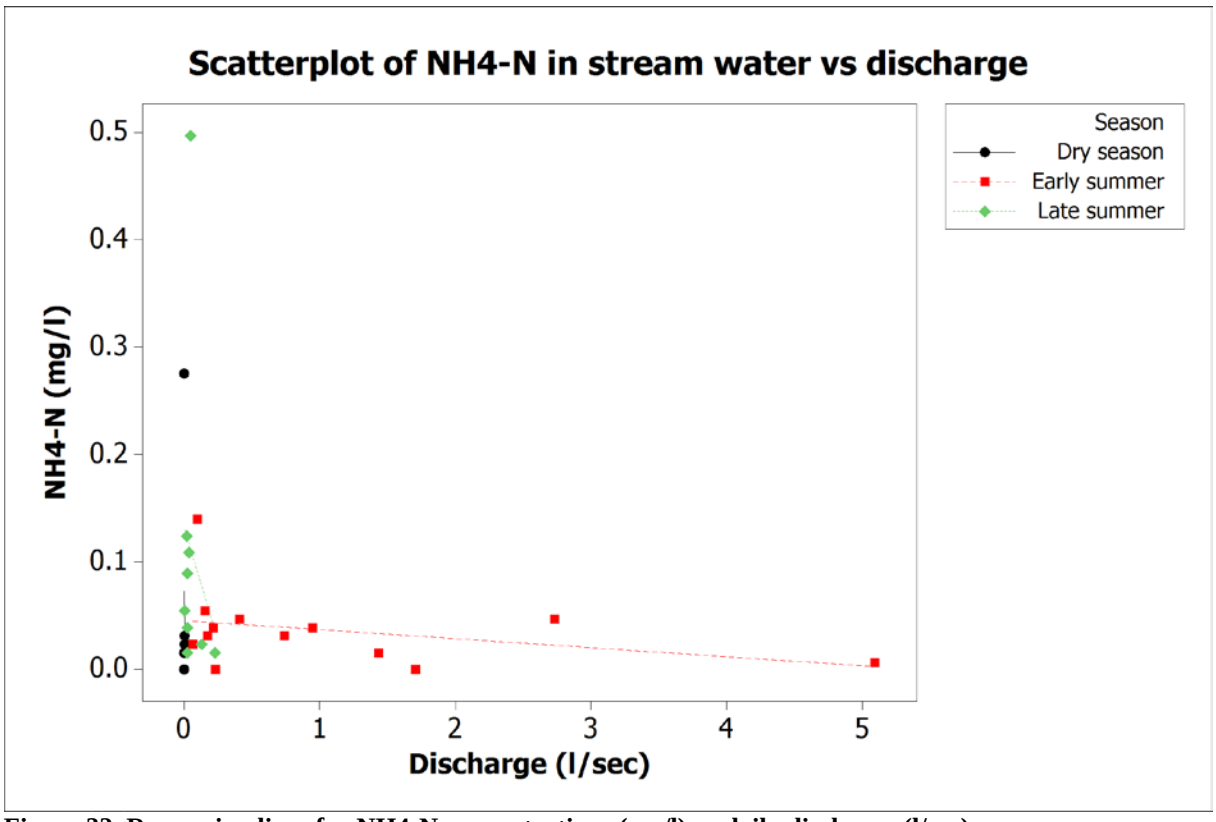

Figure 32. Regression lines for NH4-N concentrations (mg/l) vs daily discharge (l/sec).

NO_3-N concentrations were correlated with discharge during early summer ($p = 0.002$; $r^2 = 0.563$) and late summer ($p = 0.008$; $r^2 = 0.608$), but not during the dry season ($p = 0.441$). NH_4-N concentrations did not show correlation with discharge at any time, with p values of 0.675, 0.257 and 0.604 for the dry season, early summer and late summer respectively.

3.4.3 Modelling

A number of difficulties were encountered parameterizing and running the SUTRA model, and I was unable to gain any useful results from the attempted simulations. The simulations either did not seem to respond to precipitation input, or they gave unrealistic results when they did. When trying to run long-term simulations or simulation with high temporal resolution in order to get results that could be compared with *in situ* measurements, the model most often encountered unknown errors and stopped running early in the simulation. I was unable to resolve the unexpected program terminations, and the modelling work was aborted.

4 Discussion

4.1 Classification of dominant runoff process (DRP)

Using the DRP decision scheme from Scherrer & Naef (2003), the hill slope seems to classify as either SSF1 (subsurface flow) or SSF2 (delayed subsurface flow), depending on whether we define the soil depth as less than or more than 50 cm in depth. Due to the regolithic nature of the sub-50 cm soil, this is difficult to establish, but either of these classifications could apply. The main difference between these two types, in addition to the delay factor, is the degree of water exchange between macropore flow and matrix. Possibly, the results from the chemical analysis may further constrain this problem.

4.2 Soil physical and hydrological parameters

Hypothesis: If episode water is channelled laterally through the upper O/A and AB horizons, we should expect a difference in soil physical and hydrological characteristics at the transition between upper and lower layers, specifically at the transition to the B horizon, 15-20 cm down.

4.2.1 Water retention characteristic

Hypothesis: There is be a marked difference in the water retention characteristic between the O/A-AB horizons and B1.

The results show a gradual steepening of the pF curve with depth, with decreasing water content at saturation (h = 0) and increasing water content at wilting point (pF 4.2). This indicates that there is generally more potential soil water variability in the upper horizons and that little water needs to be added to the deeper soil horizon to increase the potential from 4.2 to 2. However, it is important to note that remaining soil water at matrix potentials greater than pF 2 (field capacity) is mostly capillary and is not easily available for runoff generation. Thus, the most interesting part of the pF curve may be the drainable range, between saturation and pF 2. Unfortunately, as mentioned in the results section, soil moisture content at pF 2 may be underestimated in the measurements, and thus the drainable porosity may be overestimated. The water retention characteristics will therefore be discussed further together with the soil moisture response, where drainable porosity is compared with the difference between measured maximum and minimum soil moisture content.

Shape of pF curves

All curves show a sudden shape change from the -3000 cm pressure and stronger, where the evacuation is performed on disturbed samples. This may be due to the fact that disturbed samples will achieve a better contact with the ceramic pressure plates than undisturbed samples. However, some soils do display a water retention curve with dual or multiple inflection points (Stolte et al. 1994), indicating that there are, in some cases, natural "threshold points" where water retention characteristics change suddenly with increasing potential. The van Genuchten model only accounts for a single inflection point in the water retention curve, making it problematic to fit the observed data to the curve shape expressed in the Van Genuchten equation.

Some samples show a sudden increase in soil water content with increasing underpressure between the -1000 cm and the -3000 cm pressure. This does clearly not reflect the reality and as such must be a measuring error, but it is difficult to tell where the error has occurred, and there may be several concurrent factors in play. I will try to identify some of them:

1) Insufficient contact between samples and ceramic plates: Ensuring contact with the porous ceramic plates is very important, and if at some point during the procedure with the disturbed samples I have not managed to achieve this, this could lead to air getting between the samples and the plates, preventing water from being led out of the samples through the ceramic plate.

2) Insufficient saturation of ceramic plates or leaky connections: If the plates were insufficiently saturated or there was air leakage in the equipment, this could also cause air to enter the system and prevent water from being properly led out of the samples.

3) The effect seems to grow stronger with depth and vary by profile. At 3.5 cm, the averages for each depth show no increase at -3000 cm. At 10 cm, only T1-2 exhibits this characteristic, and at 25 cm and 50 cm, only T1-5 does not change in this fashion. This would indicate that the effect is strongest at T1-3 through T1-4, somewhat less at T1-1 and not at all at T1-5. This points to porosity or bulk density being controlling factors, as these properties vary with depth and profile: Porosities are highest at T1-2 to T1-4, lower at T1-1 and lowest at T1-5, and the inverse is the case for bulk density. Profiles T1-2 to T1-4 also stand out by being the most clay-rich, indicating that a high clay content may exacerbate the effect.

4) In the grinding of the samples, closed capillary pore spaces are destroyed, increasing the connectivity of the soil. Such capillary pores may not participate in the water transport, and may even not get filled up during saturation. The result of this will be to increase the water storage capacity of the soil. In addition, clay aggregates are broken up into individual clay particles, effectively increasing the specific surface of the soil. This may again lead to stronger adhesion of water at the particle surface, increasing the water content at wilting point. This corresponds to the fact that the effect seems strongest where the soils are most clay-rich.

When we compare the regular curves with the curves using disturbed samples also at -500 cm and -1000 cm, we see that the soil water content increase now takes place at the -500 cm step, confirming that this shift is a result of disturbing the samples. Also, the soil moisture content at -500 cm sometimes exceeds saturation values, which would seem to indicate that values for disturbed samples are unreliable.

All taken together, the discrepancies point to a measuring or equipment error, which may be exacerbated by soil physical properties such as porosity / bulk density and particle size distribution. Which controls this, whether it is pore structure, specific surface or other factors, is beyond the scope of this thesis and needs further study.

4.2.2 Bulk density and porosity

Hypothesis: Bulk density shows a sudden increase and porosity shows a sudden decrease at the transition to B1.

Bulk density shows a marked increase between the O/A and the AB horizon. This is to be expected, as the O/A horizon contains more organic matter, which has a lower particle density than mineral particles, and because porosity is higher due to root and invertebrate pores and lack of compaction. However, at the transition between AB and B1, bulk densities are more notable for their similarities than for their differences. Except for T1-5, where there is a sudden and unexpected increase in bulk density and decrease in porosity not seen in the other profiles, the 10 cm and 25 cm measurements are remarkably similar.

If we pool the 3.5 and 10 cm results for bulk density and porosity, we do see a statistically significant difference ($p = 0.003$ for bulk density; $p = 0.02$ for porosity) between the pooled O/A and AB horizons compared with the B1 horizon. However, this result is strongly influenced by the extreme values in the O/A horizon, which is much thinner than the AB horizon. In addition, while the results are statistically significant, they may not have a

significant effect: The change in bulk density is from 1.32 in the O/A-AB horizon to 1.44 in the B1. Porosity in these horizons are 47.28 % and 43.80 %, respectively.

If porosity and bulk density are controlling factors, it is uncertain whether we should expect subsurface runoff over the B1 horizon.

4.2.3 Hydraulic conductivity

Hypothesis: Hydraulic conductivity is significantly lower in the B1 horizon than in the horizons above.

There seems to be a significant difference, both statistically ($p < 0.000$) and physically, indicating that the hydraulic conductivity is on average 16.3 times greater in the AB horizon than in the B1 and B2 horizons collectively, even though bulk density and porosity do not differ significantly. This is probably due to a greater proportion of macropores to micropores in the A/B horizon than in the B horizon and lends support to the hypothesis.

The small samples used may significantly underestimate hydraulic conductivities, particularly where there are preferential flow patterns (Davis et al. 1999). In their study, Davis *et al*. found that the use of small samples for determining K_{sat} will have a high risk of significantly underestimating K_{sat} on a catchment scale by anything between one to three orders of magnitude, since they do not take preferential flows into account. As root and invertebrate pores are more dominant in the AB horizon than further down, these are more sensitive to such underestimation, and the actual difference in K_{sat} might as such be greater than the measurements show. However, this uncertainty is not likely to affect the conclusion that subsurface runoff is generated over the B1 horizon.

4.3 Dye tracer experiment

Hypothesis: If water mainly flows through the AB horizon, the dye tracer should be concentrated in the upper 15-20 cm, with less dye visible in the lower horizons.

Most of the dye is concentrated in the upper 20 cm region in the upper plot and in the upper 25 cm in the lower plot. Some macropore flow is generated to lower soil horizons. There is some penetration to the B horizon, possibly through macropore structures. Altogether, the hypothesis is supported by this experiment. Assuming average drainable porosity of 13.7, 12.3 and 10.4 at 10 cm, 25 cm and 50 cm, respectively, we have an average water storage capacity of 1.2 litres per cm soil depth, indicating that 80 mm of water should have penetrated to 65 cm depth. We can see only a few instances where the dye has penetrated below 30 cm,

and this could indicate that lateral flow dominates over vertical flow at greater depths. It also suggests that there is limited macropore flow in the B horizon.

4.4 Data analysis of climate vs soil moisture and discharge

4.4.1 Soil moisture response

Hypothesis: If water flows primarily over the B horizon, soil moisture in the AB horizon (10 cm sensor) should respond quickly to precipitation, and so should discharge. Soil moisture in the lower horizons (20 and 40 cm) should be more stable and show less variability with precipitation.

There is a clear difference between the response in the 10 cm depth (AB) and the 20 (start of B1) and 40 cm (B2) depths, and the variability is far greater in the AB horizon. However, the variability seen in the TDR measurements (θ_{max}-θ_{min}) for the 20 cm and 40 cm depth is considerably smaller than the drainable porosity measured at 25 cm and 50 cm. Thus, at 20 cm, the active porosity (ϕ_A as defined in the methods section) is only 3.9 % (compared to a drainable porosity of 12.3 %) and only 5.5 % at 40 cm (ϕ_D at 50 cm = 10.4 %). This may be a result of spatial heterogeneity, accidental compaction (caused by people walking over the installation site) of the soil above the TDR sensors or simply a matter of calibration of the TDR sensors, and the differences are small enough to be due to such factors. If the values are real, however, it is interesting to note that the variation seems to occur in the middle of the range of drainable porosity. Normally, we should expect that if the entire porosity is not filled with water, the smallest pores (closest to field capacity) would be filled up first, before the larger pores are filled (which happens when approaching saturation). The results indicate that the water content is always above that found at field capacity (2 % more), but that it never (or only rarely) reaches saturation, indicated at 40 cm by a maximum soil moisture of 0.402 which is only reached once during episode 3. As we have no pressure head data, we cannot tell for sure whether soil moisture varies all the way between field capacity and saturation or whether it never reaches saturation or field capacity.

The AB horizon varies much more in soil water content than the B horizons, and this supports the notion of subsurface flow over the B horizons.

Hypothesis: If the subsurface runoff is generated due to a decrease in conductivity at the AB–B1 transition, the AB horizon soil moisture should respond to precipitation before the B1 horizon.

Over all episodes, the soil moisture response is first apparent at 40 cm, then at 20 cm and finally at 10 cm. This would seem to indicate that any subsurface flow in the AB horizon is generated by saturation from below. This is in sharp contrast to the drainable saturation (defined as water filled pore space as a fraction of the *drainable* pore space) which shows that saturation is always below 45 % at 20 cm when response starts at 10 cm. This would indicate infiltration excess generated subsurface runoff. If we also look at the time lag from precipitation to response at the three horizons, we see that at episodes 1, 4, 5 and 7 is characterised by near simultaneous response of all three layers to the precipitation. Episodes 4 and 5 are also characterised by a high intensity at the start of the rainfall, where we would expect infiltration limitation and quick response in the upper horizon and delayed response deeper down. What we do not see in any case, however, is the AB horizon responding before the deeper soil. Even if we calculate saturation as a fraction of soil moisture variability (θ_{max}-θ_{min}), the AB horizon in many cases responds before the 20 cm depth is near saturation, but the lower horizons always respond first.

There is an apparent conflict between two results: a) The fact that soil moisture almost always responds first at 40 cm, then 20 cm and finally at 10 cm, should suggest that the dominant subsurface flow mechanism is saturation from below, and b) the fact that based on drainable porosity measurements, the soil never reaches saturation, should suggest that permeability limits infiltration from upper horizons and generates infiltration excess subsurface runoff. If we do not discount the discrepancies as errors or spatial heterogeneity, but accept the result that soil moisture varies between field capacity and saturation, but never reaches either, it may be due to a lack of equilibrium. The B horizons have a lower proportion of macropores than the AB horizon, and infiltrated water thus needs more time to penetrate into the matrix. When macropore water enters the B1 horizon, functional saturation will be reached as soon as the macropores are filled. In the AB horizon, macropores constitute a greater fraction of the total pore volume, and equilibrium is reached faster. Since infiltration from the AB horizon exceeds the infiltration capacity of the functionally saturated B1 horizon, the response is then not classifiable as either saturation or infiltration excess subsurface flow, but is rather a combination of the two.

4.4.2 Discharge response

Hypothesis: There is little or no deep percolation to groundwater, and the majority of precipitated water is accounted for, either as discharge or through evapotranspiration.

Storage change in groundwater on the hill slope and in the GDZ (ΔS) may represent an important part of the water balance, but the annual ΔS in a system in equilibrium should be approximately zero. As we do not have access to groundwater levels on the hill slope or in the GDZ, we can only infer that any precipitated water not accounted for in the discharge is lost through evapotranspiration or deep percolation. Perhaps the most striking characteristic of the discharge response is the great variation in the runoff coefficient, ranging from 3 % to 52 % over an annual average of 22 %. According to figures from a previous study, the discharge coefficient from the surrounding parent catchment (approximately 16 hectares) ranges from 41.2 % to 67.0 % from 2001–2004 (Larssen et al. 2011), which is significantly higher than the 22 % we see in our sub-catchment. Even if we accept that evapotranspiration may be as high as 60 % of precipitation (Wang 2011), we are still missing at least 18 %. It is important to stress that we do not yet know the evapotranspiration, and until we have clear data on this, any loss through deep percolation is pure speculation. In light of the results so far, however, it does seem reasonable to assume that a not insignificant proportion of water is unaccounted for through discharge and evapotranspiration, and that some water does percolate through to groundwater (ΔS).

4.4.3 Runoff coefficient vs antecedent soil moisture

Hypothesis: Antecedent soil moisture controls the runoff response, and the runoff coefficient increases with antecedent soil moisture.

Previous research indicates that the runoff coefficient has a general dependence on initial state, particularly antecedent soil moisture (Longobardi et al. 2003), with runoff coefficient increasing with antecedent soil moisture. Interestingly, the observed relationship is actually negative, with a very high correlation at the 20 cm depth of -0.944. Explained variation is 87 % for a linear model and as high as 95 % for a quadratic model. However, the variation in antecedent soil moisture is less than 1 %, from 0.345 to 0.354, and the data spread may be insufficient to draw any conclusions. It is likely that the high correlation is coincidental, and that the variation in antecedent soil moisture is too small to have any controlling influence on the runoff coefficient.

4.4.4 Infiltration

Hypothesis: Episode rainwater is primarily channelled through the AB horizon

The majority of the episode rain water seems to drain off through the AB horizon. All episodes are similar, except from episode three, which receives a higher proportion of the

infiltrated water in the B2 depth. This episode is also the most precipitation intensive of the three, which may indicate that particularly intensive precipitation may be channelled into the B2 horizon. It seems clear from the data that the major part of the soil water change takes place in the AB horizon.

4.5 Chemical fingerprint analysis of water samples

The slight increase in NH_4-N from CTF and the litter zone indicates that there must occur some local production of NH_4 from local decomposition. We can also see that NH_4-N is extremely quickly transformed to NO_3 by the sharp decrease in NH_4 between the litter zone and the O/A horizon at 5 cm and the corresponding, dramatic increase in NO_3 over the same transition. It should therefore be easy to identify Hortonian overland flow by correlating stream water NH_4-N concentrations with discharge.

Hypothesis: If episode precipitation generates Hortonian overland flow rather than being channelled through the soil, the water will pass through the litter zone, and we should find elevated concentrations of NH_4 in the stream water at intense episodes, as identified by high precipitation or discharge.

We can see no statistically significant correlation between NH_4-N concentrations and discharge or precipitation. It would then seem unlikely that Hortonian overland flow is generated at any time.

From the positive correlation of stream water NO_3-N and discharge, it seems reasonable to assume that NO_3 is quickly washed out with rain water and has little time to be taken up by plants or be transformed to gaseous N during episodes, and a short retention time gives elevated NO_3 concentrations in stream water. Inversely, it seems that in the dry season, with little rainfall and long retention times, and in late summer, with irregular and intensive rainfall, NO_3 often has ample time to be transformed by denitrification or taken up by plants.

We did not see any relationship between stream water NH_4-N concentrations and discharge, but we did find an inverse relationship between NO_3-N and NH_4-N. Since NH_4^+ is quickly transformed to NO_3^- in the soil and we have seen that there is no significant NH_4^+ leaching to stream water during episodes, we can expect NH_4^+ dilution during episodes. However, under certain conditions we may find dissimilatory nitrate reduction to ammonium (DNRA) (Burgin & Hamilton 2007; Otte et al. 1999; Schmidt et al. 2011). Traditionally, this was thought to occur only under strongly reducing conditions, which we find directly upstream of the stream water sample point, but it has also been demonstrated that the bacterium genus *Thioploca* may

oxidise sulphur by reducing internally stored nitrate to ammonium. Thus, some local NH_4^+ production may occur, which may help to explain the increased NH_4-N concentrations.

Water exchange, and thus element exchange, between the upper and lower horizons should reasonably depend on the conditions in the lower horizons during the episode, specifically the degree of saturation in the horizon directly below at the time of soil water response at a particular depth. In the case of saturation subsurface runoff there should be saturation contact across the horizons and favourable conditions with respect to water exchange (Scherrer & Naef 2003), and we can expect that newly infiltrated soil water is mixed with old, stored soil water before reaching the surface in a stream. However, in the case of infiltration excess subsurface flow there will be less contact between soil water across the horizons and thus limited exchange. It would be interesting to analyse soil water for spatial variation, but the available data does not have the required temporal resolution to identify short-term variability over episodes.

4.6 Modelling

There are a number of reasons why modelling using SUTRA failed. What follows is a brief discussion of the weaknesses of the approach.

4.6.1 Effects of scale

The modelled system has a scale which is too large to account for all heterogeneities such as local microtopography, rocks etc., but small enough for such heterogeneities to still have a significant effect on results. Slope curvature, for instance, will slow down the water flow and have a significant impact on modelling results, and this needs to be reflected in the model setup. The digital elevation model used as background for the model setup had an equidistance of 2 m, which does not give enough information to accurately represent the actual microtopography. The system is also small enough that small rocks and dimples will significantly divert water flow at this scale, as seen in the dye tracer experiment. All this taken together will make it difficult to calibrate the model on the basis of real measurements.

4.6.2 Macroporosity

The times I did get a result from modelling which responded to input driver data, the soil moisture most often responded by reaching saturation in all horizons very quickly. While it is uncertain whether the system gets quickly saturated or not, as we've seen in the discussion of the TDR measurements, we at least know that it drains again quickly, and this was not reflected in the modelling results. It has been documented that macropores have a significant

effect on hydraulic conductivity through preferential flow networks (Beven & Germann 1982; Bronstert & Plate 1997; Cheng 1988; Lamy et al. 2009; Nieber & Sidle 2010; Noguchi et al. 2001; Sidle et al. 2001), and that macropore impact increases with saturation (Bronstert & Plate 1997; Ridolfi et al. 2003). SUTRA employs a single-permeability approach, which does not account for the effect of macroporosity. As a result, SUTRA may not accurately predict the increased drainage rate which occurs when the system approaches saturation and models saturation very quickly as a response to intensive episodes which are quite common in TieShanPing.

4.6.3 Software errors

During simulations over long time or with high temporal resolution, the program very often encountered unexpected program terminations, and I have not been able to identify the reason behind this. One cause may be that the interpolation of input parameters results in too sharp transitions in soil physical properties, which again causes the software to encounter problems in solving the relevant differential equations. It may also be that SUTRA is not particularly well suited to cope with a high degree of heterogeneity in a medium-sized model domain.

5 Conclusions

5.1 Main findings

The study supports the initial hypothesis that episode rainwater is primarily channelled through the O/A and AB horizons, that no overland flow is generated and that vertical transport to deeper soil horizons is limited by soil physical characteristics in the B1 layer. The subsurface runoff response may be described as a combination of functional saturation of the B1 horizon and subsequent infiltration excess.

The discharge response suggests that groundwater levels buffer the discharge response to some degree, but without frequent groundwater measurements it is difficult to determine how much. The low discharge coefficient suggests that a not insignificant amount of water may escape the sub-catchment through deep percolation to groundwater and is thereby is lost from the water balance. Before we can make any estimations of the amount, however, we need more detailed information on evapotranspiration and change in groundwater levels. It is also difficult to predict runoff coefficient from initial conditions, as antecedent soil moisture variation seems too small to have a controlling effect on runoff response.

Soil water content seems to vary only within a fraction of the drainable porosity (defined as the difference between field capacity and saturation), and the difference between θ_{min} and θ_{max} for the entire monitoring period and saturation is quite small. This is likely due to lack of equilibrium, as infiltrated soil water fills up large and medium-sized pores quickly, but needs more time to penetrate to the smaller matrix pores. Given enough time to achieve equilibrium, the soil moisture will probably vary across the entire range of drainable porosity, but during episodes the changes take place too fast for equilibrium to be established.

5.2 Recommendations for future efforts

5.2.1 Methods

5.2.2 Soil water retention characteristic

New methods or better equipment for determining the soil water retention characteristic in the laboratory are necessary. Since the measurement method used here is an indirect method with several points where measurement errors may occur, it is somewhat unreliable in its nature. A better approach may be to use a combination of tension infiltrometers and TDR probes, ensuring that soil matrix potential and soil water content can be measured simultaneously, preferably solely on undisturbed samples.

5.2.3 Hydraulic conductivity

In order to avoid problems of underestimating the hydraulic conductivity due to small sample containers, in situ measurement techniques for K_{sat} should be considered as an alternative to laboratory measurements, particularly in macropore-dominated soils such as we see in the TieShanPing catchment.

5.2.4 *In situ* soil moisture measurements

In order to determine when and why subsurface flow occurs, we need detailed information on soil moisture and corresponding matrix potential to establish the degree of saturation in the individual soil horizons. In systems as flashy as the TieShanPing hill slope, it is also necessary to measure this at more frequent intervals (1-5 minutes) during episodes, as changes sometimes seem to occur very suddenly, at less than 10-minute intervals. In order for these measurements to form a calibration basis for subsequent modelling, soil moisture measurement equipment should also be placed on locations that are representative for several types of soil and/or microtopography, with at least two measuring stations. In order to determine the degree of groundwater buffering, groundwater level measurements should be taken at similar intervals as soil moisture measurements.

5.2.5 Sampling

Where possible, all episode sampling should be automatic. Many episodes occur during the night, and by the time we can reach the field for sampling, we will have missed the first and most interesting part of the episode. In addition, it is not always recommended to perform manual sampling during the night, particularly in areas with potentially dangerous wildlife.

For water chemistry to be of use in hydrological analyses, samples should be taken very frequently during episodes, if possible at intervals as low as 5 minutes during high-intensity episodes. A volume-proportional sampling regime with a minimum sampling frequency of one or two weeks in dry periods may be sufficient to achieve the required temporal resolution, if necessary in combination with specified time intervals when discharge exceeds a certain threshold.

5.2.6 Modelling

For future modelling to have a necessary degree of accuracy, a higher spatial resolution for microtopography and slope is necessary. Digital elevation models may not have the sufficient resolution to accurately represent the microtopography to the degree necessary in such heterogeneous systems, and manual levelling may be required to achieve this.

More importantly, the model to be used should take macroporosity into account, particularly in systems such as TieShanPing, where macroporosity is likely to be a dominant controlling factor for hydraulic conductivity in wet periods. HYDRUS 2D/3D (Simunek & van Genuchten 2008) is such a model, and there are others on the market which account for preferential flow, e.g. MACRO 4.3 and S1D DUAL. All these may be suitable for future modelling efforts and should be evaluated at the start of future projects.

6 References

Aber, J. D., Nadelhoffer, K. J., Steudler, P. & Melillo, J. M. (1989). NITROGEN SATURATION IN NORTHERN FOREST ECOSYSTEMS. *Bioscience*, 39 (6): 378-386.

Aber, J. D. (1992). Nitrogen cycling and nitrogen saturation in temperate forest ecosystems. *Trends in Ecology & Evolution*, 7 (7): 220-224.

Argus Holdings, L. (2010). *Argus ONE Home Page*. Available at: http://www.argusint.com/ (accessed: 28 May 2011).

Aubertin, G. M. (1971). *Nature and extent of macropores in forest soils and their influence on subsurface water movement*, vol. NE-192: For. Serv. Res. Pap. NE (U.S.D.A.). 33 pp.

Beven, K. & Germann, P. (1982). Macropores and waterflow in soils. *Water Resources Research*, 18 (5): 1311-1325.

Bittelli, M. & Flury, M. (2009). Errors in Water Retention Curves Determined with Pressure Plates. *Soil Science Society of America Journal*, 73 (5): 1453-1460.

Blake, G. R. & Hartge, K. H. (1986). Particle Density. In Klute, A. (ed.) *Methods of soil analysis - Part 1*, pp. 377-382. Madison Wis.: American Society of Agronomy : Soil Science Society of America.

Bronstert, A. & Plate, E. J. (1997). Modelling of runoff generation and soil moisture dynamics for hillslopes and micro-catchments. *Journal of Hydrology*, 198 (1-4): 177-195.

Burgin, A. J. & Hamilton, S. K. (2007). Have We Overemphasized the Role of Denitrification in Aquatic Ecosystems? A Review of Nitrate Removal Pathways. *Frontiers in Ecology and the Environment*, 5 (2): 89-96.

Busch, G., Lammel, G., Beese, F., Feichter, J., Dentener, F. & Roelofs, G.-J. (2001). Forest ecosystems and the changing patterns of nitrogen input and acid deposition today and in the future based on a scenario. *Environmental Science and Pollution Research*, 8 (2): 95-102.

Børresen, T. & Haugen, L. E. (2003). *Soil Physics, JORD221, Field and Laboratory Methods*. Ås, Norway: Department of plant and environmental sciences, Agricultural University of Norway. 36 pp. Unpublished manuscript.

Børresen, T. (2009). *The influence of structure on soil water retention at high underpressures*. Ås.

Chen, X. Y. (2006). *Nitrogen status and dynamics in selected subtropical forested catchments in South China under elevated atmospheric nitrogen deposition*. Ås: Norwegian University of Life Sciences, Department of Plant and Environmental Sciences. 1 b. (flere pag.) pp.

Cheng, J. D. (1988). Subsurface stormflows in the highly permeable forested watersheds of southwestern British Columbia. *Journal of Contaminant Hydrology*, 3 (2-4): 171-191.

Davis, S. H., Vertessy, R. A. & Silberstein, R. P. (1999). The sensitivity of a catchment model to soil hydraulic properties obtained by using different measurement techniques. *Hydrological Processes*, 13 (5): 677-688.

Dise, N. B. & Wright, R. F. (1995). Nitrogen leaching from European forests in relation to nitrogen deposition. *Forest Ecology and Management*, 71 (1-2): 153-161.

Famiglietti, J. S., Rudnicki, J. W. & Rodell, M. (1998). Variability in surface moisture content along a hillslope transect: Rattlesnake Hill, Texas. *Journal of Hydrology*, 210 (1-4): 259-281.

Hall, S. J. & Matson, P. A. (1999). Nitrogen oxide emissions after nitrogen additions in tropical forests. *Nature*, 400 (6740): 152-155.

Horton, R. E. (1933). The role of infiltration in the hydrolgical cycle. *Trans., Am. Geophys. Union*, 14: 446-460.
IMPACTS. (2004). Integrated Monitoring Program on Acidification of Chinese Terrestrial Systems-IMPACTS. Annual Report-Results 2003. In Larssen, T., Tang, D. & He, Y. (eds), SNO 4905-2004 (2004): Norwegian Institute for Water Research, Oslo, Norway. 94 pp.
Kirkby, M. (1988). Hillslope runoff processes and models. *Journal of Hydrology*, 100 (1-3): 315-339.
Koba, K., Osaka, K., Tobari, Y., Toyoda, S., Ohte, N., Katsuyama, M., Suzuki, N., Itoh, M., Yamagishi, H., Kawasaki, M., et al. (2009). Biogeochemistry of nitrous oxide in groundwater in a forested ecosystem elucidated by nitrous oxide isotopomer measurements. *Geochimica et Cosmochimica Acta*, 73 (11): 3115-3133.
Krogstad, T., Jørgensen, P., Sogn, T., Børresen, T. & Kolnes, A. G. (1991). *Manual for kornfordelingsanalyse etter pipettemetoden: forbehandling og pipetteringsprosedyre : dataprogrammer for veiing, beregning og utskrift*. Rapport. Ås: Instituttet. 41 bl. pp.
Lamy, E., Lassabatere, L., Bechet, B. & Andrieu, H. (2009). Modeling the influence of an artificial macropore in sandy columns on flow and solute transfer. *Journal of Hydrology*, 376 (3-4): 392-402.
Larssen, T., Duan, L. & Mulder, J. (2011). Deposition and Leaching of Sulfur, Nitrogen and Calcium in Four Forested Catchments in China: Implications for Acidification. *Environmental Science & Technology*, 45 (4): 1192-1198.
Leijnse, T. (2009). *SUTRA version 2.1, adaptions by Toon Leijnse, version 4*. 4 ed.
Longobardi, A., Villani, P., Grayson, R. B., Western, A. W. & Mssanzi. (2003). *On the relationship between runoff coefficient and catchment initial conditions*. Modsim 2003: International Congress on Modelling and Simulation, Vols 1-4 - Vol 1: Natural Systems, Pt 1; Vol 2: Natural Systems, Pt 2; Vol 3: Socio-Economic Systems; Vol 4: General Systems. Nedlands: Univ Western Australia. 867-872 pp.
McGlynn, B. L., McDonnel, J. J. & Brammer, D. D. (2002). A review of the evolving perceptual model of hillslope flowpaths at the Maimai catchments, New Zealand. *Journal of Hydrology*, 257 (1-4): 1-26.
Meerveld, I. T.-v. & Weiler, M. (2008). Hillslope dynamics modeled with increasing complexity. *Journal of Hydrology*, 361 (1-2): 24-40.
Nieber, J. L. & Sidle, R. C. (2010). How do disconnected macropores in sloping soils facilitate preferential flow? *Hydrological Processes*, 24 (12): 1582-1594.
Noguchi, S., Tsuboyama, Y., Sidle, R. C. & Hosoda, I. (2001). Subsurface runoff characteristics from a forest hillslope soil profile including macropores, Hitachi Ohta, Japan. *Hydrological Processes*, 15 (11): 2131-2149.
Otte, S., Kuenen, J. G., Nielsen, L. P., Paerl, H. W., Zopfi, J., Schulz, H. N., Teske, A., Strotmann, B., Gallardo, V. A. & Jorgensen, B. B. (1999). Nitrogen, carbon, and sulfur metabolism in natural Thioploca samples. *Applied and Environmental Microbiology*, 65 (7): 3148-3157.
Reeuwijk, L. P. (ed.) (2002). *Procedures for Soil Analysis*. 6 ed. Technical Paper 9: ISRIC, Wageningen.
Ridolfi, L., D'Odorico, P., Porporato, A. & Rodriguez-Iturbe, I. (2003). Stochastic soil moisture dynamics along a hillslope. *Journal of Hydrology*, 272 (1-4): 264-275.
Rutsinda, J. (2010). *Grain size distribution and clay mineralogy in eutrophic lake-sediments. Case study, Årungen*. Master thesis. Ås, Norway: Norwegian University of Life Sciences, Department of plant and environmental sciences. 80 pp.
Scherrer, S. & Naef, F. (2003). A decision scheme to indicate dominant hydrological flow processes on temperate grassland. *Hydrological Processes*, 17 (2): 391-401.

Schmidt, C. S., Richardson, D. J. & Baggs, E. M. (2011). Constraining the conditions conducive to dissimilatory nitrate reduction to ammonium in temperate arable soils. *Soil Biology and Biochemistry*, 43 (7): 1607-1611.
Sidle, R. C., Noguchi, S., Tsuboyama, Y. & Laursen, K. (2001). A conceptual model of preferential flow systems in forested hillslopes: evidence of self-organization. *Hydrological Processes*, 15 (10): 1675-1692.
Simunek, J. & van Genuchten, M. T. (2008). Modeling nonequilibrium flow and transport processes using HYDRUS. *Vadose Zone Journal*, 7 (2): 782-797.
Simunek, J., van Genuchten, M. T. & Sejna, M. (2008). Development and Applications of the HYDRUS and STANMOD Software Packages and Related Codes. *Vadose Zone J*, 7 (2): 587-600.
Stolte, J., Freijer, J. I., Bouten, W., Dirksen, C., Halbertsma, J. M., Vandam, J. C., Vandenberg, J. A., Veerman, G. J. & Wosten, J. H. M. (1994). COMPARISON OF 6 METHODS TO DETERMINE UNSATURATED SOIL HYDRAULIC CONDUCTIVITY. *Soil Science Society of America Journal*, 58 (6): 1596-1603.
Stolte, J. (ed.) (1997). *Manual for soil physical measurements*. 3 ed. Technical Paper 37: DLO Winand Staring Centre, Wageningen.
Tietema, A. (1998). Microbial carbon and nitrogen dynamics in coniferous forest floor material collected along a European nitrogen deposition gradient. *Forest Ecology and Management*, 101 (1-3): 29-36.
USGS. (2010a). *SutraGUI Version 2.2.2.0*: U.S. Geological Survey. Available at: http://water.usgs.gov/nrp/gwsoftware/sutra-gui/sutra-gui.html (accessed: 28 June 2011).
USGS. (2010b). *Water Resources of the United States - SUTRA version 2.2*: U.S. Geological Survey. Available at: http://water.usgs.gov/nrp/gwsoftware/sutra/sutra.html (accessed: 28 June 2011).
van Genuchten, M. T. (1992). *The RETC code for quantifying the hydraulic functions of unsaturated soils [microform] : project summary / M.Th. van Genuchten, F.J. Leij, and S.R. Yates*. Ada, OK :: U.S. Environmental Protection Agency, Robert S. Kerr Environmental Research Laboratory.
Voss, C. I. & Provost, A. M. (2002). *SUTRA: A model for saturated-unsaturated, variable-density ground-water flow with solute or energy transport*. Version 2.1 ed. U.S. Geological Survey Water-Resources Investigations Report, 2002-4231. p. 279.
Wang, Y. (2011). *Estimation of runoff coefficient and evapotranspiration in TSP*. Hole.
WeatherHawk. (2011). *WeatherHawk 232 Direct Connect Weather Station*: WeatherHawk. Available at: http://www.weatherhawk.com/s232dc (accessed: 27 May 2011).
Weiler, M. & McDonnell, J. (2004). Virtual experiments: a new approach for improving process conceptualization in hillslope hydrology. *Journal of Hydrology*, 285 (1-4): 3-18.
Weiler, M. & McDonnell, J. R. J. (2006). Testing nutrient flushing hypotheses at the hillslope scale: A virtual experiment approach. *Journal of Hydrology*, 319 (1-4): 339-356.
Wrage, N., Velthof, G. L., van Beusichem, M. L. & Oenema, O. (2001). Role of nitrifier denitrification in the production of nitrous oxide. *Soil Biology and Biochemistry*, 33 (12-13): 1723-1732.

7 Appendix

Appendix I: Statistics

Appendix II: Soil profile descriptions

Appendix III: Precipitation and discharge

Other data is available electronically on request

Appendix I: Statistics

Bulk density

One-way ANOVA: Bulk density versus Depth

```
Source  DF      SS      MS      F      P
Depth    3  0.7483  0.2494  14.23  0.000
Error   53  0.9292  0.0175
Total   56  1.6776

S = 0.1324   R-Sq = 44.61%   R-Sq(adj) = 41.47%


                           Individual 95% CIs For Mean Based on
                           Pooled StDev
Level   N    Mean   StDev  -----+---------+---------+---------+----
3.5    15  1.2055  0.1969  (----*-----)
10     15  1.4430  0.1047                (----*-----)
25     15  1.4419  0.0887               (-----*-----)
50     12  1.5039  0.1056                    (-----*------)
                           -----+---------+---------+---------+----
                              1.20      1.32      1.44      1.56

Pooled StDev = 0.1324
```

One-way ANOVA: Bulk density versus Upper/middle/lower

```
Source              DF      SS      MS     F      P
Upper/middle/lower   2  0.3252  0.1626  6.49  0.003
Error               54  1.3524  0.0250
Total               56  1.6776

S = 0.1583   R-Sq = 19.39%   R-Sq(adj) = 16.40%


                           Individual 95% CIs For Mean Based on
                           Pooled StDev
Level    N    Mean   StDev  ---+---------+---------+---------+------
Upper   30  1.3243  0.1965  (----*-----)
Middle  15  1.4419  0.0887          (-------*-------)
Lower   12  1.5039  0.1056              (--------*---------)
                           ---+---------+---------+---------+------
                            1.30      1.40      1.50      1.60

Pooled StDev = 0.1583
```

Porosity

One-way ANOVA: Pore volume (%) versus Depth

```
Source  DF      SS     MS     F      P
Depth    3   508.4  169.5  7.70  0.000
Error   53  1166.9   22.0
Total   56  1675.3

S = 4.692   R-Sq = 30.35%   R-Sq(adj) = 26.41%


                          Individual 95% CIs For Mean Based on
```

```
                          Pooled StDev
Level   N    Mean  StDev  -----+---------+---------+---------+----
3.5    15  50.451  6.063                       (------*------)
10     15  44.110  5.747     (------*------)
25     15  43.804  2.985    (------*------)
50     12  43.109  2.431  (-------*-------)
                          -----+---------+---------+---------+----
                            42.0      45.5      49.0      52.5

Pooled StDev = 4.692
```

One-way ANOVA: Pore volume (%) versus Upper/middle/lower

```
Source              DF      SS     MS     F      P
Upper/middle/lower   2   206.8  103.4  3.80  0.028
Error               54  1468.4   27.2
Total               56  1675.3

S = 5.215   R-Sq = 12.35%   R-Sq(adj) = 9.10%


                           Individual 95% CIs For Mean Based on Pooled StDev
Level    N    Mean  StDev     +---------+---------+---------+---------
Upper   30  47.281  6.640                         (-------*-------)
Middle  15  43.804  2.985         (----------*----------)
Lower   12  43.109  2.431     (-----------*------------)
                              +---------+---------+---------+---------
                             40.0      42.5      45.0      47.5

Pooled StDev = 5.215
```

Hydraulic conductivity

Two-Sample T-Test and CI: log K (cm d-1); Soil horizon

```
Two-sample T for log K (cm d-1)

Soil
horizon   N   Mean  StDev  SE Mean
AB       28   1.63   1.04     0.20
B        23  0.419  0.825     0.17


Difference = mu (AB) - mu (B)
Estimate for difference:  1.213
95% CI for difference:  (0.689; 1.738)
T-Test of difference = 0 (vs not =): T-Value = 4.65  P-Value = 0.000  DF = 48
```

Water balance

Regression Analysis: Cr versus Antecedent soil moisture 20 cm

```
The regression equation is
Cr = 20.22 - 57.17 Antecedent soil moisture 20 cm


S = 0.0754816   R-Sq = 89.2%   R-Sq(adj) = 87.0%


Analysis of Variance
```

```
Source      DF        SS        MS      F      P
Regression   1  0.235306  0.235306  41.30  0.001
Error        5  0.028487  0.005697
Total        6  0.263793
```

Polynomial Regression Analysis: Cr versus Antecedent soil moisture 20 cm

```
The regression equation is
Cr = 904.9 - 5123 Antecedent soil moisture 20 cm
     + 7252 Antecedent soil moisture 20 cm**2


S = 0.0468225   R-Sq = 96.7%   R-Sq(adj) = 95.0%


Analysis of Variance

Source      DF        SS        MS      F      P
Regression   2  0.255024  0.127512  58.16  0.001
Error        4  0.008769  0.002192
Total        6  0.263793


Sequential Analysis of Variance

Source     DF        SS      F      P
Linear      1  0.235306  41.30  0.001
Quadratic   1  0.019718   8.99  0.040
```

Regression Analysis: Runoff (mm) versus Infiltration (mm)

```
The regression equation is
Runoff (mm) = - 42.51 + 2.615 Infiltration (mm)


S = 8.28326   R-Sq = 58.5%   R-Sq(adj) = 50.2%


Analysis of Variance

Source      DF       SS       MS     F      P
Regression   1  483.220  483.220  7.04  0.045
Error        5  343.062   68.612
Total        6  826.282
```

Chemistry

Correlations: Rain; Stream water NO3-N; Stream water NH4-N Dry season

```
                  Rain_Dry season  NO3-N_stream_Dry season
NO3-N_stream_Dry            -0.092
                             0.863

NH4-N_stream_Dry             0.993            -0.162
                             0.000             0.759


Cell Contents: Pearson correlation
               P-Value
```

Correlations: Rain; Avg soil NO3-N; Avg soil NH4-N Dry season

```
                   Rain_Dry season  Avg soil NO3-N
Avg soil NO3-N             -0.852
                            0.148

Avg soil NH4-N             -0.898             0.930
                            0.102             0.022


Cell Contents: Pearson correlation
               P-Value
```

Correlations: Rain; Stream water NO3-N; Stream water NH4-N Early summer

```
                  Sum_rain_Early s  NO3-N_stream_Ear
NO3-N_stream_Ear             0.665
                             0.013

NH4-N_stream_Ear            -0.050            -0.448
                             0.871             0.125


Cell Contents: Pearson correlation
               P-Value
```

Correlations: Rain; Avg soil NO3-N; Avg soil NH4-N Early summer

```
                  Rain_Early summer  Avg soil NO3-N
Avg soil NO3-N             -0.249
                            0.686

Avg soil NH4-N             -0.641             0.396
                            0.244             0.509


Cell Contents: Pearson correlation
               P-Value
```

Correlations: Rain; Stream water NO3-N; Stream water NH4-N Late summer

```
                  Sum_rain_Late su  NO3-N_stream_Lat
NO3-N_stream_Lat             0.606
                             0.001

NH4-N_stream_Lat             0.039            -0.233
                             0.848             0.234


Cell Contents: Pearson correlation
               P-Value
```

Correlations: Rain; Avg soil NO3-N; Avg soil NH4-N Late summer

```
                  Rain_Late summer  Avg soil NO3-N
Avg soil NO3-N             0.644
                           0.085

Avg soil NH4-N             0.365            -0.186
                           0.373             0.660


Cell Contents: Pearson correlation
               P-Value
```

Correlations: Sum_rain; Avg soil NO3-N; Avg soil NH4-N

```
                      Sum_rain  Avg soil NO3-N
Avg soil NO3-N          -0.208
                         0.423

Avg soil NH4-N          -0.381           0.259
                         0.131           0.300


Cell Contents: Pearson correlation
               P-Value
```

Correlations: Sum_rain; NO3-N_stream; NH4-N_stream

```
                    Sum_rain  NO3-N_stream
NO3-N_stream           0.385
                       0.008

NH4-N_stream           0.053        -0.306
                       0.726         0.037


Cell Contents: Pearson correlation
               P-Value
```

One-way ANOVA: Discharge versus Season

```
Source   DF      SS     MS      F      P
Season    2   40.47  20.23  18.23  0.000
Error   322  357.46   1.11
Total   324  397.93

S = 1.054   R-Sq = 10.17%   R-Sq(adj) = 9.61%


                                  Individual 95% CIs For Mean Based on
                                  Pooled StDev
Level           N   Mean  StDev  -----+---------+---------+---------+----
Dry season    151  0.005  0.047  (----*----)
Early summer   91  0.839  1.092                       (-----*-----)
Late summer    83  0.447  1.745            (------*-----)
                                  -----+---------+---------+---------+----
                                     0.00      0.35      0.70      1.05

Pooled StDev = 1.054
```

One-way ANOVA: pH stream versus Season

```
Source  DF     SS     MS     F      P
Season   2  0.743  0.371  3.54  0.037
Error   44  4.614  0.105
Total   46  5.357

S = 0.3238   R-Sq = 13.87%   R-Sq(adj) = 9.95%


                                   Individual 95% CIs For Mean Based on
                                   Pooled StDev
Level          N    Mean   StDev  --+---------+---------+---------+-------
Dry season     6  4.4867  0.1954              (------------*-------------)
Early summer  13  4.1508  0.1482  (---------*--------)
Late summer   28  4.4140  0.3925                   (-----*-----)
                                   --+---------+---------+---------+-------
                                   4.00      4.20      4.40      4.60
```

```
Pooled StDev = 0.3238
```

One-way ANOVA: NO3-N_stream (mg/l) versus Season

```
Source  DF      SS     MS      F      P
Season   2   49.35  24.68  11.83  0.000
Error   44   91.81   2.09
Total   46  141.17

S = 1.445   R-Sq = 34.96%   R-Sq(adj) = 32.01%


                              Individual 95% CIs For Mean Based on
                              Pooled StDev
Level          N   Mean  StDev  ------+---------+---------+---------+---
Dry season     6  2.896  1.866  (---------*---------)
Early summer  13  5.002  1.056                      (------*-----)
Late summer   28  2.678  1.503     (---*----)
                              ------+---------+---------+---------+---
                                  2.4       3.6       4.8       6.0

Pooled StDev = 1.445
```

One-way ANOVA: NH4-N_stream (mg/l) versus Season

```
Source  DF       SS       MS     F      P
Season   2  0.01443  0.00722  1.05  0.360
Error   44  0.30348  0.00690
Total   46  0.31791

S = 0.08305   R-Sq = 4.54%   R-Sq(adj) = 0.20%


                                 Individual 95% CIs For Mean Based on
                                 Pooled StDev
Level          N     Mean    StDev  ---+---------+---------+---------+------
Dry season     6  0.05759  0.10755  (------------------*-------------------)
Early summer  13  0.03632  0.03588  (------------*-------------)
Late summer   28  0.07636  0.09233                (--------*--------)
                                 ---+---------+---------+---------+------
                                  0.000     0.035     0.070     0.105

Pooled StDev = 0.08305
```

One-way ANOVA: Avg soil pH versus Season

```
Source  DF       SS       MS     F      P
Season   2  0.15479  0.07739  8.80  0.003
Error   15  0.13196  0.00880
Total   17  0.28675

S = 0.09379   R-Sq = 53.98%   R-Sq(adj) = 47.84%


                               Individual 95% CIs For Mean Based on
                               Pooled StDev
Level         N    Mean   StDev  -----+---------+---------+---------+----
Dry season    5  3.8201  0.1230                   (--------*--------)
Early summer  5  3.7817  0.1157               (--------*--------)
Late summer   8  3.6165  0.0506  (------*------)
                               -----+---------+---------+---------+----
                                  3.60      3.70      3.80      3.90

Pooled StDev = 0.0938
```

One-way ANOVA: Soil NO3-N (mg/l) versus Season

```
Source   DF       SS      MS      F      P
Season    2   6350.0  3175.0  37.25  0.000
Error   327  27873.9    85.2
Total   329  34223.9

S = 9.233   R-Sq = 18.55%   R-Sq(adj) = 18.06%


                                  Individual 95% CIs For Mean Based on
                                  Pooled StDev
Level           N    Mean   StDev  ---+---------+---------+---------+------
Dry season    112  20.885  12.053                            (----*----)
Early summer  117  11.108   7.941  (----*----)
Late summer   101  12.347   6.658     (----*----)
                                  ---+---------+---------+---------+------
                                  10.5      14.0      17.5      21.0

Pooled StDev = 9.233
```

One-way ANOVA: Soil NH4-N (mg/l) versus Season

```
Source   DF       SS      MS     F      P
Season    2   0.0492  0.0246  0.79  0.455
Error   327  10.2021  0.0312
Total   329  10.2513

S = 0.1766   R-Sq = 0.48%   R-Sq(adj) = 0.00%


                                  Individual 95% CIs For Mean Based on
                                  Pooled StDev
Level           N    Mean   StDev  -------+---------+---------+---------+--
Dry season    112  0.1184  0.2532            (------------*------------)
Early summer  117  0.0891  0.1304  (------------*-----------)
Late summer   101  0.1020  0.1055     (-------------*-------------)
                                  -------+---------+---------+---------+--
                                       0.075     0.100     0.125     0.150

Pooled StDev = 0.1766
```

Regression Analysis: NO3-N in stream water versus Discharge in Dry season

```
The regression equation is
NO3-N_stream (mg/l)_Dry season = 3.37 - 291 Discharge_Dry season


6 cases used, 145 cases contain missing values


Predictor              Coef  SE Coef      T      P
Constant             3.3686   0.9589   3.51  0.025
Discharge_Dry season  -291.3    340.7  -0.86  0.441


S = 1.91854   R-Sq = 15.5%   R-Sq(adj) = 0.0%


Analysis of Variance

Source          DF      SS     MS     F      P
```

```
Regression       1   2.691  2.691  0.73  0.441
Residual Error   4  14.723  3.681
Total            5  17.414
```

Regression Analysis: NO3-N in stream water versus Discharge in Early summer

```
The regression equation is
NO3-N_stream (mg/l_Early summer = 4.39 + 0.565 Discharge_Early summer


13 cases used, 78 cases contain missing values


Predictor                 Coef  SE Coef      T      P
Constant                4.3923   0.2450  17.93  0.000
Discharge_Early summer  0.5652   0.1393   4.06  0.002


S = 0.698045   R-Sq = 59.9%   R-Sq(adj) = 56.3%


Analysis of Variance

Source          DF       SS      MS      F      P
Regression       1   8.0228  8.0228  16.46  0.002
Residual Error  11   5.3599  0.4873
Total           12  13.3827
```

Regression Analysis: NO3-N in stream water versus Discharge in Late summer

```
The regression equation is
NO3-N_stream (mg/l)_Late summer = 1.41 + 12.3 Discharge_Late summer


9 cases used, 206 cases contain missing values


Predictor                Coef  SE Coef     T      P
Constant               1.4073   0.3046  4.62  0.002
Discharge_Late summer  12.279    3.350  3.66  0.008


S = 0.688368   R-Sq = 65.7%   R-Sq(adj) = 60.8%


Analysis of Variance

Source          DF      SS      MS      F      P
Regression       1  6.3646  6.3646  13.43  0.008
Residual Error   7  3.3170  0.4739
Total            8  9.6815
```

Regression Analysis: NH4-N in stream water versus Discharge in Dry season

```
The regression equation is
NH4-N_stream (mg/l)_Dry season = 0.0728 - 9.4 Discharge_Dry season


6 cases used, 145 cases contain missing values
```

```
Predictor                Coef  SE Coef      T      P
Constant              0.07284  0.05863   1.24  0.282
Discharge_Dry season    -9.39    20.83  -0.45  0.675


S = 0.117300   R-Sq = 4.8%   R-Sq(adj) = 0.0%


Analysis of Variance

Source          DF       SS       MS     F      P
Regression       1  0.00280  0.00280  0.20  0.675
Residual Error   4  0.05504  0.01376
Total            5  0.05783
```

Regression Analysis: NH4-N in stream water versus Discharge in Early summer

```
The regression equation is
NH4-N_stream (mg/l_Early summer = 0.0454 - 0.00842 Discharge_Early summer


13 cases used, 78 cases contain missing values


Predictor                   Coef   SE Coef      T      P
Constant                 0.04539   0.01237   3.67  0.004
Discharge_Early summer  -0.008418  0.007035  -1.20  0.257


S = 0.0352558   R-Sq = 11.5%   R-Sq(adj) = 3.5%


Analysis of Variance

Source          DF        SS        MS     F      P
Regression       1  0.001780  0.001780  1.43  0.257
Residual Error  11  0.013673  0.001243
Total           12  0.015452
```

Regression Analysis: NH4-N in stream water versus Discharge in Late summer

```
The regression equation is
NH4-N_stream (mg/l)_Late summer = 0.132 - 0.420 Discharge_Late summer


9 cases used, 206 cases contain missing values


Predictor                Coef  SE Coef      T      P
Constant              0.13250  0.07023   1.89  0.101
Discharge_Late summer  -0.4197   0.7727  -0.54  0.604


S = 0.158746   R-Sq = 4.0%   R-Sq(adj) = 0.0%


Analysis of Variance

Source          DF       SS       MS     F      P
Regression       1  0.00743  0.00743  0.29  0.604
Residual Error   7  0.17640  0.02520
Total            8  0.18384
```

Regression Analysis: Avg soil NO3-N versus Rain in the Dry season

```
The regression equation is
Avg soil NO3-N_Dry season = 22.1 - 3.80 Sum_rain_Dry season


4 cases used, 147 cases contain missing values


Predictor               Coef  SE Coef      T      P
Constant             22.1368   0.8273  26.76  0.001
Sum_rain_Dry season   -3.801    1.655  -2.30  0.148


S = 1.43286   R-Sq = 72.5%   R-Sq(adj) = 58.8%


Analysis of Variance

Source          DF      SS      MS     F      P
Regression       1  10.837  10.837  5.28  0.148
Residual Error   2   4.106   2.053
Total            3  14.944
```

Regression Analysis: Avg soil NO3-N versus Rain in Early summer

```
The regression equation is
Avg soil NO3-N_Early summer = 11.4 - 0.0255 Sum_rain_Early summer


5 cases used, 86 cases contain missing values


Predictor                  Coef  SE Coef      T      P
Constant                 11.389    1.051  10.84  0.002
Sum_rain_Early summer  -0.02553  0.05731  -0.45  0.686


S = 1.77744   R-Sq = 6.2%   R-Sq(adj) = 0.0%


Analysis of Variance

Source          DF      SS     MS     F      P
Regression       1   0.627  0.627  0.20  0.686
Residual Error   3   9.478  3.159
Total            4  10.105
```

Regression Analysis: Avg soil NO3-N versus Rain in Late summer

```
The regression equation is
Avg soil NO3-N_Late summer = 11.3 + 0.473 Sum_rain_Late summer


8 cases used, 207 cases contain missing values


Predictor               Coef  SE Coef     T      P
Constant              11.324    1.216  9.31  0.000
Sum_rain_Late summer  0.4734   0.2294  2.06  0.085


S = 2.98945   R-Sq = 41.5%   R-Sq(adj) = 31.8%
```

Analysis of Variance

Source	DF	SS	MS	F	P
Regression	1	38.066	38.066	4.26	0.085
Residual Error	6	53.621	8.937		
Total	7	91.687			

Regression Analysis: Avg soil NH4-N versus Rain in the Dry season

The regression equation is
Avg soil NH4-N_Dry season = 0.166 - 0.150 Sum_rain_Dry season

4 cases used, 147 cases contain missing values

Predictor	Coef	SE Coef	T	P
Constant	0.16636	0.02597	6.40	0.024
Sum_rain_Dry season	-0.15032	0.05195	-2.89	0.102

S = 0.0449893 R-Sq = 80.7% R-Sq(adj) = 71.1%

Analysis of Variance

Source	DF	SS	MS	F	P
Regression	1	0.016946	0.016946	8.37	0.102
Residual Error	2	0.004048	0.002024		
Total	3	0.020994			

Regression Analysis: Avg soil NH4-N versus Rain in Early summer

The regression equation is
Avg soil NH4-N_Early summer = 0.122 - 0.00287 Sum_rain_Early summer

5 cases used, 86 cases contain missing values

Predictor	Coef	SE Coef	T	P
Constant	0.12242	0.03641	3.36	0.044
Sum_rain_Early summer	-0.002873	0.001985	-1.45	0.244

S = 0.0615667 R-Sq = 41.1% R-Sq(adj) = 21.5%

Analysis of Variance

Source	DF	SS	MS	F	P
Regression	1	0.007942	0.007942	2.10	0.244
Residual Error	3	0.011371	0.003790		
Total	4	0.019313			

Regression Analysis: Avg soil NH4-N versus Rain in Late summer

The regression equation is
Avg soil NH4-N_Late summer = 0.0977 + 0.00282 Sum_rain_Late summer

8 cases used, 207 cases contain missing values

Predictor	Coef	SE Coef	T	P
Constant	0.09775	0.01556	6.28	0.001
Sum_rain_Late summer	0.002822	0.002934	0.96	0.373

S = 0.0382417 R-Sq = 13.4% R-Sq(adj) = 0.0%

Analysis of Variance

Source	DF	SS	MS	F	P
Regression	1	0.001353	0.001353	0.92	0.373
Residual Error	6	0.008775	0.001462		
Total	7	0.010127			

Descriptive Statistics: Average pH, NO3-N and NH4-N in soil water over all depths and profiles and pH, NO3-N and NH4-N in stream water

Variable	Season	N	Mean	StDev	Minimum	Median	Maximum
Avg soil pH	Dry season	5	3.8201	0.1230	3.6750	3.8089	4.0054
	Early summer	5	3.7817	0.1157	3.6265	3.8492	3.8754
	Late summer	8	3.6165	0.0506	3.5600	3.5962	3.6914
pH _stream	Dry season	6	4.4867	0.1954	4.1500	4.5200	4.7000
	Early summer	13	4.1508	0.1482	3.9300	4.1400	4.4800
	Late summer	28	4.4140	0.3925	3.8300	4.3250	5.9400
Avg soil NO3-N	Dry season	5	20.68	2.24	18.34	20.48	23.00
	Early summer	5	11.083	1.589	8.909	11.507	12.924
	Late summer	8	12.57	3.62	9.98	11.52	21.16
NO3-N_stream	Dry season	6	2.896	1.866	1.850	2.232	6.660
	Early summer	13	5.002	1.056	3.449	4.676	7.254
	Late summer	28	2.678	1.503	0.106	2.724	6.144
Avg soil NH4-N	Dry season	5	0.1142	0.0794	0.0160	0.1325	0.2174
	Early summer	5	0.0879	0.0695	0.0331	0.0474	0.1987
	Late summer	8	0.1052	0.0380	0.0479	0.1129	0.1524
NH4-N_stream	Dry season	6	0.0576	0.1075	0.0000	0.0194	0.2757
	Early summer	13	0.03632	0.03588	0.00000	0.03106	0.13977
	Late summer	28	0.0764	0.0923	0.0000	0.0561	0.4970

Descriptive Statistics: pH, NO3-N and NH4-N in soil water

Results for Season = Dry season

Variable	Depth	N	Mean	StDev	Minimum	Median	Maximum
pH	1	28	3.6618	0.1703	3.3200	3.6500	3.9600
	2	29	3.7597	0.1340	3.5200	3.7600	4.0300
	3	25	3.8848	0.1590	3.4600	3.9000	4.1500
	4	19	3.9658	0.1210	3.7700	3.9500	4.2500
NO3-N (mg/l)	1	30	25.24	15.50	9.89	20.60	65.64
	2	29	25.36	12.32	12.04	21.74	57.00
	3	27	16.83	5.90	1.23	17.27	36.19
	4	26	15.07	7.82	8.44	12.95	36.94
NH4-N (mg/l)	1	30	0.2557	0.4440	0.0000	0.0778	1.8667
	2	29	0.0727	0.0999	0.0000	0.0311	0.3500
	3	27	0.0640	0.0829	0.0000	0.0389	0.3422
	4	26	0.0673	0.0822	0.0000	0.0428	0.3111

Results for Season = Early summer

Variable	Depth	N	Mean	StDev	Minimum	Median	Maximum
pH	1	30	3.7183	0.1482	3.4600	3.7200	4.0200
	2	28	3.7418	0.1577	3.4500	3.7300	4.0300
	3	28	3.8293	0.1250	3.6300	3.8400	4.0300
	4	29	3.8666	0.1488	3.5700	3.8600	4.0800
NO3-N (mg/l)	1	30	9.079	4.101	4.098	8.007	22.034
	2	29	10.13	9.24	1.28	7.59	49.19
	3	28	12.27	8.92	3.69	8.83	32.65
	4	30	13.00	8.30	1.13	11.08	38.28
NH4-N (mg/l)	1	30	0.1042	0.1650	0.0000	0.0661	0.8944
	2	29	0.1167	0.1859	0.0000	0.0544	0.7933
	3	28	0.0804	0.0592	0.0078	0.0622	0.2256
	4	30	0.05543	0.04331	0.00000	0.04278	0.14778

Results for Season = Late summer

Variable	Depth	N	Mean	StDev	Minimum	Median	Maximum
pH	1	24	3.5692	0.1501	3.2100	3.5350	3.8700
	2	17	3.6247	0.0689	3.5400	3.6200	3.7500
	3	13	3.6838	0.0705	3.5700	3.7000	3.7700
	4	13	3.6931	0.0664	3.5800	3.6700	3.8100
NO3-N (mg/l)	1	30	17.43	6.49	7.57	16.40	36.75
	2	28	10.82	6.23	0.00	11.63	31.86
	3	20	9.01	4.52	1.99	9.23	23.02
	4	23	10.48	5.37	5.54	9.50	27.16
NH4-N (mg/l)	1	30	0.1021	0.0864	0.0000	0.0894	0.2644
	2	28	0.1372	0.1452	0.0000	0.0739	0.4978
	3	20	0.0786	0.0834	0.0000	0.0428	0.2489
	4	23	0.0795	0.0793	0.0000	0.0544	0.3033

Descriptive Statistics: pH, NO3-N and NH4-N in stream water by season

Variable	Season	N	Mean	StDev	Minimum	Median	Maximum
pH _stream	Dry season	6	4.4867	0.1954	4.1500	4.5200	4.7000
	Early summer	13	4.1508	0.1482	3.9300	4.1400	4.4800
	Late summer	28	4.4140	0.3925	3.8300	4.3250	5.9400
NO3-N_stream	Dry season	6	2.896	1.866	1.850	2.232	6.660
	Early summer	13	5.002	1.056	3.449	4.676	7.254
	Late summer	28	2.678	1.503	0.106	2.724	6.144
NH4-N_stream	Dry season	6	0.0576	0.1075	0.0000	0.0194	0.2757
	Early summer	13	0.03632	0.03588	0.00000	0.03106	0.13977
	Late summer	28	0.0764	0.0923	0.0000	0.0561	0.4970

Descriptive Statistics: pH, NO3-N and NH4-N in soil water by season

Variable	Season	N	Mean	StDev	Minimum	Median	Maximum
pH	Dry season	101	3.8023	0.1854	3.3200	3.8300	4.2500
	Early summer	115	3.7884	0.1562	3.4500	3.8000	4.0800
	Late summer	67	3.6296	0.1158	3.2100	3.6500	3.8700
NO3-N (mg/l)	Dry season	112	20.89	12.05	1.23	17.79	65.64
	Early summer	117	11.108	7.941	1.134	8.876	49.192
	Late summer	101	12.347	6.658	0.000	11.015	36.745

NH4-N (mg/l)	Dry season	112	0.1184	0.2532	0.0000	0.0544	1.8667
	Early summer	117	0.0891	0.1304	0.0000	0.0544	0.8944
	Late summer	101	0.1020	0.1055	0.0000	0.0700	0.4978

Descriptive Statistics: pH; NO3-N and NH4-N in stream water

Variable	N	Mean	StDev	Minimum	Median	Maximum
pH _stream	47	4.3505	0.3412	3.8300	4.2900	5.9400
NO3-N_stream	47	3.348	1.752	0.106	3.128	7.254
NH4-N_stream	47	0.0629	0.0831	0.0000	0.0388	0.4970

Descriptive Statistics: pH; NO3-N and NH4-N in soil water

Variable	N	Mean	StDev	Minimum	Median	Maximum
pH	283	3.7558	0.1738	3.2100	3.7500	4.2500
NO3-N (mg/l)	330	14.805	10.199	0.000	12.419	65.642
NH4-N (mg/l)	330	0.10300	0.17652	0.00000	0.05444	1.86667

Canopy throughfall			
Year	2001	2002	2003
Average pH	3.87	3.87	3.76
Average NO3 (mg/l)	4.526	3.596	4.030
Average NH4 (µg/l)	3914.346	2326.961	2904.192

Appendix II: Soil profile descriptions

Profile T1-1 is described by Professor Jan Mulder, profiles T1-2 throug T1-4 are described by the author, and only vegetation and soil horizon depths are included. Other characteristics are very similar along the profiles. T1-5 is described by the author without the use of a Munsell colour map or other aids, and all descriptions are subjective.

T1-1

Described by Prof. Jan Mulder.

Physiographic position: Just below (about 1 m) the summit of a small ridge, that forms the watershed divide of the studied sub-catchment. The described profile was previously sampled for undisturbed soil cores, which were used for the determination of K_{sat} (Sørbotten, unpublished data).

The terrain on which the profile is situated is sloping (6 to 13%) and the slope is convex.

Topography of the surrounding land: Rolling with steepest slopes between 8 and 16%.

Micro-topography: no characteristic features.

Vegetation and land-use: Forestry; forest is dominated by Masson pine with a mixed, dense understory (e.g. rhododendron).

The area is dominated by sedimentary rocks; the soils are developed in weathering residue.

Drainage class 4 (well drained)

The moisture condition of the soil was wet to moist throughout. No groundwater was observed.

No surface stones or rock outcrops and no evidence of erosion.

The soil profile:

Horizon	Depth	Description
O	+1-0	Partly decomposed tree litter. An abrupt, smooth boundary to the O/A horizon.
O/A	0-4	Dark reddish brown (5YR2.5/2). Rich in organic matter, clay and silt. Contains very few gravel and no stones. Weak structure and a sticky, slightly plastic consistence when wet. Common fine and very fine pores; few medium pores. Many very fine roots; very few fine roots. Abrupt, smooth boundary to AB horizon.
AB	4-17	Yellowish red (5YR5/6). Dominated by clay and silt, but slightly gravelly (2 – 15%). Moderately weak structure. Consistence when wet is non-sticky,

		plastic. Darker coloured, continuous, very thin coatings are visible along pores and roots; their nature is unclear. Common medium, fine, and very fine pores. Few fine and very fine roots; very few coarse roots. A clear, wavy boundary to the B1 horizon.
B1	17-27	Yellowish red (5YR5/8). Silty. Clay-rich horizon. Slightly gravelly and stony. The structure is moderately weak. Consistence when wet is non-sticky, plastic. Darker coloured, continuous, very thin coatings are visible along pores and roots; their nature is unclear. Common fine, and very fine pores; few medium pores. Very few fine and very fine roots; very few coarse roots. A gradual, wavy boundary to the B2 horizon.
B2	27++	Yellowish red (5YR5/8); weathered rock fragments up to 5 cm in diameter are brighter in colour (7.5YR6/8; strong brown). More clay-rich than the horizons above. Gravelly and stony (15 to 50%), many are partly weathered. Moderately weak structure. Consistence when wet is non-sticky, plastic. Few fine pores. Very few fine roots and very few coarse roots.

T1-2

Vegetation: Equal mix of Masson pine and deciduous trees. Few ferns. Root pores extend down to the AB horizon.

The soil profile:

Horizon	Depth
O	+2-0
O/A	0-6
AB	6-18
B1	18-30
B2	30++

T1-3

Vegetation: Mostly Masson pine, some deciduous trees. Few ferns.

The soil profile:

Horizon	Depth
O	+1-0
O/A	0-6
AB	6-17
B1	17-28
B2	28++

T1-4

Vegetation: Equal mix of ferns, deciduous trees and Masson pine. Root pores: many root pores in the AB horizon.

Soil profile:

Horizon	Depth

O	+3-0
O/A	0-7
AB	7-15
B1	15-28
B2	28++

T1-5

Slope 10-12 %

Vegetation: some Masson pine and Chinese fir, dense fern understory

The soil profile:

Horizon	Depth	Description
O	+1-0	Partly decomposed tree litter. Abrupt and smooth boundary to O/A horizon.
O/A	0-3	Grayish black. Rich in organic matter. Medium sized, weak structure. Many fine pores and a few large pores. Many fine and medium sized roots. Root aggregation in boundary between O and O/A horizon. Abrupt, smooth boundary to AB horizon.
AB	3-18	Grayish yellow brown. Thickly deposited erosion material with fragments of brick and human activity. Medium sized, moderately weak structure. Many fine pores, few medium sized. Common fine and coarse roots. Clear, smooth boundary to B1.
B1	18-24	Dark reddish brown. Little organic matter. From eroded clay particles from top of the profile. Horizontal sheet structure, moderately weak. A few fine pores following the sheet structure. Very few roots. Little iron precipitation, mostly rock fragments. Some signs of iron precipitation in boundary to B-B/C.
B2	24++	Dark reddish brown. Plastic, single-grain structure .

Appendix III: Precipitation and discharge

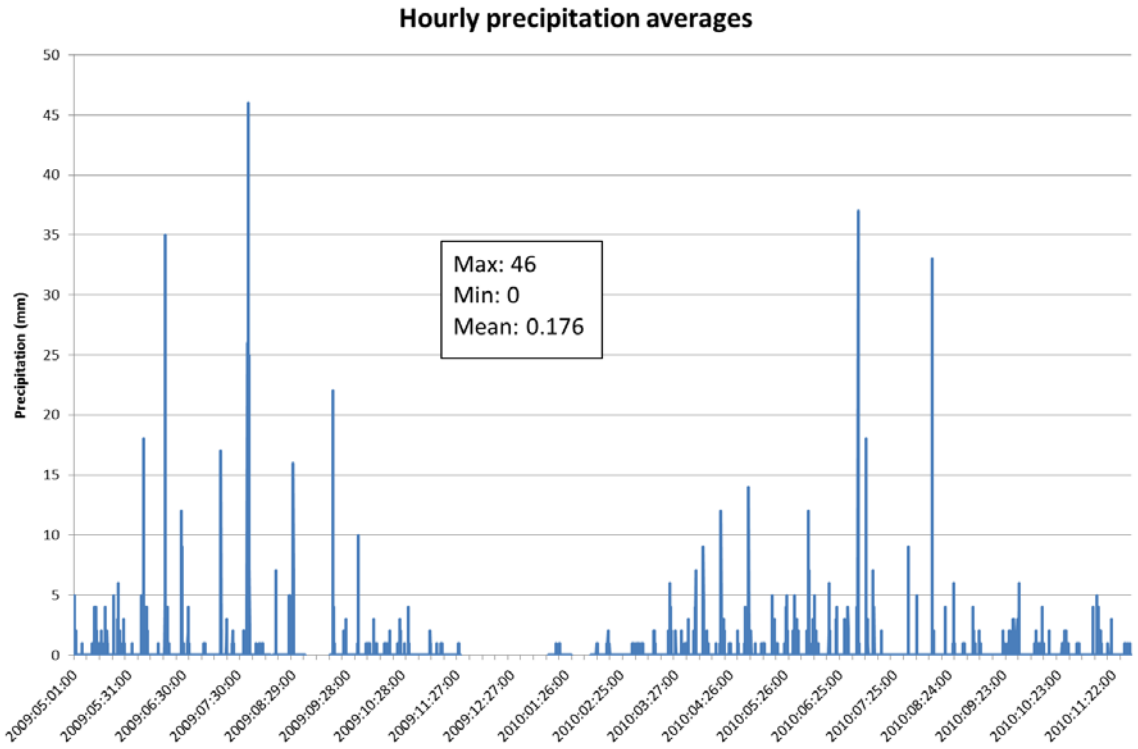

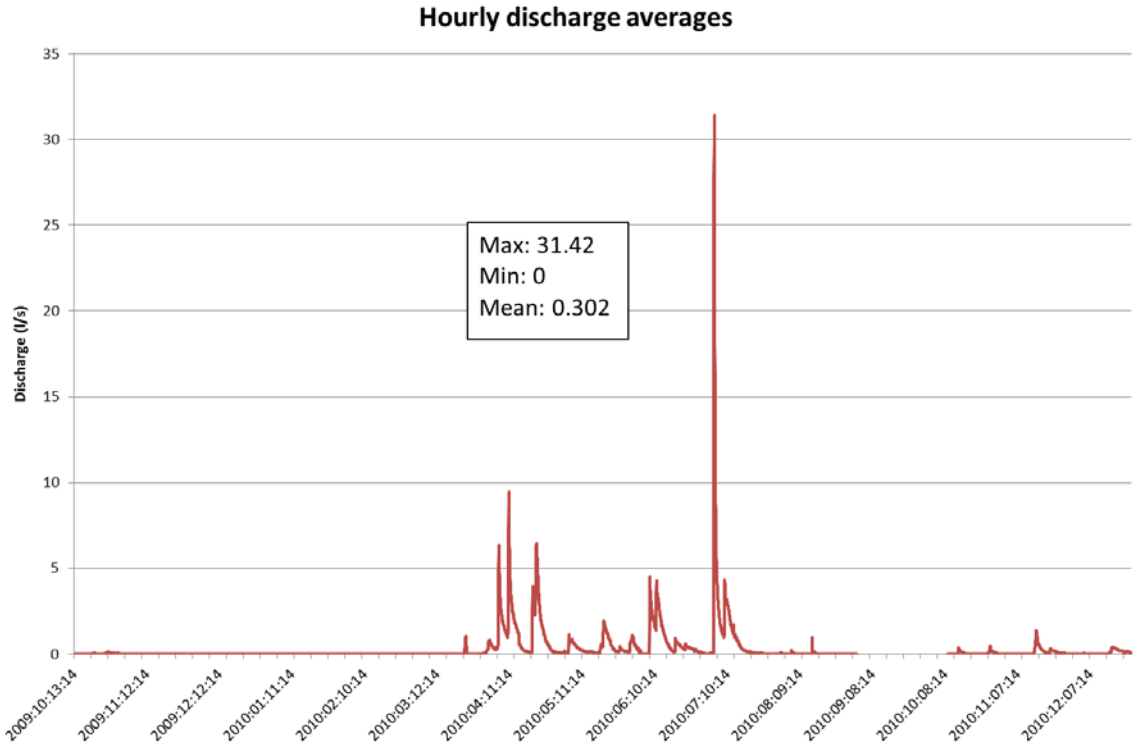

Episodes

Episode 1

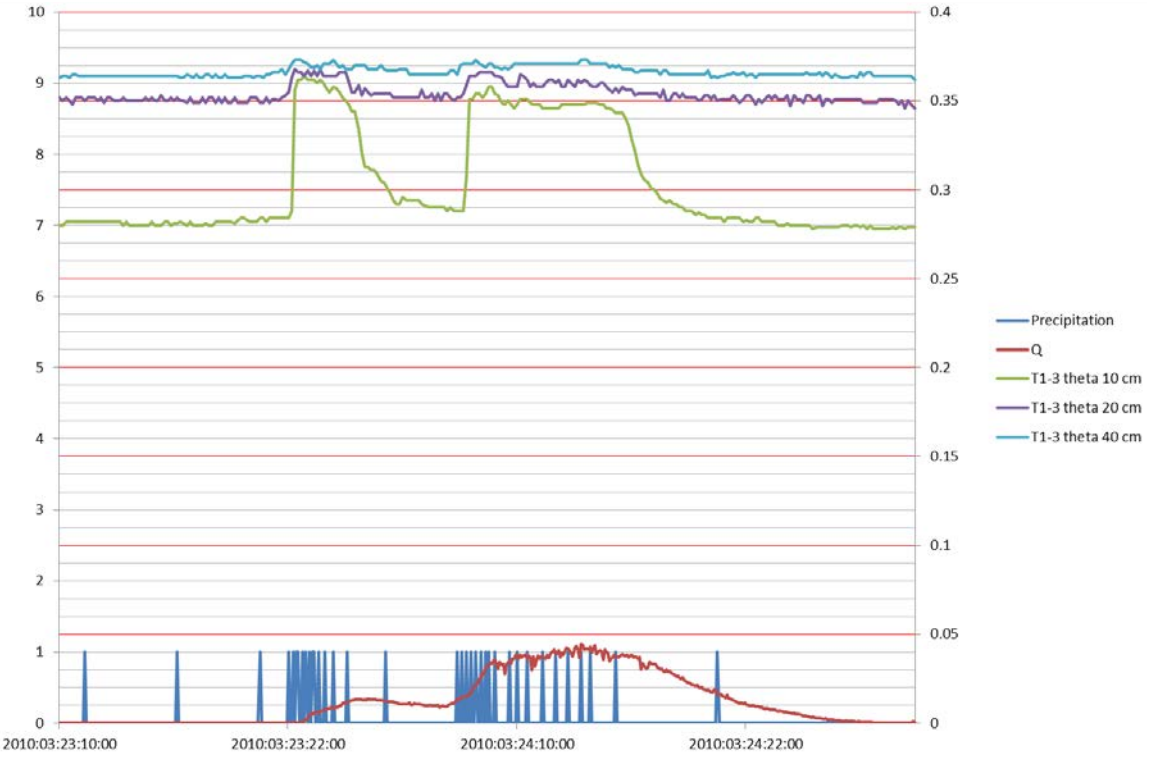

Episode 2

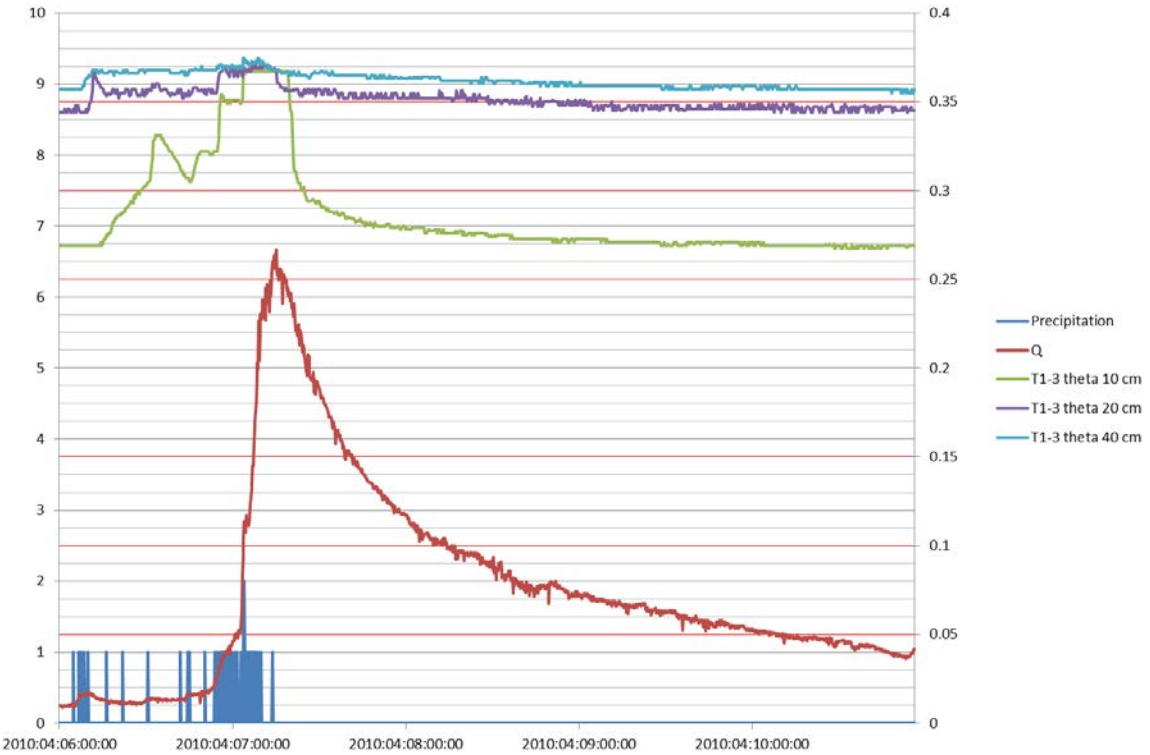

Episode 3

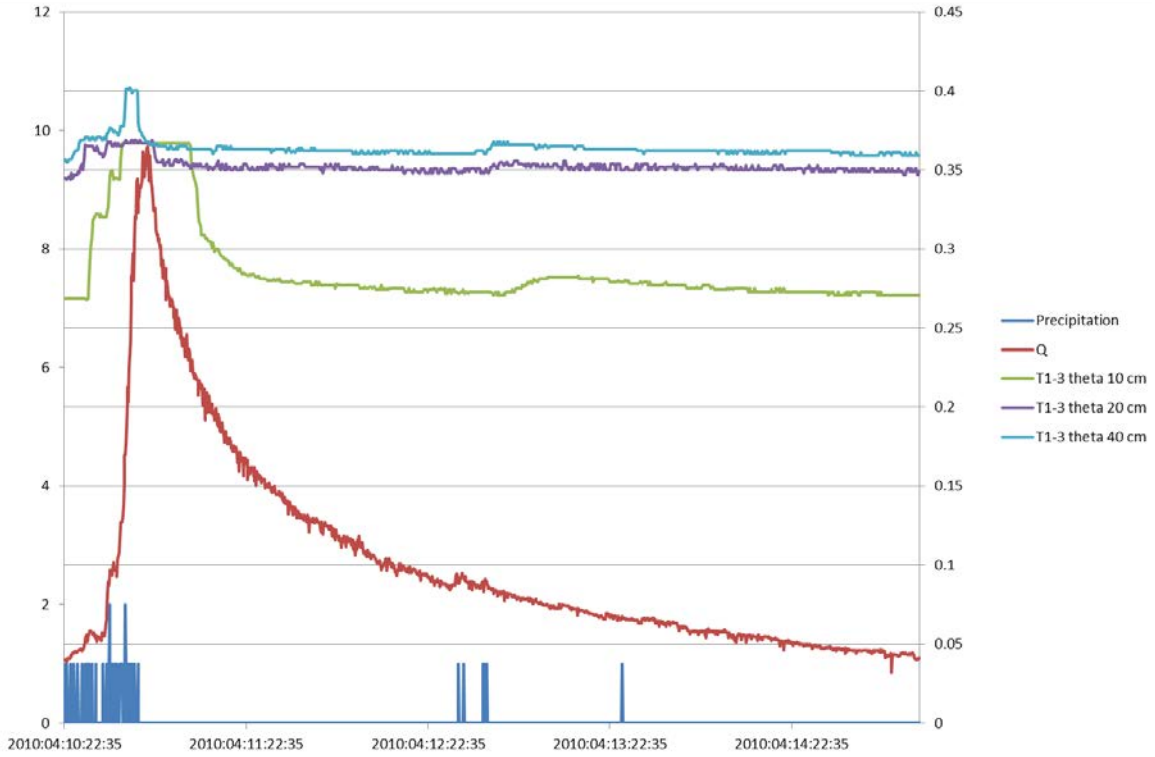

Episode 4

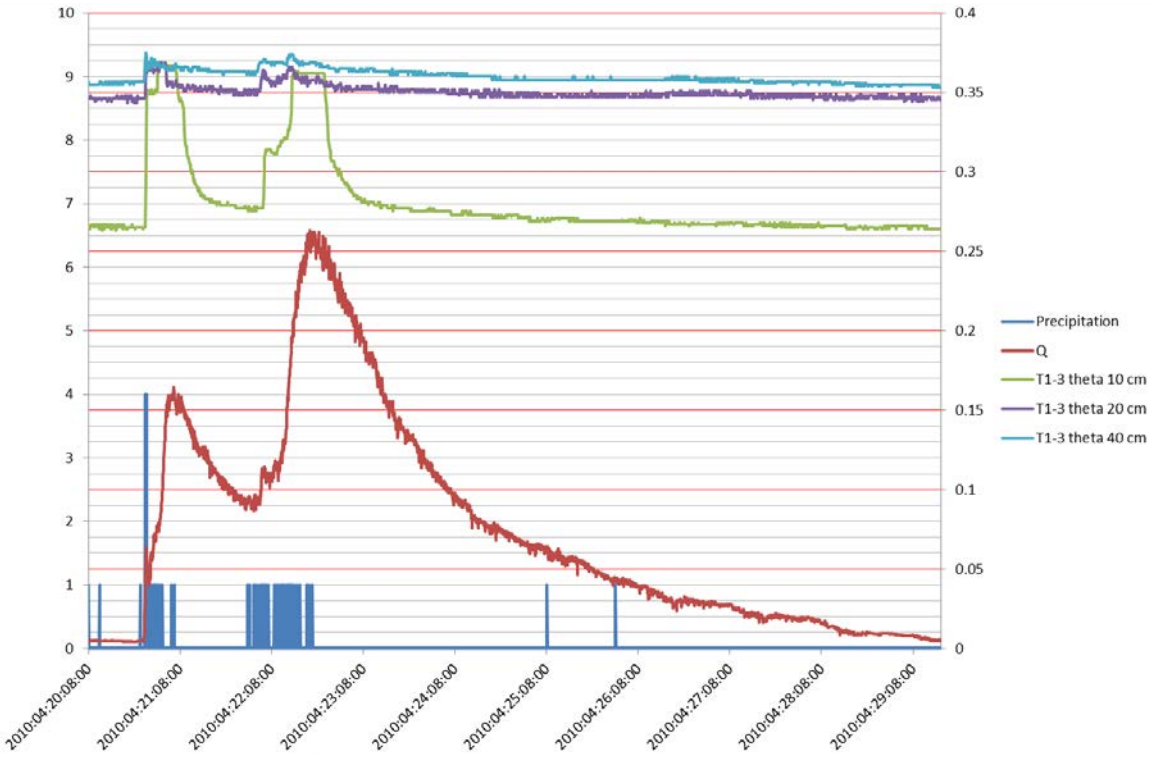

Episode 5

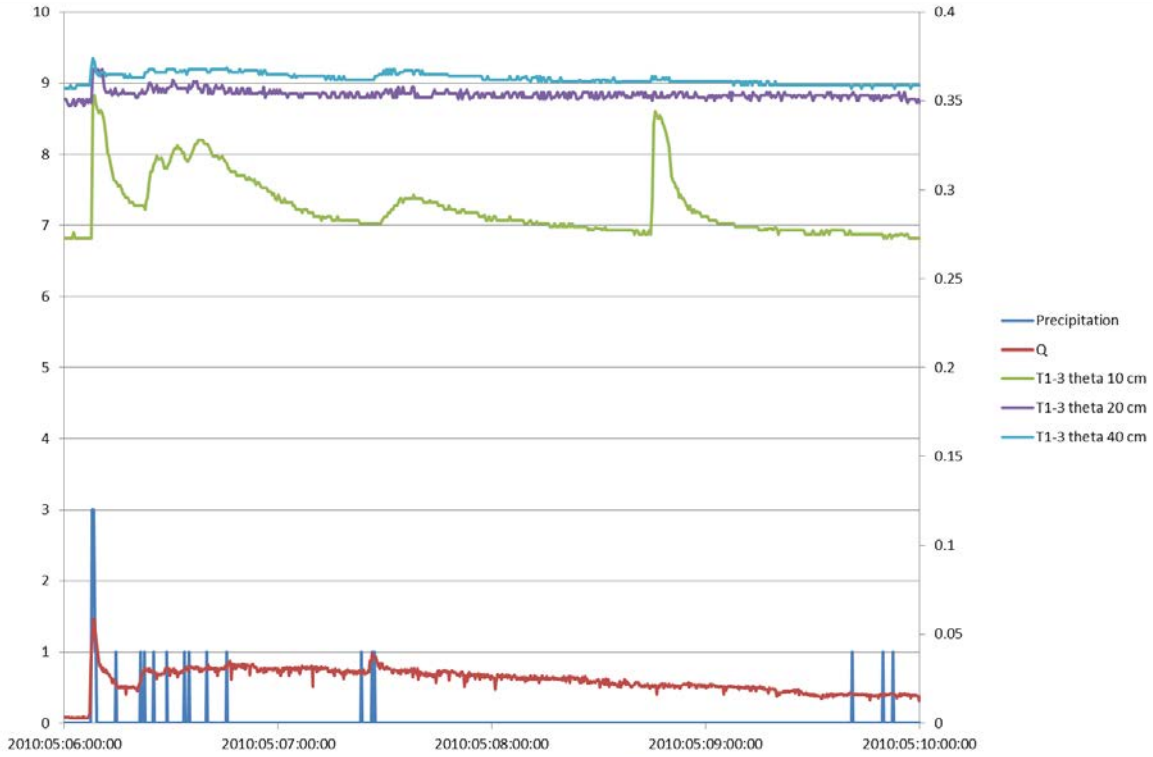

Episode 6

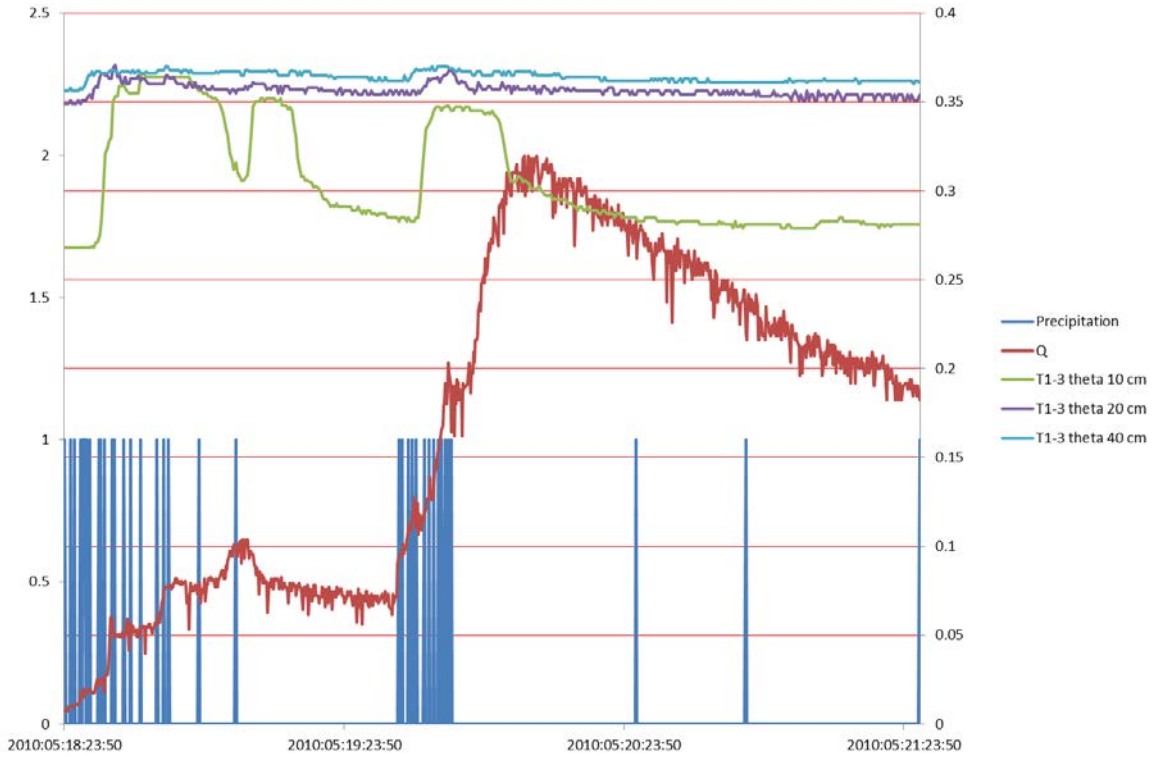

Episode 7

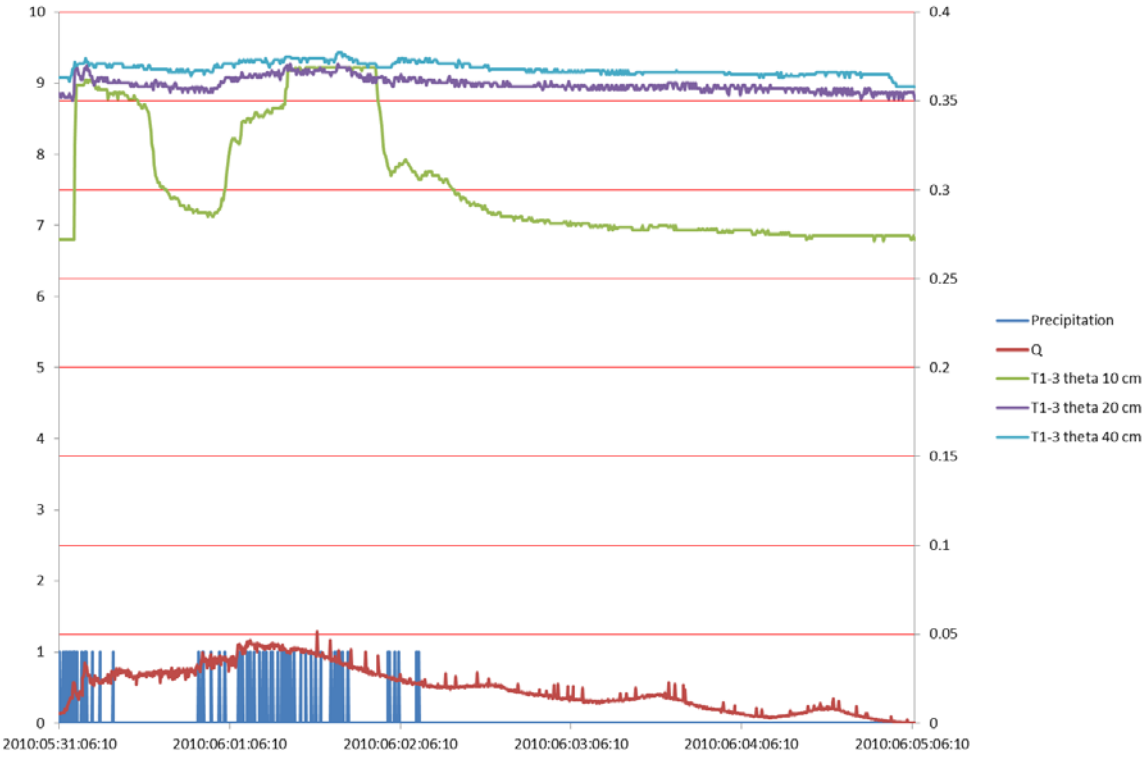
10
9
8
7
6
5
4
3
2
1
0
0.4
0.35
0.3
0.25
0.2
0.15
0.1
0.05
0
2010:05:31:06:10
2010:06:01:06:10
2010:06:02:06:10
2010:06:03:06:10
2010:06:04:06:10
2010:06:05:06:10
Precipitation
Q
T1-3 theta 10 cm
T1-3 theta 20 cm
T1-3 theta 40 cm